Phosphorus-Sulphur Donor Complexes of Palladium, Nickel and Iridium:

Preparation, Coordination and Structural Characterisation

Thesis submitted in accordance with the requirements of the

University of Cardiff for the degree of Doctor in Philosophy

by

Simon James Baker

April 2007

1

UMI Number: U584975

UMI

Dissertation Publishing

ProQuest

Abstract

Commercially available substrates for the synthesis of chiral bidentate phosphinothiolate and phosphinothioether ligands are usually limited with low molecular weights. We report the synthesis of two sterically diverse ligands and how their backbones can influence reactivity and coordination geometries. Phosphinothiol ligand 2-(diphenylphosphino)cyclohexanethiol (L^1H) has been successfully synthesised using commercially available cyclohexene sulphide and fully characterised. A second chiral bidentate phosphinothiolate ligand 9, 10-ethanoanthracene-2-diphenylphosphino-1-ethanethiol, 9-10-dihydro, (L^2H) has been synthesised via a seven step process derived from anthracene. A series of phosphinothioether ligands have been synthesised using the phosphinothiolate L^1Li and L^2K precursors. The series includes thioether moieties containing benzyl (L^1Bn, L^2Bn), 1-methyl naphthalene ($L^1$1-MN, $L^2$1-MN) and 9-methyl anthracene ($L^1$9-MAN, $L^2$9-MAN).

L^1H reacts with divalent nickel and palladium to form complexes of general formula $M(L^1)_2$ (**7**, M=Ni), (**8**, M=Pd), $[M(L^1)Cl]_2$ (**9**, M=Ni) and $M(L^1)_2MCl_2$ (**11**, M=Pd). We also report the formation of a novel dimer complex using the well researched 2-(diphenylphosphino)ethanethiol (dppet) ligand, $[M(dppet)Cl]_2$ (**10**, M=Pd). We report the first structural characterisation of a nickel phosphinothiolate bis-chelate and dimer complexes. L^2H reacts with divalent palladium to produce a number of polymeric complexes; $M(L^2)_2$ (**12**, M=Pd), $M(L^2SO_2)_2$ (**13**, M=Pd) $M[(L^2)Cl]_2$ (**14**, M=Pd) $MCl_2[Pd(L^2)_2M(H_2O)Cl_2]_2$ (**15**, M=Pd) $M[(L^1)Cl]_3$ (**16**, M=Pd). Complexes are structurally analysed via their crystallographic data and compared.

Complexation of phosphinothioether ligands using divalent nickel and palladium yield the following dihalide complexes $M(L^1Bn)Br_2$ (**17**, M=Ni), (**18**, M=Pd), $M(L^1Bn)Cl_2$ (**19**, M=Ni), (**20**, M=Pd), $M(L^1$1-MN$)Cl_2$ (**21**, M=Pd), M(1-MN$L^1$1-MN)Cl_2 (**22**, M=Pd), $M(L^1$9-MAN$)Cl_2$ (**23**, M=Pd). The resulting complexes are structurally compared to similar complexes reported in the literature. We report a similar series of phosphinothioether ligands as previously described using the phosphinothiolate precursor L^2K. Complexation of these ligands with divalent palladium resulted in the corresponding dichloride complexes $Pd(L^2Bn)Cl_2$ (**24**), $Pd(L^2$1-MN$)Cl_2$ (**26**) and $Pd(L^2$9-MAN$)Cl_2$ (**28**). NMR analysis revealed the complexes were fluxional between conformations and diastereoisomers at room temperature. Variable temperature NMR studies show the relative intensities of the inter-converting species. Finally the series of phosphinothioether ligands were coordinated using iridium cod chloride dimer to form complexes: $Ir(L^2Bn)(cod)$ (**25**), $Ir(L^2$1-MN$)(cod)$ (**27**) and $Ir(L^2$9-MAN$)(cod)$ (**29**).

DECLARATION

This work has not been accepted in substance for any degree and is not being concurrently submitted in candidature for any degree.

Signed....................................

Date........ oS | o4 | o7

STATEMENT 1

This thesis is the result of my own investigations, except where otherwise stated. Where correction services have been used, the extent and nature of the correction is clearly marked in a footnote.

Other sources are acknowledged by footnotes giving explicit references. A bibliography is appended.

Signed....................................

Date........ oS | o4 | o7

STATEMENT 2

I hereby give consent for my thesis, if accepted to be available for photocopying and for inter-library loan, and for the title and summary to be made available to outside organisations.

Signed....................................

Date........ oS / o4 | o7

Acknowledgements

I would like to thank my supervisor, Dr Nancy Dervisi, for providing me with the opportunity to carry out this work and for her guidance throughout the project. Most of all, I appreciate her support and encouragement to complete my studies. Thank you.

Thanks are due to all my friends and colleagues in the department of Chemistry, past and present. I would like to thank all the members of the group Dr Despina Koursarou and Dr Christina Carcedo for their encouragement throughout the time of my studies. I'd like to say a special thank you to Rob Jenkins for all his advice and time spent recording the low temperature NMRs and electrospray mass spectroscopy. A thank you goes to Dr Li-Ling Ooi for her time and effort recording and resolving the X-ray crystallography analysis.

I want to pay a special tribute to my family for whom all of this would not be possible without their continued support, not only through my PhD but also throughout my entire studies.

Finally I'd like to say a thank you to all the current and past members of the chemistry football team (Chemsoc) for all the enjoyable moments that we have shared over the seasons.

Table of Contents

6

List of tables

7

List of figures

9

Chapter 6

List of schemes

Chapter 1

Chapter 2

Chapter 3

13

Glossary of abbreviations and symbols
Chemicals, ligands, radicals, etc.

9-MAN	9-methyl anthracene
acac	acetylacetonate anion
Ar	aryl
BINAP	2, 2'-bis(diphenylphosphino)-1,1'-binaphthyl
BINAPHOS	(1, 1'-binaphthalen-2,2'-yl)phosphite
Bu	butyl(superscript i, s, or t refers to iso, secondary or tertiary butyl)
Br	bromide
Bn	benzyl
Cl	Chloride
COD	1, 5-Cyclooctadienyl
Cp	Cyclopentadienyl
DBU	1, 8-Diazabicyclo[5.4.0]undec-7-ene
dcm	dichloromethane
DMF	N, N-Dimethylformamide
dppet	2-(diphenylphosphino)ethanethiol
dpppt	2-(diphenylphosphino)propanethiol
DIOP	2, 3-O-isoprepylidiene-2, 3-dihydroxy-1,4 bis(diphenylphosphino)-butane
DIPAMP	1, 2-bis(phenylanisylphosphino)ethane
DMF	dimethyl formamide
DMSO	dimethyl sulphoxide, Me_2SO
DSP	bis(o-methylthiophenyl)phosphine
ES	Electrospray (Mass Spectrometry)
Et	ethyl, CH_3CH_2
h	hours
hv	Irradiation with light
iPr	Isopropyl
L	ligand
L^1H	
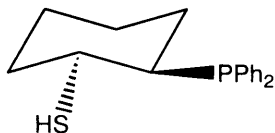
2-(diphenylphosphino)cyclohexanethiol

14
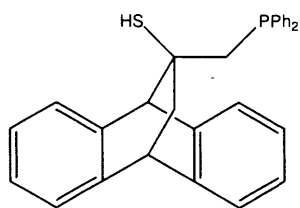
L²H

9, 10-ethanoanthracene-2-diphenylphosphino-1-ethanethiol, 9-10-dihydro

Me	methyl
NMR	nuclear magnetic resonance
1-MN	1-methyl naphthalene
OAc	acetate ion
Ph	phenyl, C_6H_5
PhMe	toluene
py	pyridine
R	alkyl group
S	solvent
SP	*o*-methylthiophenyldiphenyl-phosphine
t-BuLi	tertiary-Butyl Lithium
THF	tetrahydrofuran
tol	toluene
TSP	tris(*o*-methylthiophenyl)phosphine
X	halogen

Units, etc.

º	Degrees
Å	Angstrom unit, 10^{-10} m
Atm	atmospheres, 1 atm = 101 325 Pa
cm^{-1}	wave number
e.e.	enatiomeric excess
Hz	hertz, s^{-1}
IR	infrared
nm	nanometres, 10^{-9} m
ppm	parts per million

Chapter 1 Introduction

The coordination chemistry of bidentate phosphorus-sulphur donor ligands has been studied intermittently for over thirty years, and this work has been comprehensively reviewed [62]. To date a vast majority of phosphinothiolate and phosphinothioether complexes contain relatively low molecular weight backbones. This is due to the lack of availability and the difficulty of synthesising sulphur containing precursors for ligand preparation. In industry there is a requirement for catalytic complexes to be synthesised in a small number of synthetic steps from precursors which are inexpensive and commercially available. In this thesis we will study whether the use of such precursors affects the coordination of transition metal complexes. In this study we have synthesised two novel classes' of phosphinothiol ligands, one being synthesised from the commercially available thiirane, cyclohexene sulphide (L^1H) and the second being synthesised via a seven step synthesis derived from anthracene (L^2H).

These ligands have been reacted with suitable metal precursors to form a number of structurally diverse transition metal complexes. Through the study, coordination chemistry and modelling theories have been used to anticipate the relative geometries of such complexes. We present how the bonding of transition metal complexes compares with crystal field and molecular orbital theory.

1.1   Coordination chemistry

The geometrical arrangement of ligands varies according to the number of ligands bonded to the metal centre, and to the coordination preference of the metal. The number of ligands can vary from two to eleven per metal. One of the most common geometries is octahedral, where six ligands are coordinated to the metal in a symmetrical distribution, leading to the formation of an octahedron if lines were drawn between the ligands. Other common complexes contain four coordinated ligands which can be arranged around a central metal atom in several ways. Ligands can be placed at the corners of a square, with the metal atom at the centre of the square; this is called square planar geometry. Another way that four ligands could be arranged around the central metal atom is at the corners of a tetrahedron; this is referred to as tetrahedral geometry (**Figure 1-1**).

Octahedral   Tetrahedral   Square planar
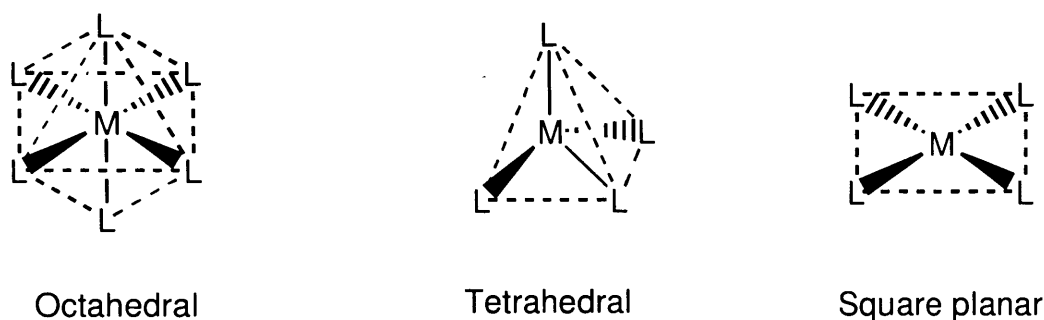
Figure 1-1 Typical coordination geometries of metal complexes

1.1.1 Crystal field theory

The geometry of a complex can be anticipated using several different models such as Crystal field theory, Molecular orbital theory and Ligand field theory, which delivers insight into the process of chemical bonding in transition metal complexes. By utilising such models, the geometries of phosphinothiol and phosphinothioether complexes can be hypothesised before any chemical reactions take place.

Crystal field theory (CFT) is a model that describes the electronic structure of transition metal compounds, all of which can be considered coordination complexes. In CFT, the metal complex is treated as a "free ion". The ligands are treated as point charges. It is assumed that the orbitals on the metal and the ligands do not overlap. Interactions between a transition metal and ligand arise from the attraction between the positively charged metal cation and negative charge on the non-bonding electrons of the ligand. It is typical to consider how the d-orbitals on a metal will be affected upon being surrounded by an array of point charged ligands. The way these point charges interact with the d-orbitals of a metal atom explains the geometries adopted by various transition metal complexes.

In the absence of ligands, all d-orbitals in a particular metal have the same energy and are said to be degenerate. When ligands coordinate to the metal, however, the ligands cause the d-orbitals to be either stabilised or destabilised. A stabilising effect from a ligand lowers the energy of the interacting d-orbital, whereas a destabilising effect raises the energy of the d-orbital. In an octahedral complex, six ligands are placed symmetrically along the axes of a Cartesian coordinate system, with the metal at the origin. Knowing the shapes of the five d-orbitals is essential in understanding octahedral geometry. There are two d-orbitals that point directly along the Cartesian axes: the dz^2

17

orbital, which points along the z-axis, and the dx²-y² orbital, which has lobes on both the x- and y-axes (**Figure 1-2**).

$d_z{}^2$

$d_{x^2-y^2}$

d_{xy}

d_{xz}

d_{yz}
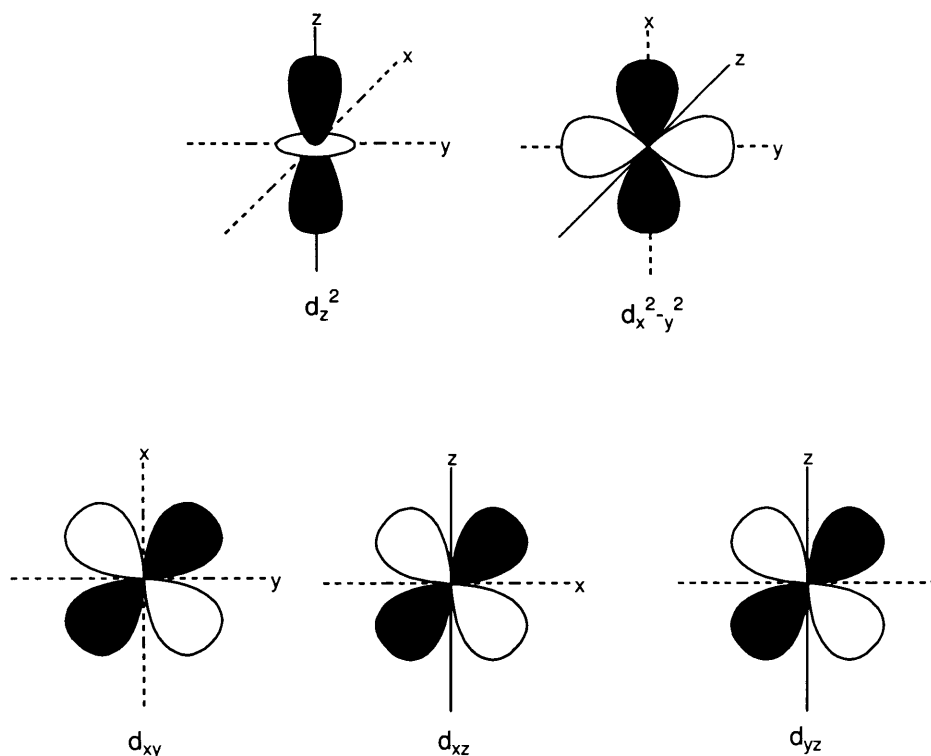
Figure 1-2: Diagram of transition metal d-orbitals $d_z{}^2$, $d_{x^2-y^2}$, d_{xy}, d_{xz} and d_{yz}

The interaction of six ligands with the dz² and the dx²-y² orbitals raises the energy of these two d-orbitals through repulsive interactions. Moreover, the energy of these two orbitals is increased by the same amount, so the dz² and the dx²-y² orbitals are degenerate. In the nomenclature of crystal field theory, these orbitals are called the e orbitals. The other three d-orbitals, the dxy, dzx, and dyz orbitals, which all have lobes in between the Cartesian axes, are repelled less by the ligands and are in effect stabilised to a lower energy. The dxy, dxz, and dyz orbitals (**Figure 1-2**) are also degenerate; collectively, they are called the t orbitals. The six bonding molecular orbitals that are formed are filled with the electrons from the ligands, and electrons from the d-orbitals of the metal ion occupy the non-bonding and, in some cases, anti-bonding MO's. The energy difference between the e and t orbitals is called Δ_o (o stands for octahedral) and is determined by the nature of the π-interaction between the ligand orbitals with the d-orbitals on the central atom. π-donor ligands lead to a small Δ_o and are called weak- or low-field ligands, whereas π-acceptor ligands lead to a large value of Δ_o and are called strong- or high-field ligands.

18

The spectrochemical series is an empirically-derived list of ligands ordered by the size of the splitting Δ that they produce. It can be seen that the low-field ligands are all π-donors, such as I^-, the high field ligands are π-acceptors, such as CN^- and CO, and ligands, such as H_2O and NH_3, which are neither, are in the middle.

$$I^- < Br^- < S^{2-} < SCN^- < Cl^- < NO_3^- < N_3^- < F^- < OH^- < C_2O_4^{2-} < H_2O < NCS^- < CH_3CN$$
$$< py \ (pyridine) < NH_3 < en \ (ethylenediamine) < bipy \ (2,2'\text{-bipyridine}) < phen \ (1,10\text{-}$$
$$phenanthroline) < NO_2^- < PPh_3 < CN^- < CO$$

We use similar logic to explain the crystal field splitting of the d-orbitals in a four-coordinate, tetrahedral complex. One way to represent a tetrahedral species is to show four ligands on alternating corners of a cube. In a tetrahedral complex, the ligands do not point directly at any of the five d-orbitals, but they come close to the d_{xy}, d_{zx}, and d_{yz} orbitals, which are directed toward the edges of the cube, these orbitals are raised in energy and are degenerate. The d_{z^2} and the $d_{x^2-y^2}$ orbitals point toward the sides of the cube and are therefore directed away from the attached ligands; these two orbitals are lowered in energy and are degenerate.

Crystal field theory also explains the four-coordinate, square planar geometry. In this case, we imagine an octahedral complex in which the ligands on the z-axis that is, those interacting most directly with the d_{z^2} orbital are removed. The d_{z^2} orbital is therefore lowered in energy. Furthermore, the other d-orbitals having z-character specifically, the d_{zx} and d_{yz} orbitals also decrease in energy. However, since the ligands are all now in the xy plane, both d-orbitals having x- and y-character namely, the $d_{x^2-y^2}$ and the d_{xy} orbitals are raised in energy (**Figure 1-3**).
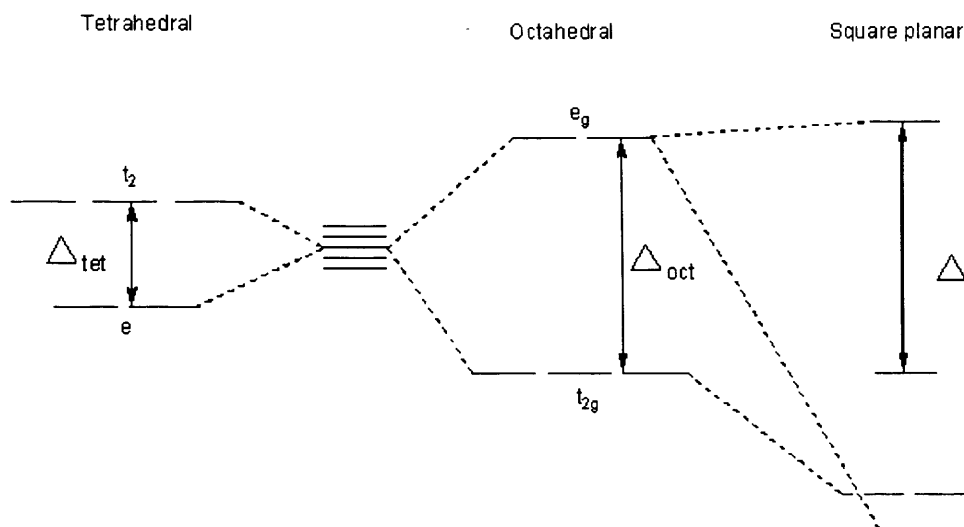
Figure 1-3: Crystal field splitting of tetrahedral, octahedral and square planar transition metal complexes

What determines whether a four-coordinate transition metal complex is tetrahedral or square planar is dependant on the number of d-electrons in the central transition metal. If the metal has eight d-electrons, as is the case for Pd^{2+}, it is energetically advantageous for the complex to adopt a square planar geometry. In this case, the eight d-electrons will achieve some stabilisation in energy by occupying the dxz, dyz, dz^2, and dxy orbitals.

1.1.2 Molecular orbital theory

Molecular orbital (MO) theory uses a linear combination of atomic orbitals (LCAO) to form molecular orbitals which cover the whole molecule. These are often divided into bonding orbitals, anti-bonding orbitals, and non-bonding orbitals. When studying the interactions of transition metal complexes the differences in energy levels of ligands and metals complexes are quite different. The ligand orbitals which are lower in energy than the metal orbitals evolve into bonding molecular orbitals when the complex is formed. This is a general result, orbitals with the lower energy are lowered even further when the molecule is formed. The bonding molecular orbital is dominated by the ligand orbitals which are closest in energy. In other words, the bonding molecular orbitals in transition metal complexes are mostly ligand in character and have a small but not zero metal character. Correspondingly, the metal orbitals evolve into anti-bonding molecular orbitals which are mostly metal in character and have a small

contribution from the ligand orbitals. With reference to octahedral complexes all these factors can be identified.

In octahedral complexes six bonding molecular orbitals are formed which are mostly ligand in character. Since each ligand contributes exactly two electrons, these are always completely filled. The filling of these orbitals is the source of the stabilisation which holds the complex together. Three of the metal d-orbitals have a symmetry which excludes interaction with the ligand orbitals therefore they are non-bonding and degenerate. Two of the metal d-orbitals interact with the ligand orbitals and produce a pair of degenerate anti-bonding orbitals which are mostly metal in character. The magnitude of this splitting (Δ_{oct}) is determined by the extent of interaction between the metal and the ligand (**Figure 1-4**). If the interaction is large, the spacing is relatively large. This is called the strong field case. With a weak interaction called the weak field case, the spacing is relatively small. This splitting result has consequences on the colour of octahedral complexes. The remaining metal orbitals also evolve into four anti-bonding molecular orbitals.
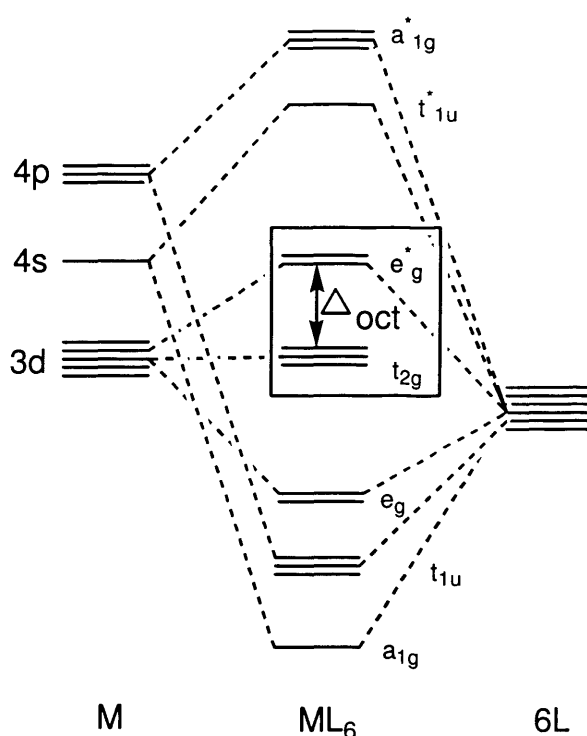
Figure 1-4: MO diagram for an octahedral metal complex

Some ligand ions in combination with certain metal ions have a preference for tetrahedral coordination. Since a tetrahedral complex has a radically different symmetry,

the metal and ligand orbitals must combine differently. The MO diagram for a tetrahedral complex is given in **Figure 1-5**. The complex has four ligands and hence there are only four bonding molecular orbitals which are mostly ligand in character. These orbitals are completely filled as each ligand contributes as before a pair of electrons. The filling of these orbitals is the source of the stability of the complex. In contrast with the octahedral case, two rather than three of the d-orbitals are non-bonding and hence entirely metal in character. Three rather than two of the d-orbitals are anti-bonding and are mostly metal in character. The pattern for the tetrahedral complex is the reverse of that for the octahedral complex. The remaining anti-bonding molecular orbitals are unoccupied and do not make an important contribution to the bonding. Tetrahedral complexes lack a centre of symmetry. This has an important consequence. The propensity to absorb light is greatly increased and tetrahedral complexes which absorb in the visible are very darkly coloured.
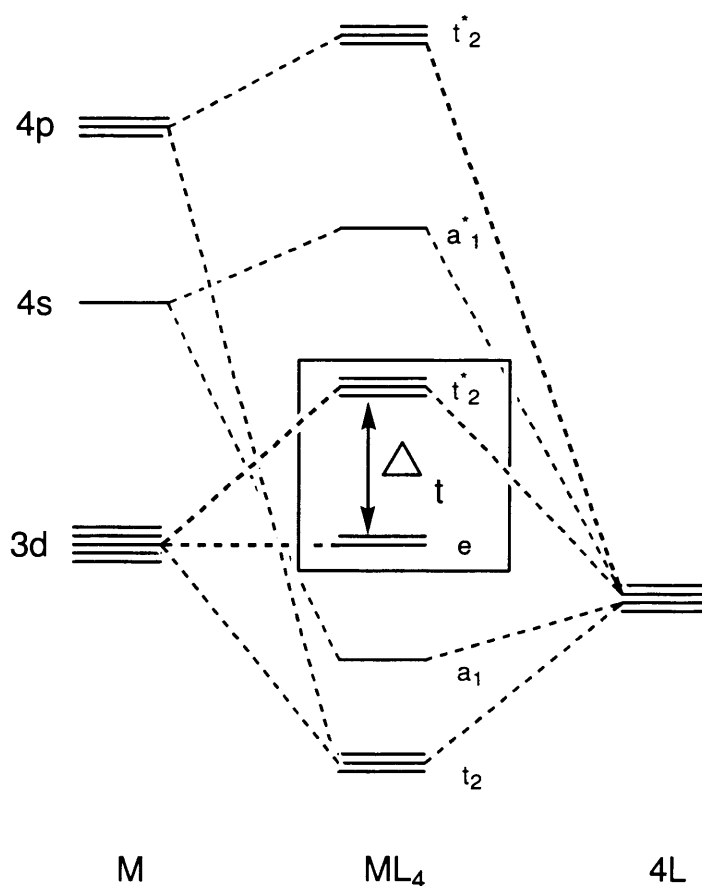
Figure 1-5: MO diagram for a tetrahedral metal complex

For purposes of completeness, a molecular orbital energy diagram of a square planar complex is given in **Figure 1-6**. The complex has four ligands and hence there are only

22

four bonding molecular orbitals which are mostly ligand in character. These orbitals are completely filled as each ligand contributes as before a pair of electrons. The filling of these orbitals is the source of the stability of the complex. In this MO model, three of the metal d-orbitals are non-bonding, one is slightly anti-bonding, and one is more anti-bonding. The arrangement of these orbitals changes depending upon ligand and metal complex. However, in every case one orbital which is anti-bonding is significantly higher in energy than the other four which is the last orbital to be filled.
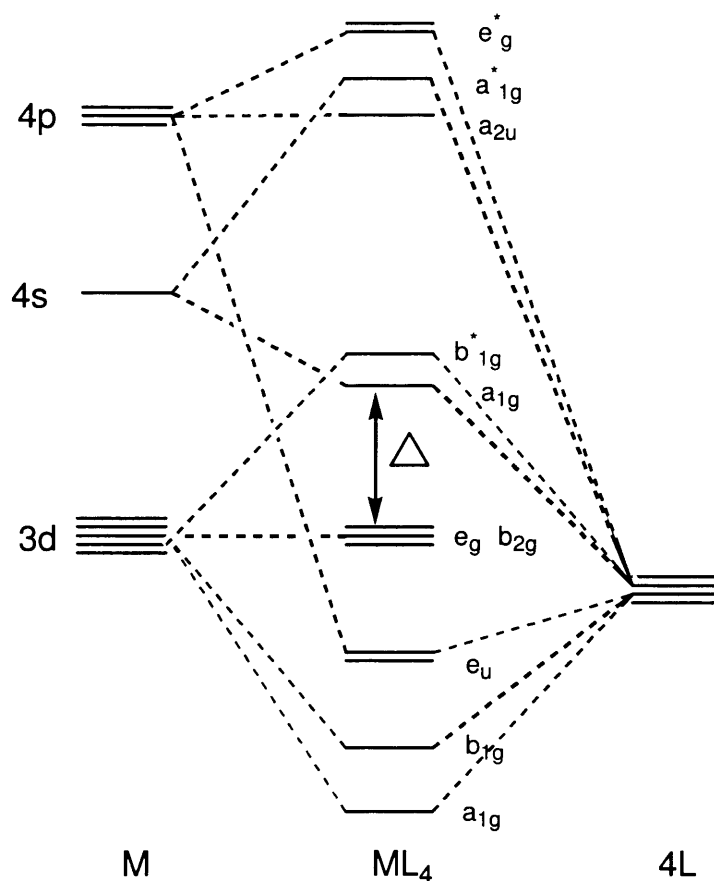
Figure 1-6: MO diagram for a square planar metal complex

We have already noted that transition metals with a d^8 configuration have a preference for square planar coordination. A combination of thermodynamics and MO theory provides an explanation for the formation of square planar complexes with d^8 species. First entropy considerations alone would argue for a loss of ligands and a reduction in the coordination number. The energetics of this conversion from octahedral to square planar coordination must be examined to discover why this is most likely with d^8 species and why square planar rather than tetrahedral coordination results. An octahedral complex contains the elements of a square planar complex. The equatorial

ligands and the metal constitute a square planar arrangement. Consider an octahedral complex of a d^8 species such as Ni^{2+}. Two of the eight d-electrons are present in the e_g^* anti-bonding molecular orbitals. If one examines the symmetry of these orbitals, one discovers that they involve the two axial metal-ligand bonds. These axial bonds are broken preferentially and the residual complex is a planar species.

1.2 Hard and soft acids and bases (HSAB)

The HSAB concept, also known as HSAB theory, is widely used in chemistry for explaining stability of compounds, reaction paths etc. 'Hard' applies to species which are small, have high charge states and are weakly polarised. 'Soft' applies to species which are big, have low charge states and are strongly polarised. A summary of the theory is that soft acids react faster and form stronger bonds with soft bases, where hard acids react faster and form stronger bonds with hard bases, all other factors being equal. The classification in the original work was based on equilibrium constants for reaction of two Lewis bases competing for a Lewis acid. **Table 1-1** summarises typical examples of hard and soft bases and acids.

Acids				Bases			
hard		**soft**		**hard**		**soft**	
Alkali metals	Li^+,Na^+,K^+	Palladium	Pd^{2+}	Hydroxyl	OH^-	Thiol	RS^-
Hydrogen	H^+	bulk Metals	M^0	Alcohol	RO^-	Phosphine	PR_3
Titanium	Ti^{4+}	Platinum	Pt^{4+}	Halogens	F^-,Cl^-	Hydride	H^-
Chromium	Cr^{3+},Cr^{6+}	Mercury	$CH_3Hg^+, Hg^{2+}, Hg_2^{2+}$	Ammonia	NH_3	Iodides	I^-
Boron trifluoride	BF_3	Silver	Ag^+	carboxylic acid	CH_3COO^-	Thiocyanate	SCN^-
Carbocation	R_3C^+	Borane	BH_3	Carbonate	CO_3^{2-}	Carbon monoxide	CO
				Hydrazine	N_2H_4	Benzene	C_6H_6

Table 1-1: Examples of 'hard' and 'soft' acids and bases

Phosphinothiols contain phosphino and thiolate donor ligands which are both classed as soft bases, therefore it would be suitable to coordinate such ligands to soft acid metals to form stable transition metal complexes. Examples of suitable metals have been highlighted in **Table 1-1.** Group 10 metals, palladium and platinum have been

extensively reported in the literature in forming stable complexes with P, S ligands [44], [53], [72].

1.3   Chelating ligands

With the ligands prepared in this study being bidentate chelating ligands a mention of the importance of chelates in chemistry must be made. Chelators are used in chemical analysis, as water softeners, shampoos, preservatives, and in medicine (chelation therapy), where they are employed to safely bind with poisonous metal agents such as mercury, arsenic, or lead to stabilise them and allow them to be excreted without further interaction with the body. Natural chelators include the porphyrin rings in hemoglobin or chlorophyll and the Fe^{3+} chelating siderophores secreted by microorganisms, and are contained in herbs such as cilantro, which has long been used as a treatment for heavy metal poisoning. A commonly used synthetic chelator is EDTA.

1.3.1   Chelate effect

It has been known for many years that coordination with chelating ligands produce complexes which have much greater thermodynamic stability than their monodentate counterparts. This can be seen by simply looking at the Gibbs free energies for adding a number of monodentates compared with adding half the number bidentate ligands to form a metal complex. A classic example is the coordination of ethylenediamine compared with the separate ligand addition of ammonia in forming Ni^{2+} complexes (**Scheme 1-1**).

$$[Ni(H_2O)_6]^{2+} + 6NH_3 \underset{}{\overset{k_1}{\rightleftharpoons}} [Ni(NH_3)_6]^{2+}$$

$$\Delta G^\circ = -49.2 \text{ kJ mol}^{-1}$$

$$[Ni(H_2O)_6]^{2+} + 3en \underset{}{\overset{k_2}{\rightleftharpoons}} [Ni(en)_3]^{2+}$$

$$\Delta G^\circ = -104.4 \text{ kJ mol}^{-1}$$
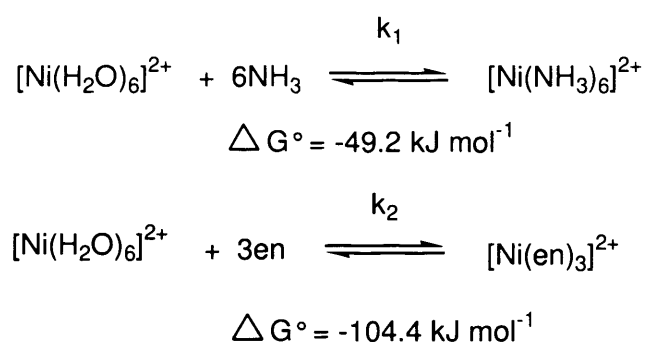
Scheme 1-1: Complex formation of Ni^{2+} using ammonia (NH_3) and ethylenediamine (en)

If we study the free energy of formation we see that the ΔH° values for each reaction are almost identical, that is, heat is evolved to about the same extent whether forming   a   complex   involving   monodentate   ligands   or   bidentate   ligands.

25

What is seen to vary significantly is the entropy ($\Delta S°$) which changes from negative (unfavourable) to positive (favourable). To explain this enhanced contribution from entropy there are two areas to concentrate on.

One explanation is to count the number of species on the left and right hand side of the equation above. It will be seen that on the bottom there are four species, whereas on the top there are seven species, a net gain of three species which occurs as the reaction proceeds. This can account for the increase in entropy since it represents an increase in the disorder of the system.

An alternative view comes from trying to understand how the reactions might proceed. To form a complex with six monodentates requires six separate favourable collisions between the metal ion and the ligand molecules. To form the tris-bidentate metal complex requires an initial collision for the first ligand to attach by one arm, the other arm is always nearby and only requires a rotation to enable the ligand to form the chelate ring. If you consider dissociation steps, then when a monodentate group is displaced, it is lost into the bulk of the solution. On the other hand, if one end of a bidentate group is displaced the other arm is still attached and it is only a matter of the arm rotating around and it can be reattached again. Both sets of conditions favour the formation of the complex with bidentate groups rather than monodentate groups. Such advantages favour the formation of bidentate phosphinothiol and phosphinothioether complexes compared to their monodentate counterparts.

1.3.2 Macrocyclic effect

Coordination chemists study macrocycles with three or more potential donor atoms in rings of greater than nine atoms as these compounds often have strong and specific binding with metals. This property of coordinating macrocyclic molecules is the macrocyclic effect. A macrocycle has donor atoms arranged in more fixed positions and thus there is less of an entropic effect in the binding energy of macrocycles than monodentate or bidentate ligands with an equal number of donor atoms. Thus the macrocyclic effect states that complexes of macrocyclic ligands are more stable than those with polydentate ligands of similar strength. With bridging phosphinothiol complexes the extended valency of sulphur could take advantage of the macrocyclic effect. The combination of both effects makes the formation of such ligands and metal complexes very desirable.

1.4 Trans effect and influence

The *trans effect* is defined as the effect of a coordinated ligand upon the rate of substitution of ligands opposite to it. It is attributed to electronic effects and it is most notable in square planar complexes, although it can also be observed for octahedral complexes. The intensity of the *trans effect* (as measured by the increase in rate of substitution of the *trans* ligand) follows this sequence:

$$F^-, H_2O, OH^- < NH_3 < py < Cl^- < Br^- < I^-, SCN^-, NO_2^-, SR_3, Ph^- < SO_3^{2-} < PR_3,$$
$$AsR_3, SR_2, CH_3^- < H^-, NO, CO, CN^- C_2H_4$$
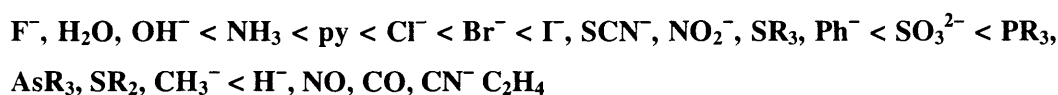
A classic example of the *trans effect* is the synthesis of cisplatin. Starting from $PtCl_4^{2-}$, the first NH_3 ligand is added to any of the four equivalent positions at random, but the second NH_3 is added *cis* to the first one, because Cl^- has a larger *trans effect* than NH_3. If, on the other hand, one starts from $Pt(NH_3)_4^{2+}$, the *trans* product is obtained instead (**Scheme 1-2**).
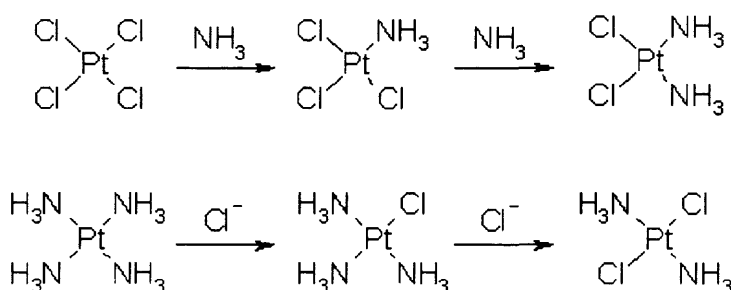
Scheme 1-2: *Trans effect* demonstrated by the synthesis of cisplatin

The *trans influence* is purely a thermodynamic phenomenon where ligands can influence the ground state properties of groups which are *trans* to them. Such properties include; Metal-ligand bond lengths, vibrational frequencies and NMR coupling constants. The *trans influence* series is based on structural data and has been given as;

$$R^-, H^- > PR_3 > CO, CNR, Cl^-, As(CH_3)_3, NH_3 > py$$

As we have previously discussed there is a preference of reacting group 10 transition metal precursors with our P, S ligands to form square planar complexes. Therefore *cis* and *trans* geometries of the resulting complexes could be observed. Phosphorus and Sulphur have different electronic properties which affect the geometries of complexes formed owing to the *trans effect*, the ligands also alter the bonding properties of groups

trans to them by their differing *trans influence*. These properties have been discussed with the inclusion of the changes in the *trans effect* and *influence* between phosphinothiolates and phosphinothioethers.

1.5 Phosphine chemistry; electronic and steric properties

There are many properties which make phosphines desirable ligands to study in co-ordination chemistry and homogeneous catalysis. One of the most useful characteristics is the ability to act as π-acids as well as σ-bases thereby assisting the stabilisation of metals in low oxidation states. This back donation is postulated to be either to empty *d*-orbitals on the phosphorus atom [1] or to occupy σ^* antibonding molecular orbitals on the phosphine [2], [3], [4], [5] (**Figure 1-7**).
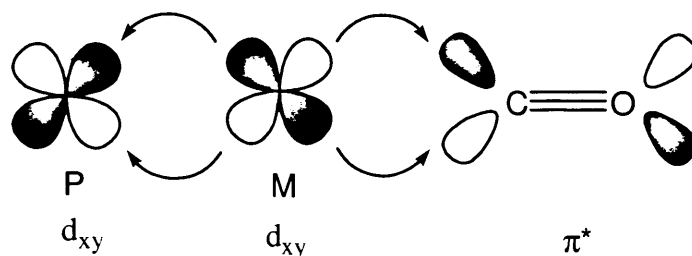
Figure 1-7: Metal phosphine back-bonding

A second desirable feature of phosphine ligands is that they have the ability to be 'tuned' for a particular purpose. Groups pendant on the phosphorus atom giving differing electronic as well as steric properties to the phosphine. The steric properties of a coordinated monodentate phosphine are often defined by the cone angle, a parameter first described by Tolman.[6] The cone angle is measured by drawing a cone such that the lines touch the outer most part of the groups bonded to the phosphorus atom, and the lines intersect at the centre of the metal atom (**Figure 1-8**)
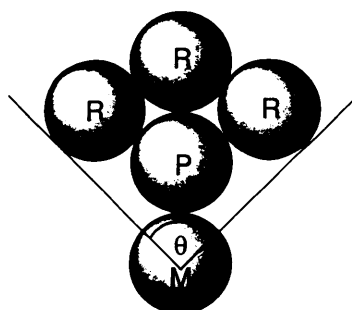
Figure 1-8: Tolman cone angle

28

A simple measurement of the σ-basicity of a phosphine is to take the pKa of the conjugate acid (i.e. the phosphonium salt), a high pKa indicating a more basic phosphine (**Table 1-2**). This method is not a true reflection of just σ-basicity, but rather a measure of the overall characteristics of the phosphine.

Phosphine	pKa
P(t-Bu)₃	11.40
P(Et)₃	8.69
P(Ph)₃	2.73

Table 1-2: Relative pKa of selected phosphines

Tolman [7] also devised a now widely accepted methodology to measure the relative π-acidity of a particular phosphine ligand. The π-acidity of a phosphine ligand has an effect upon π-acidic co-ligands coordinated to a metal atom. Because a phosphine with high π-acidity will accept more of the electron density from the metal, this lessens the available electron density shared between the other coordinated ligands bound to the same d-orbital. Synthesis of a number of phosphine metal-carbonyl species allowed Tolman to compare the relative π-acidity of the phosphine ligands by comparison of their IR spectra. As the electron density is removed from the metal by the phosphine ligand, the carbonyl ligands receive less back bonding from the metal. This has the effect of strengthening the C-O bond (the acceptor orbitals of CO are antibonding) shifting the A_1 band in the IR to a lower wave number in the IR spectrum. By comparison of the wavelength at which the A_1 band is observed, comparison of the relative π-acidity of different phosphine ligands can be made.

1.6   Sulphur chemistry

Sulphur exhibits oxidation numbers of -2, 0, +2, +4 and +6 and is most commonly seen in the sulphide ion, S^{2-}, and a typical compound is H_2S, hydrogen sulphide or hydro sulphuric acid. It has been widely used in coordination chemistry and homogeneous catalysis due to its extended valency of 2, 3, 4 and 6. Complexes range from monomeric sulphides to bridging polymeric structures. Applications of sulphur have focused around biological aspects where the oxidation properties of sulphur have been utilised.

1.6.1 Thiolates

There are many properties which make thiolates desirable ligands to study in co-ordination chemistry and homogeneous catalysis. Thiolates are generated by deprotonating their thiol counterparts in the presence of a base. The resulting thiolate is a very powerful nucleophile which drives complexation reactions. One of the most useful characteristics of thiolates is their ability to act as a σ-donor orbital and a lone pair orbital that is principally sulphur 3p in character. The lone pair orbital has the correct symmetry for π interactions with metal d orbitals (**Figure 1-9**). If the metal d-orbitals are formally occupied, the thiolate ligand may effectively act as a four electron donor $(2\sigma + 2\pi)$ [25].
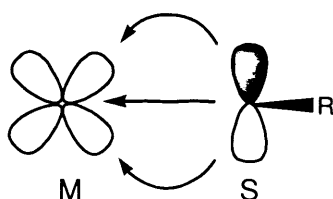
Figure 1-9: Thiolate orbital interactions with metal centres

Sulphur bridging species are well known, and *syn-anti* isomerisation proceeds via a bridge opening mechanism (**Figure 1-10**). Unidentate groups also are well known with mononuclear thiolates forming from ions such as: Zn^{II}, Cd^{II}, Mn^{II} and most commonly Fe^{II}. With their resemblance to proteins such as Desulphoredoxintype [Fe(Cys)₄], biological processes which contain thiolate linkages has increased the profile of this area of study.

syn   *anti*
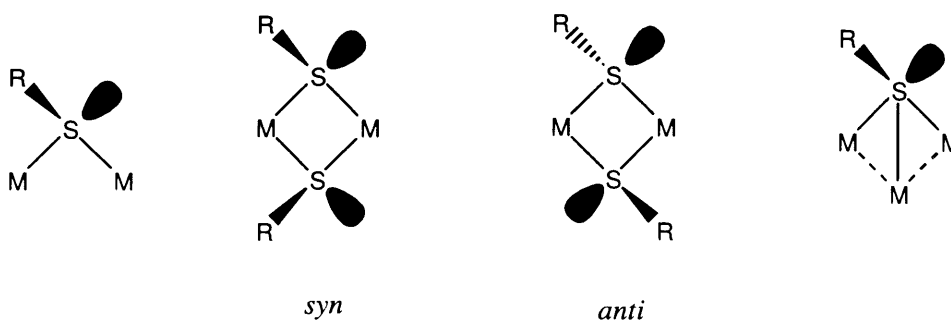
Figure 1-10: Main types of thiolate complexation

1.6.2 Thioethers

A thioether is a functional group in organic chemistry that has the structure R_2-S-R. They are relatively weak donors, but stronger binding occurs with chelating or macrocyclic thioethers. Thioethers have two lone pairs so that when one is involved in metal binding, complexes exhibit pyramidal inversion (**Figure 1-11**) of the metal-coordinated sulphur atom(s), rates and activation energies can be evaluated by total NMR bandshape analysis. $\Delta G^{\ddagger}$ values range between 45–56 kJ mol^{-1}, with chelating and bridging dithioethers, the stereochemical nonrigidity can be quite complicated.
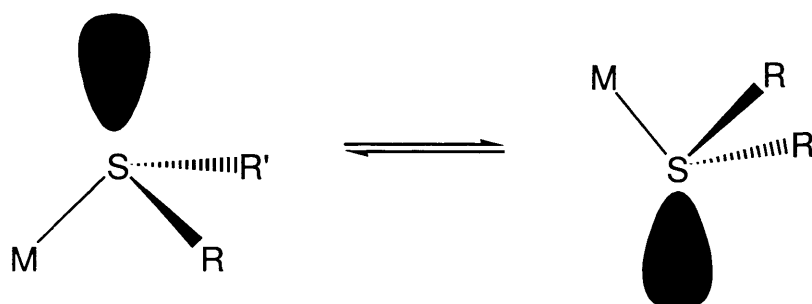
Figure 1-11: Geometry of a thioether showing the potential inversion and chirality

1.7 Mixed donor ligands

The first mixed donor ligand that utilised the effect of two different donating centres simultaneously was seen in the work of Mann and Watson [30]. Here they demonstrated the influence of two donor groups giving the chelate multifunctional properties. The chemistry of asymmetric ligands offers other significant possibilities, specific transformation of donor atoms can be carried out, potentially mirroring ligand reactivity in non-chelating complexes. Introduction of a second stereogenic centre can give different ligand donor properties through chelation on a metal which are not available with monodentate ligands. Due to their increased stability many metal centre studies can be made without the problem of competing ligand substitution reactions.

Multidentate ligands have not only shown ability in many areas of asymmetric catalysis where there is a need for more than one donor influence on selectivity. Another area of interest lies in hemilability where a ligand contains both a strongly binding donor centre and one weakly binding donor centre [40]. They can be used to

protect an active site at a metal centre until it is required to effect a transformation of a substrate.

1.8 Phosphinothiol ligands

The synthesis of phosphinothiols may seem to be a reasonably straight forward process, but it does present a number of challenges. Many simple thiirane precursor compounds are not commercially available, or even chemically well understood. This is often because they are highly unstable, the introduction of sulphur containing moieties brings with it the possibility of the unwelcome formation of phosphine sulphides and almost without exception, the compounds involved are difficult to manipulate being toxic, smelly and air-sensitive.

Synthetic methods for the formation of phosphinothiolate ligands can be summarised into three areas of study. A review was carried out finding the possible synthetic routes used in the formation of phosphinothiolates (**Table 1-3**). The review shows that the number of synthetic routes attempted was limited with a total of eleven different ligands formed for coordinating phosphinothiolate complexes. There has been reported a small number of phosphinothiolates formed as an intermediate in the formation of phosphinothioether ligands [41].

Each ligand has been categorised depending on their method of formation showing the trend of methods used over the last forty years. In a historic review we shall discuss the pros and cons of each type of synthesis and discuss the criteria used for the selection of our ligand synthesis.

Type of Synthesis	Ligand	Date	Reference
Ring-opening	$Ph_2PC_2H_4SH$	1965	[42]
Ring-opening	$MePhPC_6H_{10}SH$	1973	[43]
Electrophilic Substitution	$MePhPC_2H_4SH$	1986	[44]
Electrophilic Substitution	$Ph_2PC_3H_6SH$	1987	[45]
Electrophilic Substitution	$Ph_2PC_6H_4SH$	1989	[46]
Phosphite reduction	$Ph_2P(BINAP)SH$	1994	[47], [48]
Double Substitution	$CpFe[Ph_2PCpCH(Me)SH]$	1997	[49]
Ring-opening	$Ph_2PC_2H_3(CH_2OCH_2Ph)SH$	2002	[50]
Double substitution	$Ph_2PCpFeCpSH$	2002	[51]
Ring-opening	$Ph_2PC_2H_3\{C_6H_3(CH_3)[CH(CH_3)_2]\}SH$	2003	[52]
Ring-opening	$Ph_2PC_2H_3(Et)SH$	2003	[53]

Table 1-3: Review of phosphinothiol ligand synthesis

1.8.1 Ring opening of episulfides

Ring-opening reactions of thiiranes, [43] and to a lesser extent thietanes [140], are the preferred route for a majority of reactions for the synthesis of phosphino-thiolates. This is due to the process being a one-step regioselective reaction. Nucleophiles attack at the least sterically hindered site of the thiirane (Scheme 1-3). However this reaction does have its limitations, the attacking species must be a better nucleophile than the thiol formed on ring-opening, due to the ease of formation of poly(thioethers). This effect is also seen in reactive thiiranes where polymerisation can occur at ambient temperatures during formation or storage.

Another complication is the possibility of attack at sulphur rather than carbon. This is rare in the case of thiiranes, although alkyl- and aryllithium compounds can cause desulphurisation. However the initial attack at sulphur is the rule rather than the exception in ring-opening reactions of thietanes [140].
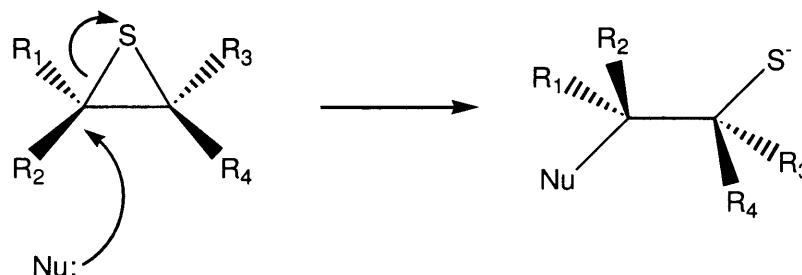
Scheme 1-3: Nucleophilic ring-opening of thiiranes

Chiral phosphines can be formed using prepared secondary organophosphides, depending on their counter ion they can change the ligands reactivity and solubility. The first recorded ring opening of an episulphide was pioneered by Geigy [42], who synthesised the first chelating phosphinothiolate ligand from ethylene sulphide (Scheme 1-4). This opened the door for a whole range of ligands [53] using the same methodology for thiiranes that are commercially available [43]. Hydrolysis of these ligands gave the resulting phosphino-thiol ligands along with an inert halide salt which plays no further part in the reaction. Compared to their phosphinothiolate counterparts, phosphino-thiols have greater stability which reduces the possibility of ligand oxidation or polymerisation.
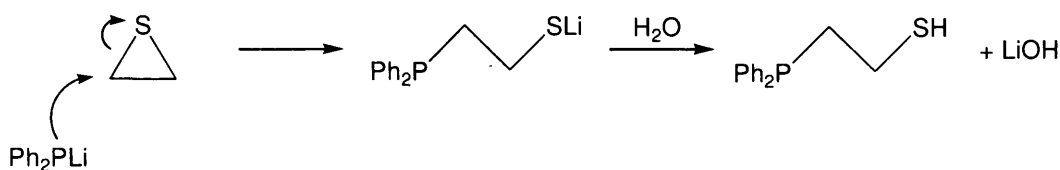
Scheme 1-4: The preparation of dppet by ring opening of ethylene sulphide

In the literature there have been reports of a number of commercially available thiiranes used in the manipulation of phosphinothiolates [43]. In terms of variety this does reduce the number of potential precursors, so synthetic routes have been found for the synthesis of these episulphides. Thiiranes may be stereo selectively synthesised from their corresponding oxiranes using different thiolating agents: phosphine sulphides [54], [55] (**Scheme 1-5**), benzothiazole-2-thiones [56], potassium thiocyanate [57] and thiourea [58], [59]. For all these methods a mechanism involving two Walden inversions, one for each oxirane carbon has been proposed, indicating for terminal chiral oxiranes, as in the case below, the stereochemistry of the resulting episulphide is opposite to that of the starting material.
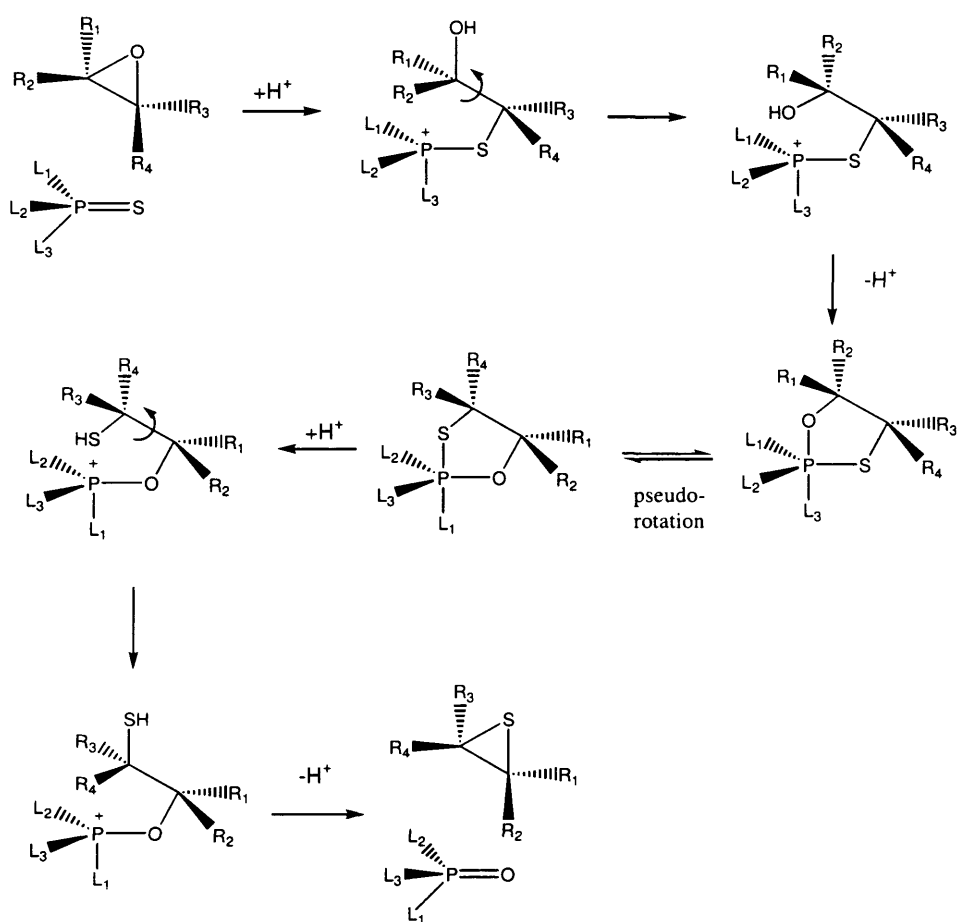
Scheme 1-5: Proposed reaction scheme for the conversion of an epoxide to the resulting episulphide

An example was reported by Brugat [50] where benzyl glycidyl ether was converted into the corresponding episulphide, benzyl thioglycidyl ether, using thiourea as the sulphur exchange agent. The thiirane was then reacted with potassium diphenylphosphide, a regioselective process where only the S_N^2 product was observed. The resulting phosphinothiol ligand has the opposite stereochemistry to the starting oxirane, but the same absolute configuration (S or R) due to a change in the C.I.P substituent order of precedence.

More recently synthesis using episulphides as precursors has moved towards chemically tuned ligands. A good example of this can be seen in the work of Duran [52] where he reported the synthesis of enantiopure complexes of group 10 metals. Through some simple organic synthetic reactions ligands are synthesised from low-cost commercially available substrates. Starting with a precursor of menthone a bulky, optically pure phosphinothiol is synthesised using potassium diphenyl phosphide followed by a water work up (**Scheme 1-6**). This synthetic mechanism can potentially be replicated to form other novel phosphinothiols using commercially available substrates.
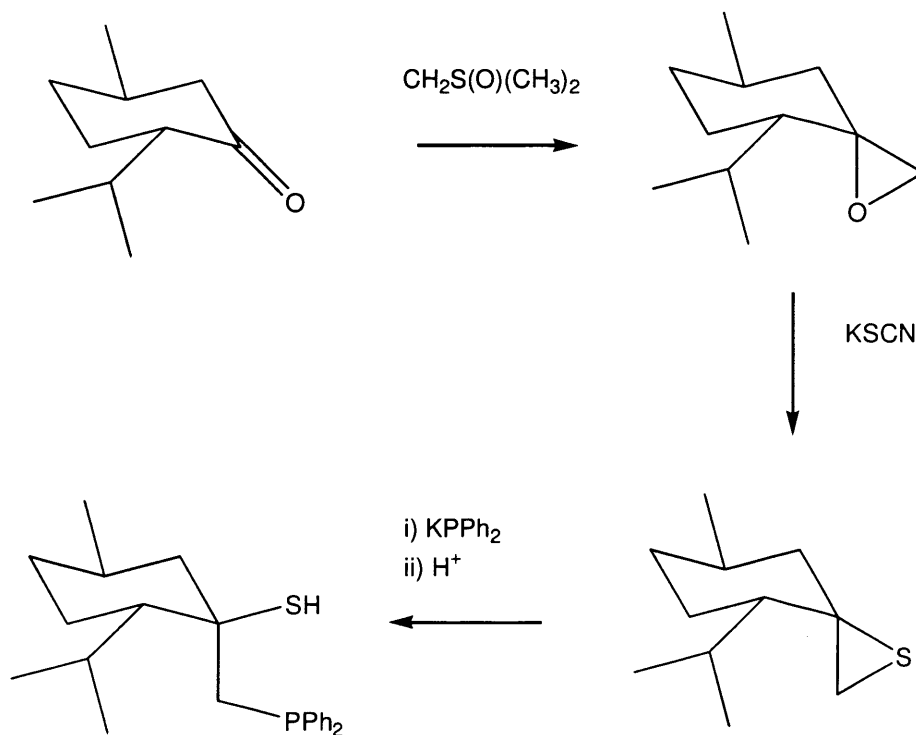
Scheme 1-6 Synthetic route of a phosphinothiol derived from (-)-menthone

1.8.2 Nucleophilic substitution

In the search for new ligands with no general synthesis available, a new form of synthesis was adopted by Block [46]. He reported a range of ligands being synthesised by *ortho*-lithiation-electrophilic substitution procedures. The systematic study of phenylene-bridged phosphinothiols had previously been hampered by the lack of a general preparative route until the discovery of *ortho*-lithiation of benzenethiol. The 2-lithiobenzenethiolate can be quenched with chloro-diphenylphosphine to give 2-(diphenylphosphino)benzenethiol (**Scheme 1-7**)
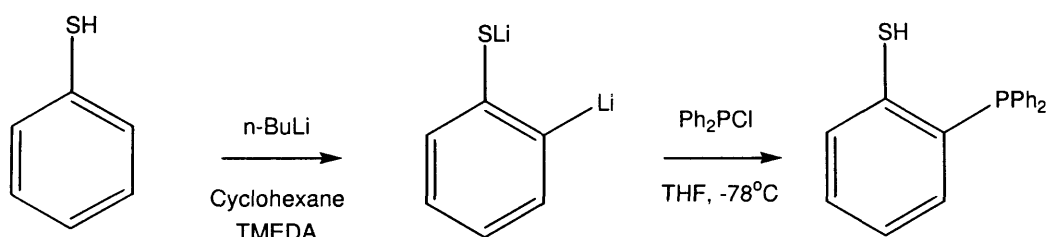
Scheme 1-7: Synthetic route for forming a new class of phosphinothiol ligands

Chirality in phosphinothiol ligands can be introduced in different ways. It can be achieved by means of the addition of a substituent in the chelate chain, as in the case of 1-methyl-2-(diphenylphosphino)ethane-1-thiol [60], or by the use of a phosphine group with different substituents, as in the case of 2-(phenylmethylphosphino)ethane-1-thiol [61], [44]. But in the both cases the resulting phosphinothiols were obtained as racemic mixtures.

It is fairly common that thiolate complexes contain phosphine moieties which, operating as ancillary ligands, are able to enhance the properties of interest. For this reason the chemistry of polydentate ligands with sulphur and phosphorus donor atoms in their frameworks has attracted increasing interest, augmented by the observations of unusual structures and reactivities in the resulting transition metal complexes [64]. They exhibit ligands which place phosphorous and sulphur in a *cis* configuration, and this should imprint electronic asymmetry on the metal centre to be transmitted to any *trans* groups.

1.8.3 Reduction of phosphinothiol oxides

Atropisomerically pure S-alkyl (R)-2-diphenylphosphino-1,1'-binaphthyl-2'-thiol derivatives have been synthesised through a multi-step reaction sequence starting from (R)-binaphthol [47]. The final step of the reaction sees the phosphine oxide sulphide deoxygenated with trichlorosilane / triethylamine to complete the synthesis (**Scheme 1-8**). This is the only example of a phosphinothiol being formed through the reduction of a phosphite such conditions are usually detrimental to a normally reactive ligand product.
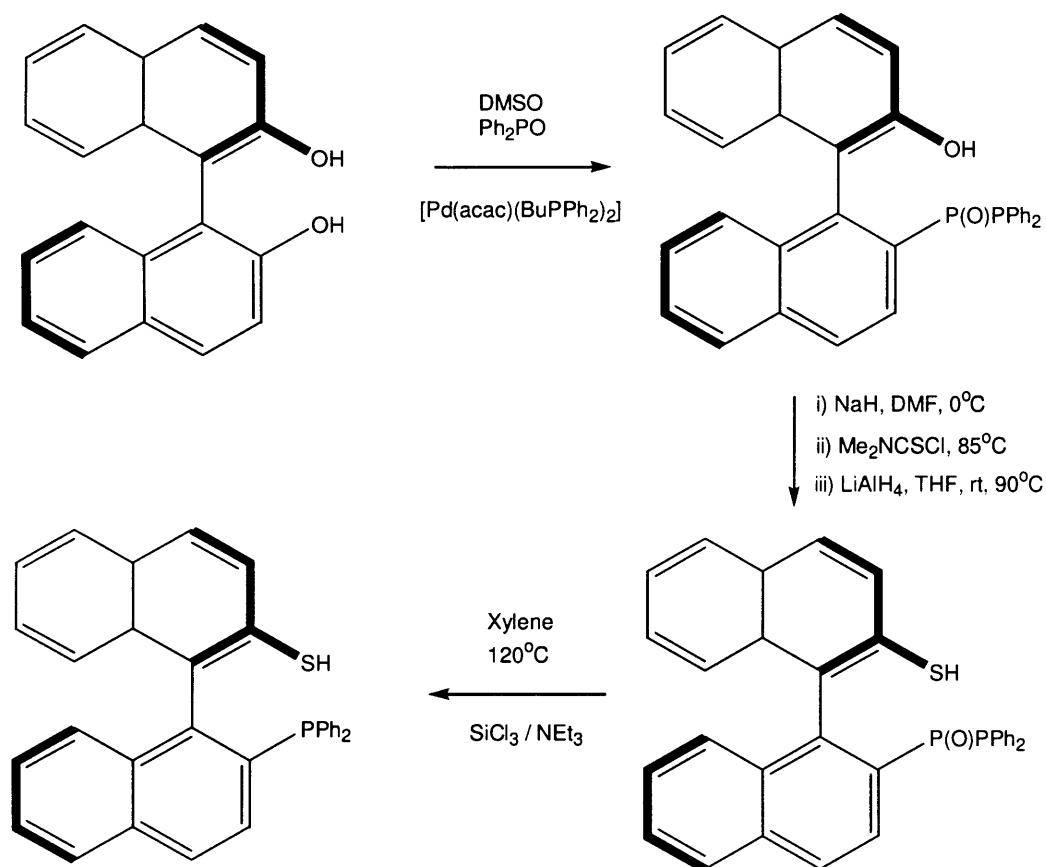
Scheme 1-8: Reduction of phosphine oxide to a phosphinothiol ligand

1.9 Phosphinothioether ligands

With the early development of phosphinothiol ligands in the mid 1960s it wasn't long before the development of phosphinothioethers was exploited and superseding that of the phosphinothiolates. The first reported phosphinothioether was done by Dyer and Meek in the form of a tetradentate ligand tris(o-methylthiophenyl)phosphane [84]. After phosphinothioethers were labelled to be less stable than the corresponding phosphine and arsines, Dyer and Meek decided to make a series of ligands containing As, P and S moieties. Comparisons show the relative stability of nickel complexes formed, opening the door for a whole range of phosphinothioether complexes to be exploited.

After synthesising the tetradentate ligand Dyer, Meek and Workman formed the first bidentate and tridentate phosphinothioether ligands [85]. The reaction scheme for all three ligands is shown below with the final step determining the ligand composition using primary, secondary or tertiary phosphides (Scheme 1-9). Two years after the synthesis of the first phosphinothioether ligand, Sieckhaus and Layloff reported a novel phosphinothioether ligand [86]. The bidentate ligand diethylphosphinoethyl ethyl sulphide (DPES) was synthesised by nucleophilic addition of 2-chloroethyl ethyl sulphide to sodium diethyl phosphide. DPES was synthesised in order to study the effects of phosphine and thioether linkages on the co-ordination number of nickel (II) halide complexes.
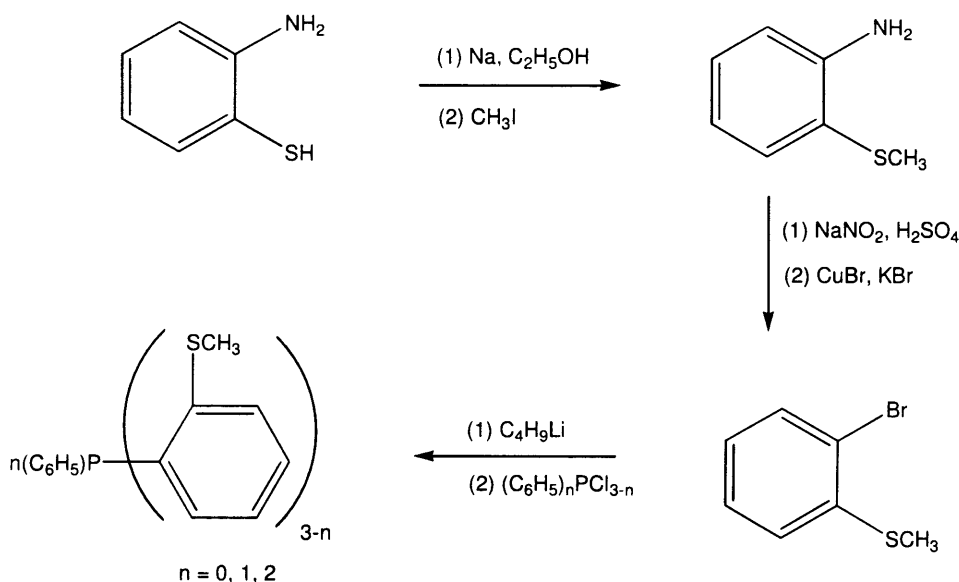
Scheme 1-9: Synthetic route for the first series of phosphinothioether ligands

This work was followed by the synthesis of 1-diphenyl-phosphino-2-methylthioethane using the standard method for that time by Ross and Dobson [87]. They also employed a new method via a Grignard synthesis (**Scheme 1-10**), similar to that employed by Mann and Miller in the preparation of a mixed nitrogen-phosphorus ligand [88].

Br + Mg → (Dry Ether) → MgBr

HPPh₂ + MgBr → (Dry Ether / Benzene) → Ph₂PMgBr + ——

Ph₂PMgBr + Cl⌐⌐⌐S → (Benzene) → Ph₂P⌐⌐⌐S + MgBrCl
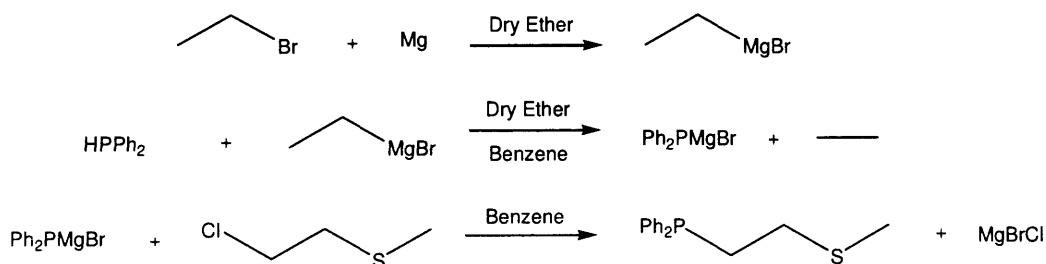
Scheme 1-10: Grignard synthesis of 1-diphenyl-phosphino-2-methylthioethane

For an extended period of time the interest in developing new phosphinothioether ligands was halted. It wasn't until the early 1990s that a new series of phosphinothioether ligands was formed using the standard methods (**Table 1-4**). These ligands had a range of different substituents on the sulphur moiety giving new electronic and steric effects [91], [41], [94].

Type of Reaction	Ligand	Date	Reference
Nucleophilic Substitution	$P(C_6H_4SMe)_3$	1965	[84]
Nucleophilic Substitution	$Ph_2PC_6H_4SMe$, $PhP(C_6H_4SMe)_2$	1967	[85]
Grignard reaction	$Ph_2PC_2H_4SMe$	1968	[86]
Nucleophilic Substitution	$Et_2PC_2H_4SEt$	1967	[87]
Ring-opening	$Ph_2PC_2H_3MeSR$	1999	[89]
Substitution (Bu-Li)	$(OC_6H_2Bu_2)_2PGlucoseCH_2SR$ R = Me, i-Pr, Ph	2000	[90]
Nucleophilic Substitution	$Ph_2PC_6H_4CH_2SR$, R = Et, Cy, $CH_2C_6H_7OHCHMe_2$	1995	[91]
Ring-opening	$Ph_2POMeC_2H_4(CHMe_2)SR$, $Ph_2POC_6H_{10}SBu$	2000	[92]
Double halide substitution	$Ph_2PCH_2C_6H_4SMe$	2002	[93]
Ring opening	$Ph_2PC_2H_3(Et)SH$	2003	[53]
Phosphite reduction	$Ph_2P(BINAP)SMe$, $Ph_2P(BINAP)S$ iso-Pr	1994	[47]
Electrophilic Substitution	$Ph_2PB_{10}H_{10}CH_2SH$	1997	[41]
Electrophilic Substitution	$CpFePh_2PCpCH(Me)S(glucose)$, $Ph_2PC_6H_4CH_2SCH_2C_6H_7OHCHMe_2$	1996	[94]

Table 1-4: Review of phosphinothioether ligand synthesis

In 1999 Hauptman developed a new strategy for the synthesis of chiral phosphinothioethers [89]. It was based on the opening of chiral non-racemic episulphides using phosphorus nucleophiles. The opening of thiiranes by phosphorus nucleophiles has been reported and in the case of terminal episulfides proceeds regioselectively to the less hindered site as described in the synthesis of phosphinothiolates. Subsequent quenching with reactive electrophiles leads to the corresponding phosphinothioether ligand (Scheme 1-11).
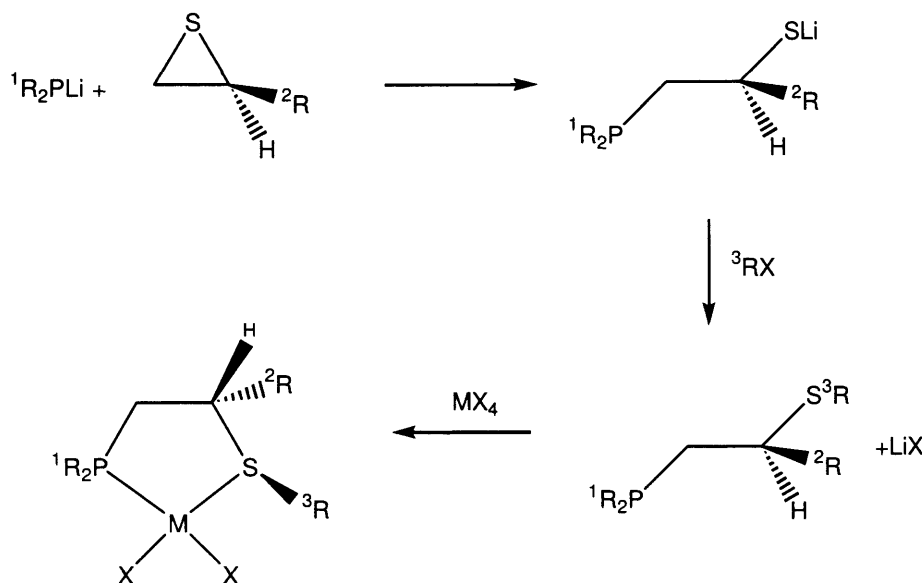
Scheme 1-11: Tuning ability of reacting electrophiles with pre-formed phosphinothiolates

The scheme above shows two nearly quantitative steps allowing chirality to be introduced to the ligand through three degrees of molecular diversity represented by ^1R, ^2R and ^3R. This approach seems to be adequate for controlling the synthesis and ease of adaptability (the first step is by-product free while the second step generates inert LiCl). Coordination of these groups of ligands to a metal centre places the modified sulphur, directly next to the metal where the key enantioselective step occurs. The presence of large groups on phosphorus make the phosphorus coordination site sterically more hindered. In addition, bulky groups both on the backbone and sulphur would cause ^2R and ^3R to be trans to each other upon ligand coordination, limiting the number of coordination modes of alkene substrate. Finally, the electronic differences between sulphur and phosphorus might lead to electronic effects that have found to be important in some cases for obtaining favourable enantiomeric excesses in such catalytic processes. All of the above arguments give us just cause in the preparation of these ligands. More examples using this new method of ligand synthesis can be seen in the work of Dervisi [53] and Evans [92].

1.10 Coordination chemistry of phosphinothiols

In comparison to the extent of phosphinothioether ligands, only a small range of phosphinothiolate ligands that have been reported, with a number of co-ordinated complexes to a range of transition metals. **Table 1-5** shows a review of publications with their respective ligands, dates and the period of time it has taken for these ligands to be fully researched. Furthermore we can identify that a limited number of large sterically demanding phosphinothioether complexes have been synthesised.

Complex Metal	Ligands	Date	Reference
Mo, Cr, W	$Ph_2PC_2H_4SH$	1975	[63]
Mo	$Ph_2PC_2H_4SH$	1979	[64]
Fe, Mn, Mo	$Ph_2PC_2H_4SH$	1980	[65]
Ir	$Ph_2PC_2H_4SH$	1983	[66]
Ti, Cu	$Ph_2PC_2H_4SH$	1985	[67]
Mo	$Ph_2PC_2H_4SH$	1999	[68]
Pd	$Ph_2PC_2H_4SH$	2000	[69]
Pd	$Ph_2PC_2H_4SH$	1984	[70]
Ni, Pd, Pt	$MePhPC_2H_4SH$	1986	[44]
Ti, Rh	$Ph_2PC_3H_6SH$	1987	[45]
Pd	$Ph_2PC_2H_4SH$, $Ph_2PC_3H_6SH$	1999	[71]
Ni, Pd, Pt	$Ph_2PC_2H_3(Et)SH$	2003	[53]
Pd	$Ph_2PC_2H_3(CH_2OCH_2Ph)SH$	2002	[50]
Au, Pd, Pt	$Ph_2PC_6H_4SH$	1994	[72]
Ir	$Ph_2PC_6H_4SH$	1995	[73]
Re	$Ph_2PC_6H_4SH$	1997	[74]
Re	$Ph_2PC_6H_4SH$	1998	[75]
Re	$Ph_2PC_6H_4SH$	1998	[76]
In	$Ph_2PC_6H_4SH$	1999	[77]
Mo	$Ph_2PC_6H_4SH$	2005	[78]
Ni, Pd, Pt	$Ph_2PC_6H_4SH$	2003	[79]
Ni, Pd	$PhP(C_6H_4SH)_2$	2002	[80]
Mo, W, Re, Fe, Ru, Os, Rh, Ir, Ni	$PhP(C_6H_4SH)_2$, $P(C_6H_4SH)_3$	1996	[81]
Au	$PhP(C_6H_4SH)_2$, $P(C_6H_4SH)_3$	2000	[82]
Ti	$P(C_6H_4SH)_3$	2005	[83]
Pd, Pt	$Ph_2PC_2H_3\{C_6H_3(CH_3)[CH(CH_3)_2]\}SH$	2003	[52]
Ni, Pd, Rh	$Ph_2PCpFeCpSH$	2002	[51]
Pd, Pt	$CpFe[Ph_2PCpCH(Me)SH]$	1997	[49]
Pt	$Ph_2CH_2P(S)Ph_2$	2004	[131]

Table 1-5: Review of chelating phosphinothiolate complexes

What is evident is the recent resurgence in the interest of phosphinothiolate complexes mostly due to their application in asymmetric catalysis. The first phosphinothiolate complex to be formed was that of group VI transitions metals with 2-(diphenylphosphino)ethanethiolate described by Doyle in the mid 1970s [63]. Over this time period interest was centred on the coordination chemistry of different combinations of ligands. With the development of crystal structure data, new complexes were needed for the study of interactions between donor ligands and metal centres. It was also the start of mimicking natural and enzymatic systems that spurred the next growth of phosphinothiolate complexes with discoveries that molybdenum was ligated by sulphur in iron-molybdenum proteins of nitrogenase [64].

The first reference to phosphinothiolates being linked catalysis was made in 1983 in the work of Stephan [66]. He referred to the involvement of thiolates and thioethers with respect to enzymatic and non-biological catalytic processes and the use of phosphine complexes in a variety of catalytic reactions. The development of these two fields led to the interest in mixed donor phosphorus-sulphur ligands. In 1985 Stephan again used the sulphur moiety to link two transition metals together forming a heterobimetallic species [67]. This formed the first sulphur bridging phosphinothiolate complex, binding titanium and copper in close proximity.

After following the development of the earliest chelating P, S ligand complexes we now turn our attention to the most extensively studied phosphinothiolate ligand. 2-(diphenylphosphino)thiobenzene ligand was first prepared along with a series of aromatic P, S ligands in the late 1980s. It wasn't until 1994 that a range of transition metals complexes were synthesied for a number of industrial applications [72]. With the interest of the biomedical industry, inorganic complexes were beginning to find application in the clinical market. Complexes of platinum gained attention with the development of treatments of throat and prostate cancer. Cisplatin is the leading example with it becoming a leading anti-cancer drug in the early 80s. The use of gold complexes as an antiarthritic drug was also coming to the attention of scientists. The formation of these complexes was being led by Dilworth with complexes of rhodium, iridium [73] and rhenium [74] being reported in the following years and his work was extended by Sousa and his group in the coordination of more rhenium [76] and indium [77] complexes.

An interesting communication was reported by Real [69] where he discovered a previously synthesised palladium bis-chelate complex Pd(Ph$_2$PC$_6$H$_4$S)$_2$, when dissolved resonated between *cis/trans* equilibrium (**Figure 1-12**). Phosphinothiolate bis-chelate complexes predominantly take a *trans* orientation due to the bulky diphenylphosphino-group being in close proximity in the *cis* form. In this case the *cis* form was isolated, characterised and reported for the first time.
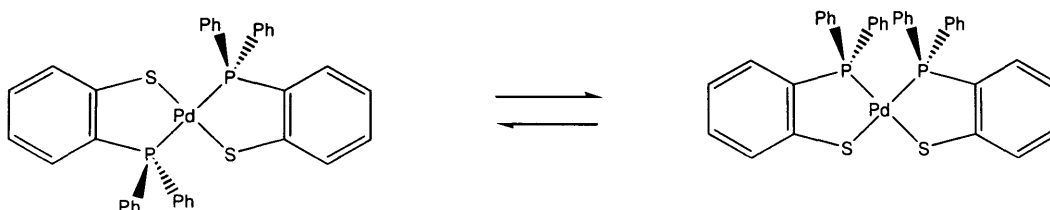
Figure 1-12: Chemical equilibrium of the inter-converting palladium bis-chelates

1.11 Phosphinothioether coordination

In the early development of phosphinothioether complexes Meek and Dyer formulated complexes of nickel and compared them to those formed with an arsenic donor atom. With the collaboration of Workman, a series of complexes were synthesised using their ligands: *o*-methylthiophenyldiphenyl-phosphine (SP), bis(*o*-methylthiophenyl)phosphine (DSP) and tris(*o*-methylthiophenyl)phosphine (TSP). The behaviour between the d^8 metal ions, palladium (II) and nickel (II) were studied, with regard to the types of complexes formed. In addition they studied the different coordinating properties of sulphur, phosphorus and arsenic in structurally similar polydentate ligands. In the final series of phosphinothioether ligands Dyer and Meek formed complexes of cobalt using ligands containing sulphur, selenium and arsenic. During the early development of phosphinothioether complexes the coordination chemistry of a small number of ligands were reported due to their limited applications.

It was not until 1975 that Doyle discovered another route to synthesising phosphinothioether complexes [63]. He performed a reaction between chromium, molybdenum and tungsten phosphinothiolate complexes and methyl or allyl halides to generate the corresponding thioether complexes. This approach of forming thioether complexes using alkyl halides was extended in the research of Roundhill [97], [98], [70], studying the equilibrium and conversion of palladium methylthioether complexes into their corresponding palladium phosphinothiolate complexes.

Complex Metal	Ligands	Date	Ref
Ni	$P(C_6H_4SMe)_3$	1965	[84]
Pd	$Ph_2PC_6H_4SMe$, $PhP(C_6H_4SMe)_2$, $P(C_6H_4SMe)_3$	1967	[85]
Ni	$Ph_2PC_6H_4SMe$, $PhP(C_6H_4SMe)_2$	1967	[95]
Co	$Ph_2PC_6H_4SMe$	1967	[96]
Ni	$Et_2PC_2H_4Set$	1967	[86]
Cr, Mo, W, Mn	$Ph_2PC_2H_4SMe$	1968	[87]
Cr, Mo, W	$Ph_2PC_2H_4SMe$, $Ph_2PC_2H_4SCH_2CHCH_2$	1975	[63]
Pd	$Ph_2PC_6H_4SMe$	1979	[97]
Pd	$Ph_2PC_6H_4SMe$	1980	[98]
Pd	$Ph_2PC_6H_4SMe$	1984	[70]
Pt	$Ph_2PC_6H_4SMe$	1986	[99]
Pd, Rh	$Ph_2P(BINAP)SMe$, $Ph_2P(BINAP)S(i-Pr)$	1994	[47]
Rh	$Ph_2PC_6H_4SMe$, $Ph_2PC_2H_4SMe$	1995	[100]
Pd	$Ph_2PC_6H_4CH_2SR$, R = Et, Cy, $CH_2C_6H_7OHCHMe_2$	1995	[91]
Pd	$PhP(C_2H_2)(CH_2CHCMeCMe)SPh$	1996	[101]
Pd	$CpFePh_2PCpCH(Me)S(glucose)$, $Ph_2PC_6H_4CH_2SCH_2C_6H_7OHCHMe_2$	1996	[94]
Pd	$CpFePh_2PCpCH(Me)S(glucose)$, $Ph_2PC_6H_4CH_2SCH_2C_6H_7OHCHMe_2$	1996	[102]
Rh, Ir, Pt	$CpFePh_2PCpCH(Me)S(glucose)$, $Ph_2PC_6H_4CH_2SCH_2C_6H_7OHCHMe_2$	1997	[103]
Pd	$Ph_2PC_6H_4S(C_5O_4)$	1997	[104]
Pd, Rh	$Ph_2PC_2H_3MeSR$	1999	[89]
Ir	$(OC_6H_2Bu_2)_2PGlucoseCH_2SR$ R = Me, i-Pr, Ph	2000	[90]
Pd	$Ph_2PC_2H_4SMe$	2000	[105]
Pd, Rh, Ir	$Ph_2POMeC_2H_4(CHMe_2)SR$, $Ph_2POC_6H_{10}SBu$	2000	[92]
Pd, Rh, Ir	$Ph_2POMeC_2H_4(CHMe_2)SR$, $Ph_2POC_6H_{10}SBu$	2002	[106]
Pd	$PhPC_2H(CN)[SCHC(Me)C(Me)]$	2002	[134]
Rh, Ir	$Ph_2PB_{10}H_{10}CH_2SH$	2002	[107]
Pd, Rh	$Ph_2PC_2H_4SC_6H_4OC_2H_4PPh_2$	2002	[108]
Pd	$Ph_2PCH_2C_6H_4SMe$	2002	[93]
Pd	$Ph_2PC_2H_3(Et)SMe$	2003	[53]

Table 1-6: Review of chelating phosphinothioether complexes

1.12 Catalysis

Chiral chelating ligands find wide applications as auxiliaries in a variety of organic transformations. In particular diphosphines have been shown to be effective in catalytic reactions such as hydrogenations [8], [9], carbonylations [10], [11], [12], hydroformylations [113], allylic substitutions, C-C [114] and C-N [115] coupling reactions.

Chelating chiral diphosphines are classical ligands extensively used in metal-catalysed enantioselective processes [16]. Besides the asymmetry introduced by the chelate ring, many of these diphosphines have two donor atoms with similar electronic and steric properties (e.g. DIOP [17], BINAP [18]). In order to decrease the symmetry of the bidentate ligand, diphosphines with different substituents at each phosphorus have been synthesized (DIPAMP [19]), and some chemical changes have been introduced (BINAPHOS [20]). In this case, electronic differences between the two donors may control reaction selectivities via operation of the *trans* effect and *trans* influence. In addition, steric differences between the two co-ordination sites of the chelate can control the catalyst regioselectivity by accommodation of the more bulky side of the participating ligand adjacent to the least hindered side of the chelate.

DIOP

DIPAMP

BINAP

BINAPHOS
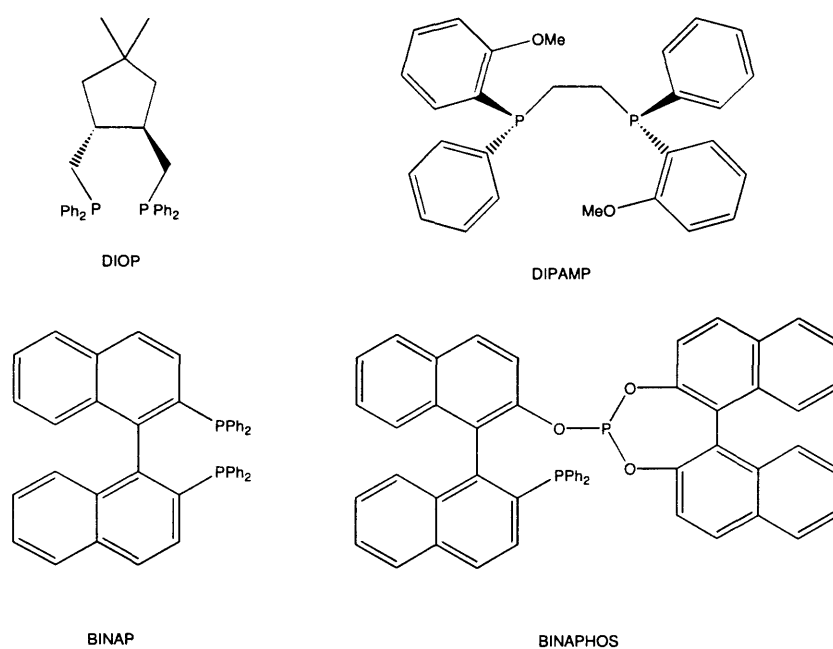
Figure 1-13: Structures of phosphine ligands

Sulphur is often talked about as being a poison of catalysts, arising from its passivation of many platinum-metal based heterogeneous catalyst systems, especially in the petrochemical industry, by the formation of various sulfide phases. However homogeneous catalysis have different requirements of reactivity and, as seen, homogeneous catalysis systems containing sulphur can display enhanced activity compared with more traditional systems [21], [22], [23], [24].

Reports in the literature have shown sulphur complexes to be in the form of thiolato-bridged complexes of palladium or platinum and demonstrating an enhanced

45

catalytic activity for allylic aminations [26], and alkylations [27], [28]. Recent reports point to the particular nature of catalytic carbonylation systems that incorporate thiolato ligands. Aminothiolato complexes of palladium with triphenylphosphine catalyse the conversion of styrene to 2-phenylpropionic acid in high yield and excellent regioselectivity [29].

In recent years, however, there has been great interest in developing chiral bidentate systems as suitable candidates for catalytic precursors where only one of the donor atoms is phosphorus. Catalytic precursors have been recently developed using chiral bidentate systems where only one of the donor atoms is phosphorus. For example, mixed P, O [31], [32] and P, N donor [36] ligands have been exclusively applied in catalysis with respect to closed chelating systems. Phosphino-oxazolines in particular have found applications that cover a wide range of catalytic processes; hydroboronations [33], allylic aminations [34], allylic alkylations [35], [36] and substitutions [37], [38], [39].

The development of P, S donor ligands for catalytic applications has also been of interest recently, it was thirty three years after the synthesis of 2-(diphenylphosphino)ethanethiol when Polo and Real [69] used the same ligand for applications in enantioselective catalysis (Scheme 1-12). The key elements for phosphinothiol selection were their steric asymmetry and differing electronic influences of the ligand coordination sites, with key intermediates that control the stereochemistry of the products of reactions that are thought to be dependent on two adjacent coordination sites, such as catalytic palladium mediated carbonylations.
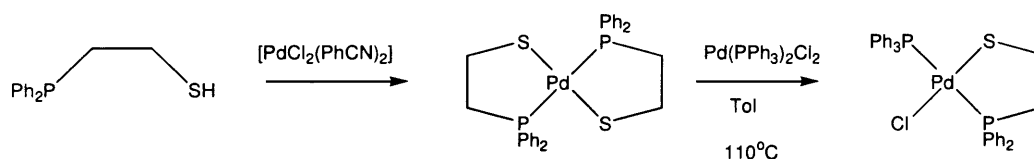
Scheme 1-12: Formation of a palladium complex used for carbonylation reactions

Finally the interest in phosphinothioether ligands was somewhat slow until the early 1990s where palladium allyl phosphinothioether complexes were shown to have potential application to the catalytic allylic alkylations [91]. Reports on catalytic reactions using phosphinothioether ligands are scarce partially owing to fear of metal poisoning by sulphur. The use of these ligands has been reported for the carbonylation of methanol [100], the reduction of ketones by hydrogen transfer [47], [109], and the hydroformylation of

styrene [47]. Pregosin has synthesised and structurally characterised a number of metal complexes bearing chiral P, S-donor ligands In particular, palladium complexes with ligands such as 2,3,4,6-tetra-O-acetyl-1-[(diphenylphosphino)benzyl]thio-D-glucopyranose and were shown to carry out allylic alkylation [94], [102], [103].

1.13 Aims of the project

Using the information gathered from literature sources we concluded that there has been limited research for the development of phosphinothiolate and phosphinothioether ligands and their relating complexes thus far. Although studies of simple backboned phosphinothiolate complexes have been carried out, the same efforts have not been made at developing novel ligands of the same class. Two areas have been identified for further study, the first being a lack of conformationally confined ligands, limiting the relative positioning of the coordinating sulphur and phosphorus moieties. The second being the development of high molecular weight ligands, due to the ease of synthesis using simple commercially available substrates the size of P, S ligands has been limited to simple backboned ligands which have little influence of the coordinated metal centre.

It is our aim to synthesise two phosphinothiolate ligand backbones with contrasting appearances, the first being synthesised using a simple commercially available substrate with a confined backbone leaving the coordinating functional groups with limited flexibility. The second ligand is to have a more intricate backbone, created using a number of synthetic steps, to enable the ligand to have an influence on any coordinated species.

L¹H   L²H
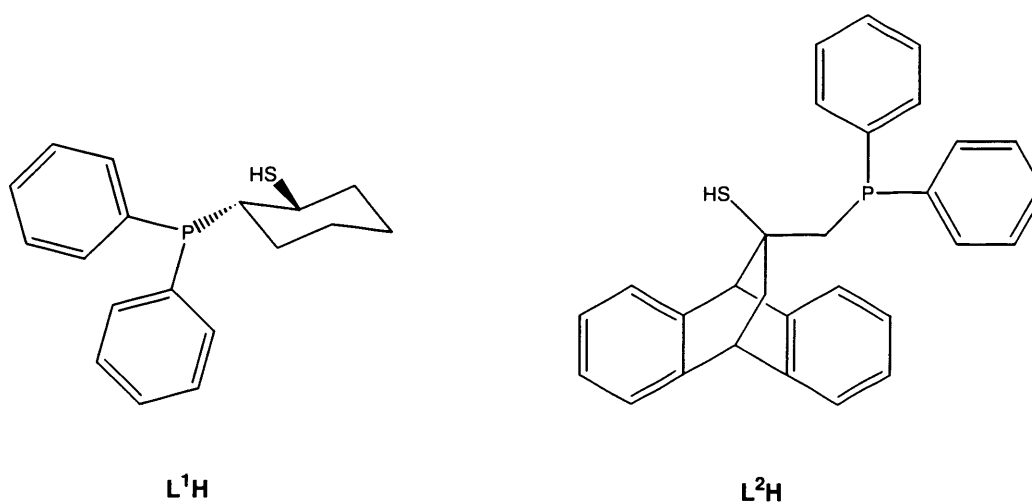
Figure 1-14: Structures of ligands L¹H and L²H

47

Using a strategy developed by Hauptman [89] we would then convert the resulting phosphinothiolate ligand into a series of phosphinothioether ligands via a simple one-step nucleophilic substitution. The number of possible halide precursors is limitless, we concluded that using electron donating substituents would increase reactivity due to the more stable intermediate and give higher yields for ligand synthesis. Our second criterion for selecting halides was made by varying and comparing relative steric properties. We wanted to study whether the size of substituents on the thioether moiety would induce electronic and steric constraints on the coordinated species.

Chapter 2 Ligand synthesis

2.1   Phosphinothiol ligands

Of the various mixed donor ligands the study of phosphorus and sulphur centred bidentate ligands are especially interesting. Both phosphorus and sulphur are excellent ligand donor atoms for a wide range of metals, while the low ionisation energy of sulphur and the existence of several lone pairs of electrons offer the possibility of a vast sulphur based chemistry of complexes.

After the literature review of synthetic routes for phosphinothiols we came to the conclusion that ring opening of episulphides would provide the best opportunity to form our sterically diverse ligands. This is followed by conversion into a series of phosphinothioethers through classical nucleophilic substitutions which could be achieved irrespective of the ligands steric differences.

2.1.1   Synthesis of 2-(diphenylphosphino)cyclohexanethiol L^1H

Herein we report the synthesis and stereochemical analysis of phosphinothiol L^1H (**Figure 1-1**). Using a racemic starting material with two chiral centres one would expect up to four stereoisomer structures being synthesised. The advantage of using a conformationally confined backbone is that they can limit the number of possible stereoisomers formed. The starting cyclohexane sulphide has an episulphide ring which can only be accommodated in an equatorial position on the cyclohexyl substituent due to geometric constraints. Due to the S_N^2 type addition of diphenyl phosphine the ligand species adopts a *trans* position with respect to the sulphur moiety. This again limits the number of stereoisomers possible for synthesis.

L^1H
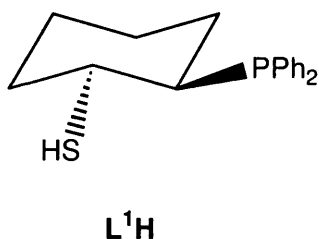
Figure 2-1: Diagram of 2-(diphenylphosphino)cyclohexanethiol L^1H

The racemic phosphinothiolate ligand L^1Li was prepared as a representative example for this class of ligand, the reaction sequence for its synthesis is shown in **Scheme 2-1**. Due to the conformationally confined starting material there are two

49

possible forms of cyclohexene sulphide with the episulphide positioned in the equatorial position. Therefore when nucleophilic addition by lithium diphenylphosphide occurs the resulting enantiomers are formed. These enantiomers are non-distinguishable by NMR spectroscopy therefore only one compound would be observed.
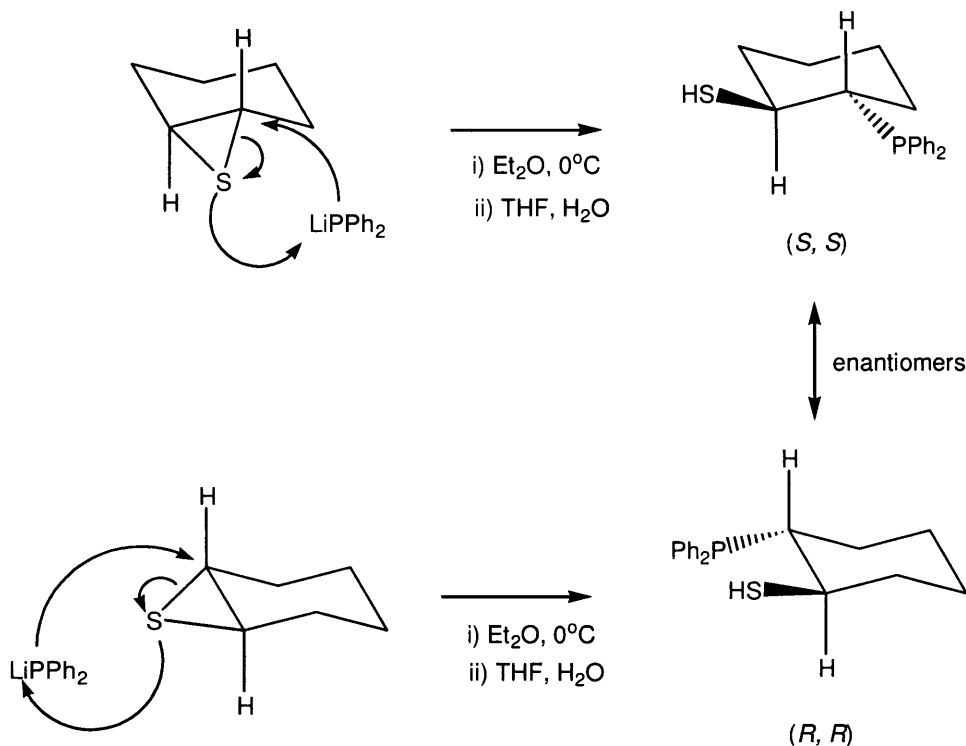
Scheme 2-1: Formation of 2-(diphenylphosphino)cyclohexanethiol L^1H

Subsequent reaction of cyclohexene sulphide with lithium diphenylphosphide followed by hydrolysis via a water work-up afforded the required phosphinothiol L^1H in reasonable yield (76%). Excess of diphenylphosphine was removed by subsequent washings with diethyl ether to give the phosphinothiolate as a fine white powdery solid. In deuterated degassed chloroform a ^1H NMR spectrum of L^1H shows the expected observation of one isomer due to the spectroscopic equivalence of enantiomers. The spectra consisted of eleven protons in the saturated hydrocarbon region representing the thiol and cyclohexyl backbone and ten protons in the aromatic region for the diphenyl phosphino- group. The resulting ligand is air sensitive and ^{31}P $\{^1H\}$ NMR shows a sharp singlet at δ_P -6.3, the oxidised form of the ligand is distinctively visible at δ_P 22.0.

2.1.2 Synthesis of 9, 10-ethanoanthracene-2-diphenylphosphino-1-ethanethiol, 9-10-dihydro, L^2H

With a design based on an anthracene precursor, we utilised the ability of anthracene to form bridging compounds via a Diels-Alder addition. To give the proposed ligand a degree of flexibility the P, S moieties are connected using an ethylene bridge forming a chiral centre (**Figure 2-2**). This Diels-Alder reaction proceeds using elevated temperatures as anthracene is more reactive with a higher electron affinity than that of benzene and naphthalene.

L^2H
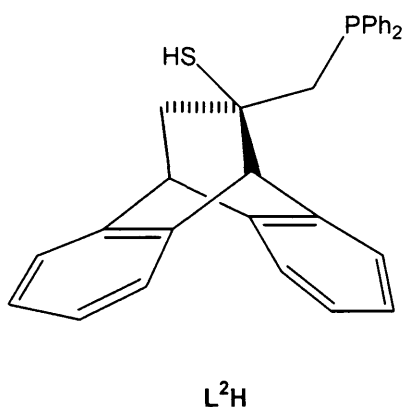
Figure 2-2: Diagram of 9,10-ethanoanthracene-2-diphenylphosphino-1-ethanethiol, 9-10-dihydro, L^2H

The racemic ligand L^2H was prepared from anthracene in a seven-step synthesis according to **Scheme 2-2**. The first step of the synthesis is a Diels-Alder reaction of anthracene with butyl acrylate at 170°C to give 9, 10-ethanoanthracene-11-carboxylic acid, 9-10-dihydro, butyl ester **1** in good yield (94%) with no further purification needed. Alcohol **2** was easily formed from the reduction of ester **1** using lithium aluminium hydride keeping a steady reflux by the drop-wise addition of the dissolved precursor. This white crystalline solid was converted to its corresponding bromide **3** giving a by-product of triphenyl phosphine oxide that was separated with a crude column using 9:1 petroleum ether: ethyl acetate solution giving reasonable yields (62%).
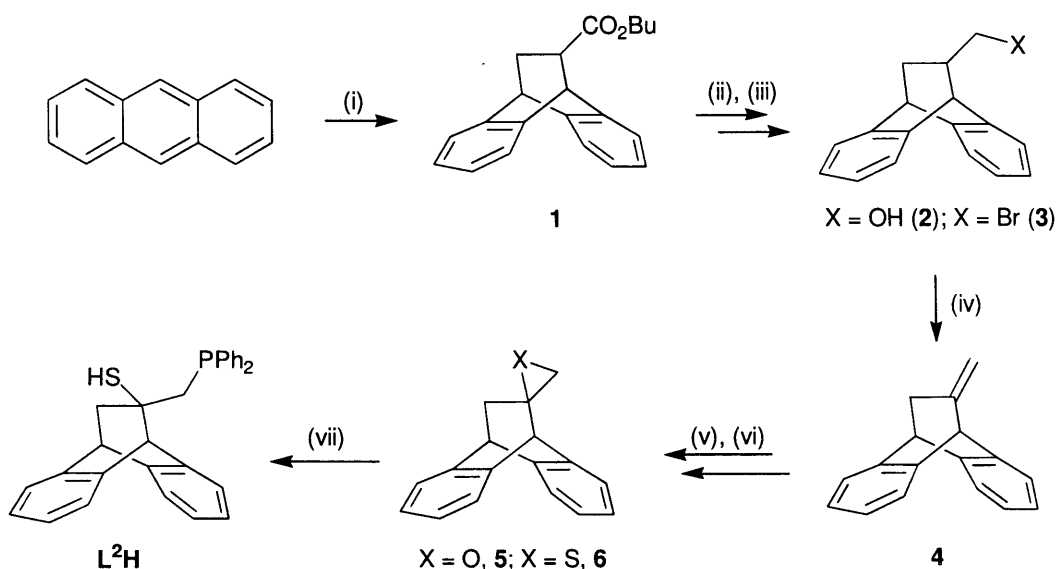
Scheme 2-2: Seven step synthesis of ligand **L²H** Reagents and conditions: (i) butyl acrylate, 170°C, 24h; (ii) LiAlH₄, ether, rt, 2h; (iii) CBr₄, PPh₃, imidazole, 80°C, 24h; (iv) DBU, 140°C, 24h; (v) chloroperbenzoic acid, HCCl₃, 0°C, 24h; (vi) SC(NH₂)₂, methanol, rt, 72 hours; (vii) KPPh₂, THF, 0°C, 1h, H₂O

Bromide **3** was reduced to alkene **4** by heating a solution of compound **3** with diazabicyclo [5.4.0] undec-7-ene (DBU) at 140 °C. The salt by-product was removed by column chromatography with the same solvent system giving the alkene pure in good yields (60-80%). Novel epoxide **5** was formed by the reaction alkene **4** with chloroperbenzoic acid, which gave the best yields at low temperatures (0°C). Washing the compound with a sodium hydroxide solution (10%) removed excess acid leaving the epoxide **5** as a white crystalline solid. Compound **5** was transformed into the corresponding episulphide **6** (Spiro[9, 10-ethanoanthracene-1-2-thiirane] 9-10-dihydro) using thiourea [58], [59]. This reaction was somewhat slow, even when using a large excess of the sulphur transfer agent. The reaction yields were moderate (50-75%), but as the reagents are easily available the reaction was still convenient. Regioselective ring opening of the thiirane **6** with one and a half equivalence of KPPh₂ followed by a water work-up gave ligand **L²H** in good yield (75%) and purity. For industrial applications this reaction mechanism is not as suitable as the previously synthesised ligand **L¹H** with the large number of synthetic steps leading to an overall yield of less than 10%. Potassium diphenyl phosphide is a commercially available substrate and was chosen in preference to that of the lithium counterpart. The larger potassium counter-ion causes the resulting ligand to precipitate out of solution and therefore leaving no requirement for washing. The novel phosphinothiol proved to be unstable in air with the tertiary phosphine oxidising. Compounds **1-6** were structurally characterised in solution by NMR spectroscopy. Reaction progress was monitored using ¹H NMR spectroscopy following

the shift in characteristic bridgehead protons (H^9, H^{10}) ranging from δ_H 3.55-4.64 (**Table 2-1**). In compound L^2H, the methylene protons (H^{13}, H^{14}) near the phosphine are diastereotopic showing a $^2J_{HP}$ coupling constant with the phosphorus atom, seen in the ^1H NMR spectrum. The phosphorus NMR spectrum of L^2H shows a single sharp resonance at δ_P −23.0. The ligand proved to be stable towards sulphur transfer from the tertiary carbon to the phosphorus [52].

Compound	$\delta_H{}^9$	$\delta_H{}^{10}$
1	4.60	4.27
2	4.34	4.17
3	4.40	4.20
4	4.64	4.26
5	3.62	4.27
6	3.57	4.28
L^2H	4.57	4.23

Table 2-1: Characteristic ^1H NMR signals of bridgehead protons H^9 and H^{10} for compounds **1-6** and L^2H

2.2 Phosphinothioether synthesis

In the past years there have been a number of coordinated dialkyl sulfides complexes with relatively little studied due to the instability of many of the complexes formed. The generation of chelates with greater stability has allowed many complexes to be successfully prepared and studied, as we have discussed in Chapter 1.

Phosphinothioether ligands generally have an advantage over their phosphinothiolate counterparts having added steric bulk in the region of catalytic activity. On complexation an extra degree of chirality is introduced into the molecule, the sulphur centre becomes chiral on complexation which is placed directly next to the metal where the key enantioselective step occurs. This combined with the presence of large groups on phosphorus, make the phosphorus coordination site sterically more hindered. In addition, bulky groups both on the backbone and sulphur would cause bonded alkyl groups and the carbon backbone to be *trans* to each other upon ligand coordination, limiting the number of coordination modes. Finally, the electronic differences between sulphur and phosphorus might lead to electronic effects that have been found to be important in some cases for obtaining favourable enantiomeric excesses in catalytic processes [119]. All of the above arguments give us just cause for the preparation of these ligands.

2.2.1 Synthesis of 2-(diphenylphosphino)cyclohexanethioether L^1R ligands

In the literature there have been a number of examples phosphinothioether ligands where the starting material is the corresponding phosphinothiolate ligand [41], [47], [53]. Such a route of synthesis gives us the opportunity to fine tune the corresponding ligands by easily changing the steric and electronic properties of the thioether moiety. Following the synthetic route proposed by Hauptman [89] we propose the systematic synthesis of a number of sterically diverse phosphinothioether ligands L^1R (**Scheme 2-3**).

LiS ⟍PPh₂ + RX ⟶ RS ⟍PPh₂ + LiX
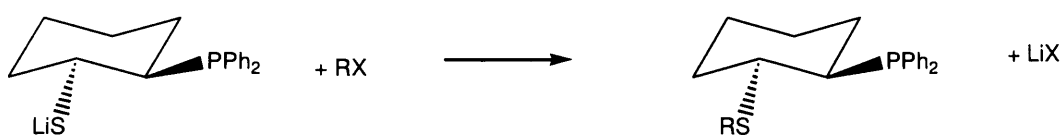
Scheme 2-3: Reaction scheme of the tuning ability of reacting electrophiles with performed phosphinothiolates.

The selection of halides for such a classical nucleophilic substitution is done keeping in mind their reactivity to ensure elevated temperatures are not required, which would result in the decomposition of targeted phosphinothioethers. For the first synthesis we decided to use the least sterically hindered halide compound to combine with our phosphinothiolate ligand L^1Li. To increase the likelihood of nucleophilic attack we selected benzyl bromide for our initial reactions, due to its increased activity and the electron donating ability of the benzyl substrate. Synthesis of phosphino-thioether L^1Bn was prepared in one step from the reaction of phosphinothiolate L^1Li dissolved in THF followed by the drop-wise addition of benzyl bromide (**Scheme 2-4**).

LiS ⟍PPh₂ + [benzyl bromide] ⟶ (THF) ⟶ [product] PPh₂ + LiBr
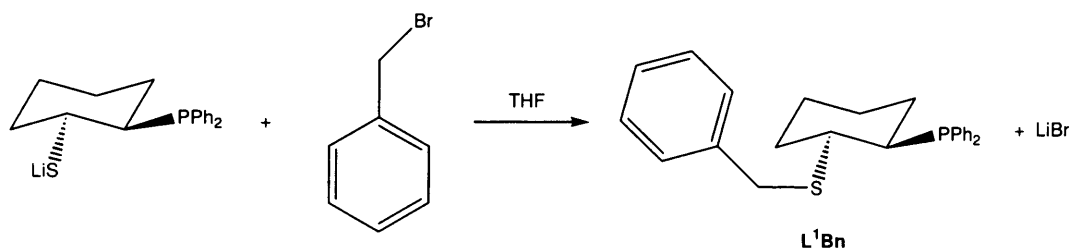
L^1Bn

Scheme 2-4: Reaction scheme of the formation of phosphinothioether ligand L^1Bn

After one hour a ${}^{31}P$ NMR spectrum of L^1Bn revealed a single sharp resonance at δ_P -11.7. To confirm the completion of the reaction a ${}^1H$ NMR spectrum shown the presence of two protons in a region of the spectrum characteristic of benzylic protons.

54

These benzylic protons were shifted from that of benzyl bromide to δ_H 3.56 showing the addition of the benzyl group forming the desired phosphinothioether L^1Bn. The increased proton integration in the aromatic region of the spectrum gave further evidence of the addition of the thioether moiety. As we have previously seen for phosphinothiol ligand L^1H, one preferred isomer of the free phosphinothioether ligand L^1Bn is observed using spectroscopic analysis. This method does have its drawbacks with the formation of a by-product which can influence resulting complexes (Chapter 5).

After the successful synthesis of L^1Bn using an aryl methyl bromide we decided to use the less reactive methyl aryl chlorides for the nucleophilic addition step. This revised method would produce a by-product of LiCl which could be removed through an aqueous work-up. The systematic synthesis of phosphinothioether ligands was carried out using benzyl chloride, 1-chloromethyl naphthalene and 9-chloromethyl anthracene (Scheme 2-5).
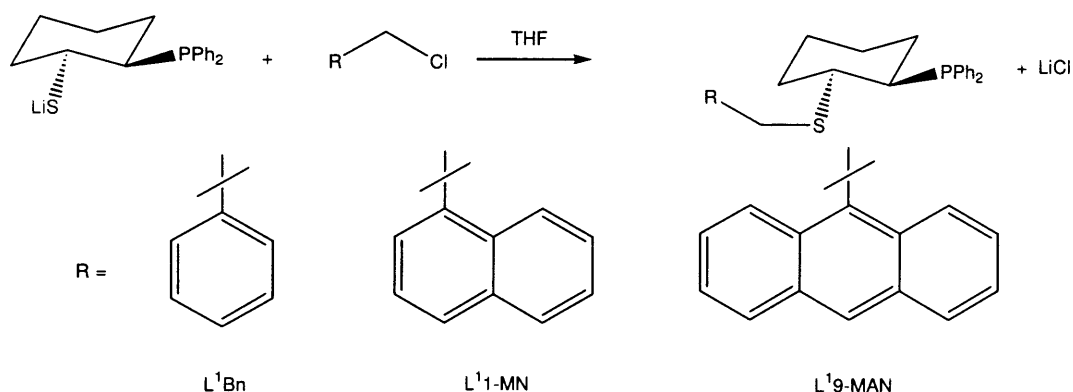
Scheme 2-5: Reaction scheme showing the formation of phosphinothioether ligand L^11-MN

This method resulted in the formation of phosphinothioether ligands L^1Bn, L^11-MN and L^19-MAN after washing giving good yields. All spectroscopic data were recorded using ligands dissolved in deuterated degassed chloroform. Single peaks were observed in the ^{31}P NMR spectra for all ligands in the region δ_P -11.8. ^1H NMR spectroscopy reveals the presence of benzylic, methyl naphthalene and methyl anthracene thioether moieties in the CH_2 and aromatic region. ^{13}C NMR data shows a total of seven signals in the saturated region of the spectra indicating addition of the thioether moieties for all ligands. The final ligand synthesis modification relates to the halide addition step. For early ligand synthesis reactions benzyl chloride and 1-methyl naphthalene were added directly to the reaction through a syringe, therefore leading to

less control over halide addition. To rectify this control all halides were diluted to a standard concentration using the preferred solvent of THF before being transferred to the reaction mixture.

2.2.2 Synthesis of 9, 10-ethanoanthracene-2-diphenylphosphino-1-ethanethioether, 9-10-dihydro L^2R ligands

Phosphinothioether ligands previously reported, in general have contained simple low molecular weight backbones [53], [85], [89]. Therefore interactions between the backbone and the thioether moiety have not been observed. We plan to synthesis a phosphinothioether with a large sterically encumbering backbone generating interactions between its own substituents, the coordinated metal and the thioether moiety. After the successful generation of a series of phosphinothioether ligands from L^1Li, we replicated similar phosphinothioether ligands using the phosphinothiolate precursor L^2K.

Following the seven step synthesis outlined previously, phosphinothiolate L^2K was synthesised and washed in anhydrous degassed THF. The high reactivity of ligand L^1K forms the corresponding phosphinothioether which then dissolves in solution (**Scheme 2-6**). Reactions times were dependant on the type of halide, benzyl chloride reacted over a twelve hour period whereas 9-methyl anthracene reacts to completion within two hours. All phosphinothioether ligand synthesis produced a by-product of LiCl which was removed through an aqueous work-up to leave the products in reasonable yields (69-76%).
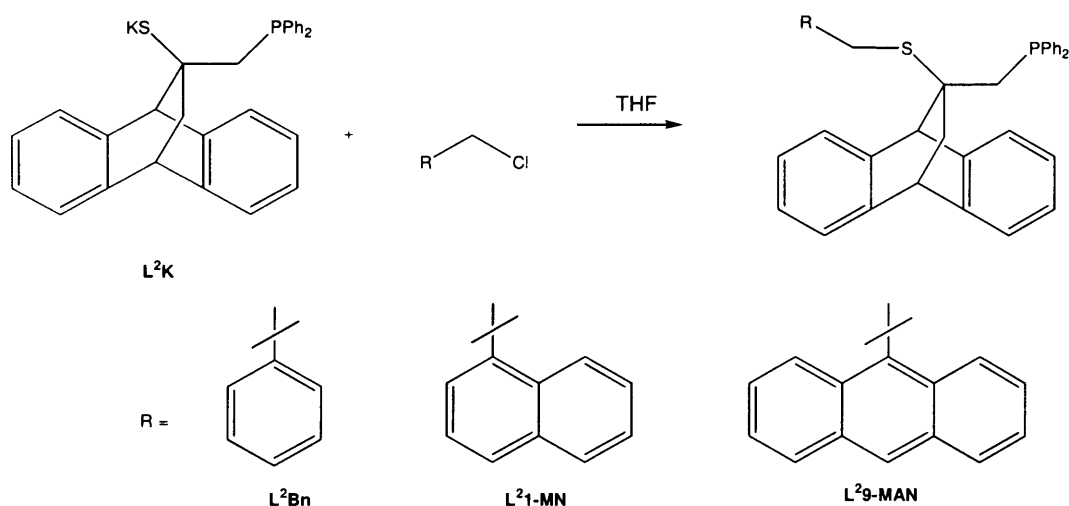
Scheme 2-6: Reaction scheme for the formation of ligands L^2Bn, L^21-MN and L^29-MAN

With the presence of one chiral centre, it was expected to see the single stereoisomer present for each reaction as the two enantiomers are non-distinguishable through spectroscopic techniques. The ^{31}P NMR spectra of the ligand solutions revealed the presence single signals between δ_P -23.7 and -24.7. ^{13}C NMR spectra of all ligands show the presence of six saturated carbons, confirming the presence of the thioether moiety. ^{1}H NMR spectroscopy reaffirmed the synthesis of one stereoisomer with the observation of one set of saturated hydrocarbon signals on the backbone of the ligand and the new methylene protons from the thioether moiety. Methylene protons were identified in the ^{1}H NMR spectra for all phosphinothioethers in the range of δ_H 2.97-4.58 depending on the electron donating abilities of the thioether groups.
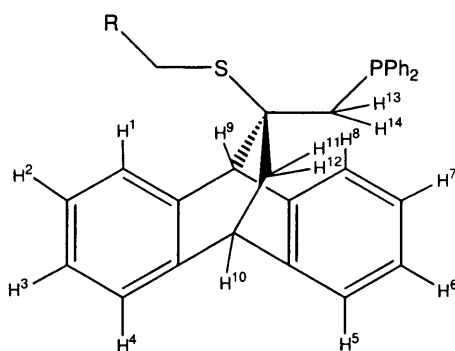
Figure 2-3: ^{1}H NMR numbering scheme for L^2R

With data for a whole series of ligands it is beneficial to compare each spectrum to evaluate the interactions of changes in the thioether group and how they effect the environment of the backbone of the ligand. All NMR data is tabulated below to show how the proton environments are effected by the change in thioether electron-density. Nearly all signals are shifted downfield with the increase in thioether size and electron donating ability, except for the bridge-head (H^{10}) proton of the benzyl ligand L^2Bn which is shifted slightly more downfield to that of the methylnaphthalene thioether, as shown in Table 2-2.

Proton	L^{2}Bn	L^{2}1-MN	L^{2}9-MAN
H^9	4.44	4.46	4.64
H^{10}	**4.14**	4.12	4.27
H^{11}	1.82	1.82	2.02
H^{12}	1.94	1.94	2.02
H^{13}	2.49	2.53	2.80
H^{14}	2.25	2.32	2.70
H^{15}	2.97	3.55	4.39
H^{16}	3.39	3.92	4.58

Table 2-2: Comparison of ^{1}H NMR data between synthesised ligands.

With the successful synthesis of a range of phosphinothiolate and phosphinothioether ligands we will coordinate and structurally compare complexes formed. From these results we will identify the influences ligand backbones have on electronic and steric properties of ligand-metal bond interactions.

2.3 Experimental

Materials and methods

All manipulations were preformed using standard Schlenk techniques under a nitrogen atmosphere, except where otherwise noted. All metal complexes were prepared under an inert atmosphere but after their formation they are air-stable. All other reagents were used as received. Solvents were purified by standard literature methods [141]. Mass spectra were obtained in FAB (Fast Atom Bombardment) mode in a 3-nitrobenzyl alcohol matrix. NMR spectra were obtained on Bruker Avance AMX 400 or Jeol Eclipse 300 spectrometers and referenced to external TMS.
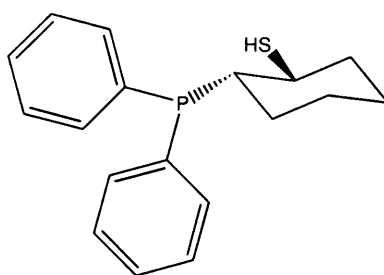
Preparation of HSC₆H₁₀PPh₂ L¹H. Diphenyl phosphine (1.63 g, 8.76 mmol) was diluted with anhydrous diethyl ether (30 ml) whilst stirring under argon. The solution was then cooled to 0°C using an ice bath and followed by addition of n-BuLi (2.5 M, 1.52 ml, 8.76 mmol) drop-wise over a period of five minutes turning the solution bright yellow. After stirring for thirty minutes cyclohexene sulphide (1.00 g, 8.76 mmol) dissolved in anhydrous diethyl ether (20 ml) was added to the reaction drop-wise at 0°C whilst stirring under argon. After stirring for 2 hours the phosphinothiolate precipitates from solution in the form of a white solid. This solid was filtered and washed with diethyl ether (3 x 30 ml). The L^1Li was then hydrolysed using degassed water (1 ml), dissolved in (20ml) and then dried using magnesium sulphate. Evaporation of the solvent left the desired product in the form of a white solid. Yield 1.627 g (60%). δ_H (CDCl₃, 400MHz) 0.90 (1H, m, Cy), 1.19 (2H, m, Cy), 1.44 (2H, m, Cy), 1.57 (1H, m, Cy), 1.75 (1H, m, Cy), 2.08 (2H, m, Cy / S*H*), 2.30 (1H, m, Cy), 2.77 (1H, m, Cy), 7.06-7.23 (5H, m, Ar*H*), 7.23-7.41 (5H, m, Ar*H*), 7.60 (1H, m, Ar*H*). δ_C (125 MHz, ppm, CDCl₃) 24.58 (1C, s, Cy), 25.10 (1C, d, Cy, $^2J_{CP}$ = 2.5), 26.50 (1C, s, Cy), 36.07 (1C, s, Cy), 40.84 (1C, d, Cy, $^2J_{CP}$ = 18.9), 43.26 (1C, d, Cy, $^2J_{CP}$ = 13.8), 128.21 (1C, s, Ph), 128.34 (1C, s, Ph), 128.40 (1C, s, Ph), 129.29 (1C, s, Ph), 129.54 (1C, s, Ph), 131.17 (1C, s, Ph), 131.26 (1C, s, Ph), 132.34 (1C, s, Ph), 135.52 (1C, s, Ph), 135.65

(1C, s, Ph), 136.92 (1C, d, Ph, $^2J_{CP}$ = 13.8), 139.16 (1C, d, Ph, $^2J_{CP}$ = 13.8). δ_P (CDCl$_3$, 121MHz) – 6.3.
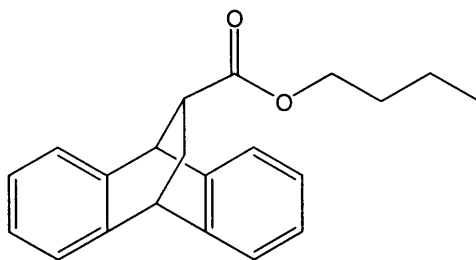
Preparation of C$_{16}$H$_{12}$CO$_2$Bu 9, 10-ethanoanthracene-11-carboxylic acid, 9-10-dihydro, butyl ester 1. Anthracene (19.31 g, 0.11 mol) was added to butyl acrylate (13.138 g, 0.11 mol) in a sealed vessel. The mixture was heated to 170°C and stirred for 24 hours. Using column chromatography the resulting product was separated leaving a white crystalline solid. Yield (24.148 g (73%). ^{1}H NMR (CDCl$_3$, 400MHz) 0.85 (3H, t, CH_3, $^3J_{HH}$ = 7.4), 1.25 (2H, m, CH_2), 1.48 (2H, m, CH_2), 1.93 (1H, m, CH_2), 2.10 (1H, m, CH_2), 2.79 (1H, m, CH), 3.90 (2H, m, CH_2), 4.27 (1H, t, CH, $^3J_{HH}$ = 2.6), 4.60 (1H, d, CH, $^2J_{HH}$ = 2.5), 7.00 (4H, m, ArH), 7.20 (4H, m, ArH). δ_C (125MHz, CDCl$_3$) 13.85 (1C, s, CH$_3$), 19.27 (1C, s, CH$_2$), 30.82 (1C, s, CH$_2$), 43.97 (1C, s, CH$_2$), 44.27 (1C, s, CH), 47.09 (1C, s, CH), 64.67 (1C, s, CH$_2$), 123.38 (1C, s, ArC), 124.86 (1C, s, ArC), 125.46 (1C, s, ArC), 125.83 (1C, s, ArC), 126.29 (1C, s, ArC), 128.30 (1C, s, ArC), 140.19 (1C, s, ArC), 142.63 (1C, s, ArC), 143.84 (1C, s, ArC), 144.13 (1C, s, ArC), 173.64 (1C, s, C=O).
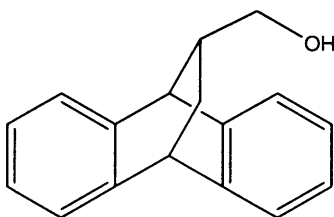
Preparation of C$_{17}$H$_{14}$OH 9, 10-ethanoanthracene-11-methanol, 9-10-dihydro 2. Into a two-necked flask fitted with a dropping funnel and reflux condenser lithium aluminium hydride (0.30 g, 7.88 mmol) was mixed with dried ether (20 ml). To this grey mixture, ester 1 (2.238 g, 7.30 mmol) dissolved in dry diethyl ether (30 ml) was added drop-wise maintaining a steady reflux and stirred for 2 hours. The reaction was quenched with water (1 ml, 56 mmol) producing a white precipitate. The mixture was

then washed with diethyl ether (20 ml) and CH_2Cl_2 (20 ml). The organic phases were combined and dried over magnesium sulphate. Removal of the solvent left a white crystalline solid. Yield 1.35g (73%). ^1H NMR (CDCl$_3$, 400MHz) 1.00 (1H, m, CH_2), 1.25 (1H, t, OH, $^3J_{HH}$ = 5.1), 1.88 (1H, dt, CH_2, $^2J_{HH}$ = 2.8, $^3J_{HH}$ = 10.1), 2.10 (1H, m, CH), 2.90 (1H, m, CH_2), 3.28(1H, q, CH_2, $^4J_{HH}$ = 5.1), 4.17 (1H, t, CH, $^3J_{HH}$ = 2.7), 4.34 (1H, d, CH, $^2J_{HH}$ = 2.3), 7.03 (4H, m, ArH), 7.19 (4H, m, ArH). δ_C (125MHz, CDCl$_3$) 31.08 (1C, s, CH$_2$), 40.99 (1C, s, CH$_2$), 44.08 (1C, s, CH), 45.57 (1C, s, CH), 66.10 (1C, s, CH), 123.18 (1C, s, ArC), 123.50 (1C, s, ArC), 123.61 (1C, s, ArC), 125.37 (1C, s, ArC), 125.44 (1C, s, ArC), 125.69 (1C, s, ArC), 125.70 (1C, s, ArC), 125.74 (1C, s, ArC), 125.76 (1C, s, ArC), 126.04 (1C, s, ArC) , 140.54 (1C, s, ArC), 143.89 (1C, s, ArC).
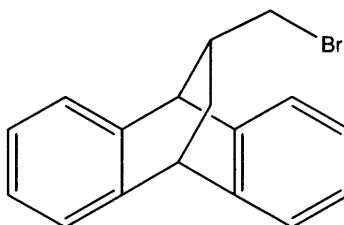
Preparation of $C_{17}H_{14}Br$ 9, 10-ethanoanthracene, 11-(bromo-methyl)-9-10-dihydro 3. Using a round bottom flask fitted with a reflux condenser alcohol 2 (1.250 g, 5.29 mmol) was dissolved in dry acetonitrile (20 ml) followed by carbon tetrabromide (3.001 g, 9.05 mmol) and imidazole (0.101 g, 1.48 mmol). Triphenylphosphine (1.95 g, 7.43 mmol) was then added slowly at 0°C causing the reaction to slightly warm. The reaction was then stirred and refluxed at 80°C for 24 hours. The resulting bright orange solution was then evaporated and the desired product separated using column chromatography leaving a pale yellow solid. Yield 0.980 g (62%). ^1H NMR (CDCl$_3$, 400MHz) 1.12 (1H, m, CH_2), 2.00 (1H, m, CH_2), 2.28 (1H, m, CH), 2.73 (1H, t, CH_2, $^3J_{HH}$ = 9.8), 3.02 (1H, t, CH_2, $^3J_{HH}$ = 6.3), 4.20 (1H, t, CH, $^3J_{HH}$ = 2.6), 4.40 (1H, d, CH, $^2J_{HH}$ = 2.3), 7.04 (4H, m, ArH), 7.18 (4H, m, ArH). δ_C (125MHz, CDCl$_3$) 34.97 (1C, s, CH$_2$), 38.19 (1C, s, CH$_2$), 41.18 (1C, s, CH), 44.33 (1C, s, CH), 47.35 (1C, s, CH), 123.42 (1C, s, ArC), 123.61 (1C, s, ArC), 124.00 (1C, s, ArC), 125.78 (1C, s, ArC), 126.00 (1C, s, ArC), 126.03 (1C, s, ArC), 126.16 (1C, s, ArC), 126.45 (1C, s, ArC), 139.67 (1C, s, ArC), 143.34 (1C, s, ArC), 143.48 (1C, s, ArC), 143.65 (1C, s, ArC).
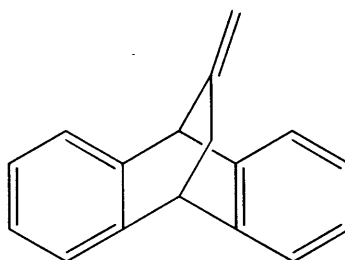
Preparation of C₁₇H₁₄ 9, 10-ethanoanthracene, 9-10-dihydro-11-methylene 4.

Bromide **3** (2.009 g, 6.70 mmol) was added to diazabicyclo[5.4.0]undec-7-ene (1.320 g, mmol) in a sealed vessel. The mixture was then heated to 140°C and stirred for 24 hours. The resulting brown oil was washed over a silica filter stick using ethyl acetate. The solvent was evaporated leaving a white solid. Yield 0.190 g, (51%). ^{1}H NMR (CDCl₃, 400MHz) 2.38 (2H, d, CH_2, $^2J_{HH}$ = 2.2), 4.26 (1H, t, CH, $^3J_{HH}$ = 2.4), 4.60 (1H, s, CH), 4.64 (1H, s, CH_2), 5.05 (1H, s, CH_2), 7.02 (4H, m, ArH), 7.20 (4H, m, ArH). δ_C (125MHz, CDCl₃) 35.08 (1C, s, CH₂), 40.99 (1C, s, CH), 44.08 (1C, s, CH), 45.57 (1C, s, =CH₂), 66.10 (1C, s, =C), 123.18 (1C, s, ArC), 123.50 (1C, s, ArC), 123.61 (1C, s, ArC), 125.37 (1C, s, ArC), 125.44 (1C, s, ArC), 125.69 (1C, s, ArC), 125.74 (1C, s, ArC), 125.76 (1C, s, ArC), 126.04 (1C, s, ArC), 128.25 (1C, s, ArC), 140.54 (1C, s, ArC), 143.89 (1C, s, ArC).
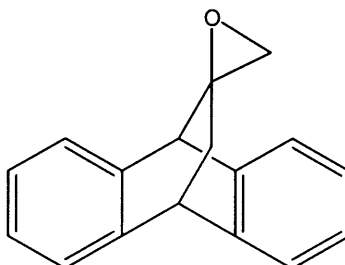
Preparation of C₁₇H₁₄O 9, 10-ethanoanthracene-1, 2-oxide, 9-10-dihydro 5.

Chloro-perbenzoic acid (0.660 g, 3.83 mmol) was dissolved in chloroform (5 ml) in a sealed vessel. The solution was then cooled to 0°C and alkene **4** (0.50 g, 2.29 mmol) was added under constant stirring. The clear solution was stirred at 0°C for 24 hours. The excess chloro-perbenzoic acid was removed by washing an excess of 10% sodium hydroxide (10 ml) and then water (2 x 20 ml). The solution was then dried over magnesium sulphate and removal of the solvent left a white solid. Yield 0.468 g (87%).
^{1}H NMR (CDCl₃, 400MHz) 1.75 (1H, dd, CH_2, $^2J_{HH}$ = 2.7, $^2J_{HH}$ = 13.3), 2.10 (1H, dd, CH_2, $^2J_{HH}$ = 2.6, $^2J_{HH}$ = 13.3), 2.69 (1H, d, CH_2, $^2J_{HH}$ = 6.3), 2.88 (1H, d, CH_2, $^2J_{HH}$ =

4.6), 3.62 (1H, s, CH), 4.27 (1H, t, CH, $^3J_{HH}$ = 2.6), 7.05 (4H, m, ArH), 7.23 (4H, m, ArH). ^{13}C NMR (125MHz, CDCl$_3$) 34.75 (1C, s, CH_2), 44.33 (1C, s, CH_2), 52.47 (1C, s, CH), 54.05 (1C, s, CH), 62.65 (1C, s, C), 123.67 (1C, s, ArC), 123.72 (1C, s, ArC), 124.78 (1C, s, ArC), 125.19 (1C, s, ArC), 126.07 (1C, s, ArC), 126.21 (1C, s, ArC), 126.49 (1C, s, ArC), 126.61 (1C, s, ArC), 140.56 (1C, s, ArC), 140.64 (1C, s, ArC), 143.05 (1C, s, ArC), 144.00 (1C, s, ArC).
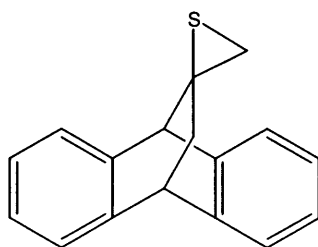
Preparation of C$_{17}$H$_{14}$S Spiro[9,10-ethanoanthracene-1-2-thiirane], 9-10-dihydro 6.
Epoxide **5** (0.677 g, 2.88 mmol) and thiourea (0.318 g, 4.18 mmol) was dissolved in methanol (15 ml). This solution was then stirred at room temperature for 3 days. The sulphide was obtained after extraction with diethyl ether (2 x 20 ml). The ether fractions were combined and extracted with saturated 10% sodium chloride (10 ml) solution and subsequently dried over magnesium sulphide. Removal of the solvent left a white solid. Yield 0.540 g (75%). ^{1}H NMR (CDCl$_3$, 400MHz) 2.12 (1H, dd, CH_2, $^3J_{HH}$ = 2.6, $^2J_{HH}$ = 13.2), 2.30 (1H, dd, CH_2, $^3J_{HH}$ = 2.7, $^2J_{HH}$ = 13.2), 2.40 (1H, s, CH_2), 2.53 (1H, s, CH_2), 3.57 (1H, s, CH), 4.28 (1H, t, CH, $^3J_{HH}$ = 2.5) 6.76-7.39 (1H, m, ArH). δ_C (125MHz, CDCl$_3$) 34.15 (1C, s, CH_2), 40.74 (1C, s, CH_2), 44.90 (1C, s, CH), 50.10 (1C, s, CH), 56.87 (1C, s, C), 123.57 (1C, s, ArC), 123.71 (1C, s, ArC), 124.21 (1C, s, ArC), 124.43 (1C, s, ArC), 126.12 (1C, s, ArC), 126.13(1C, s, ArC), 126.36 (1C, s, ArC), 126.58 (1C, s, ArC), 142.06 (1C, s, ArC), 142.49 (1C, s, ArC), 142.89 (1C, s, ArC), 143.27 (1C, s, ArC).
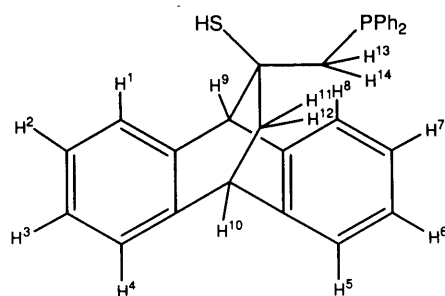
9, 10-ethanoanthracene-2-diphenylphosphino-1-ethanethio), 9-10-dihydro, L^2H.

Sulphide **6** (1.01 g, 4,04 mmol) was dissolved in dry, degassed THF (30 ml) and added drop-wise to a solution of potassium diphenylphosphide (12.1 ml, 0.5M, 6.1 mmol) at 0°C whilst stirring under argon. After 1 hour the ligand L^2K precipitated from the solution as a white solid. The ligand was washed with THF (3 x 30 ml) to remove any excess phosphide before being quenched with deoxygenated water (15 ml). The product was then extracted with dichloromethane (2 x 20 ml) and dried under $MgSO_4$. Removal of the solvent left the product as a white powder. Yield 1.23 g (75%). ^1H NMR ($CDCl_3$, 400 MHz): δ_H 2.10 (3H, m, $H^{11/12}$ / H^{13} / SH,) 2.43 (1H, dd, H^{14}, $^3J_{HP} = 5.1$, $^2J_{HH} = 14.8$), 4.07 (1H, t, H^{10}, $^3J_{HH} = 2.5$) 4.43 (1H, s, H^9), 6.82-7.31 (18H, m, ArH). ^{13}C NMR (125 MHz, $CDCl_3$): δ 43.61 (1C, s, CH), 44.84 (1C, d, CH$_2$, $^2J_{CP} = 6.2$), 46.64 (1C, s, CH), 49.86 (1C, d, CH$_2$, $^2J_{CP} = 18.0$), 56.58 (1C, d, C, $^2J_{CP} = 8.8$), 122.23 (1C, s, ArC), 122.24 (1C, s, ArC), 124.54 (1C, s, ArC), 124.68 (1C, s, ArC), 124.86 (1C, s, ArC), 125.27 (1C, s, ArC), 125.31 (1C, s, ArC), 127.32 (1C, s, ArC), 127.34 (1C, s, ArC), 127.38 (1C, s, ArC), 127.40 (1C, s, ArC), 127.50 (1C, s, ArC), 131.66 (1C, s, ArC) 131.81 (1C, s, ArC), 132.19 (1C, s, ArC), 132.35 (1C, s, ArC), 137.69 (1C, s, ArC), 137.79 (1C, s, ArC), 138.14 (1C, s, ArC) 138.23 (1C, s, ArC), 139.94 (1C, s, ArC), 140.62 (1C, s, ArC), 141.12 (1C, s, ArC), 141.23 (1C, s, ArC). ^{31}P NMR ($CDCl_3$, 121MHz): δ_P −23.0; exact mass calculated for $C_{29}H_{25}SP+H^+$ requires m/z 437.1493, found m/z 437.1510 (ES).
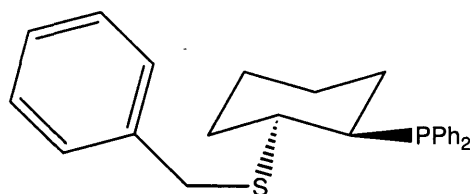
Preparation of C₇H₇SC₆H₁₀PPh₂ L¹Bn. Diphenyl phosphine (1.71 g, 9.21 mmol) was diluted with dry, degassed THF (30 ml) whilst stirring under argon. The solution was then cooled to 0°C using an ice bath, followed by the addition of n-BuLi (2.5 M, 1.60 ml, 9.23 mmol) drop-wise turning the solution bright yellow. After one hour of stirring cyclohexene sulphide (1.05 g, 9.22 mmol) was dissolved in anhydrous THF (20 ml) and added to the reaction drop-wise at 0°C whilst stirring under argon turning the solution colourless. After one hour of stirring benzyl bromide (1.58 g, 9.25 mmol) was added drop-wise. Removal of the solvent left a white crystalline solid. Yield 2.62 g (73%). δ_H (CDCl₃, 400MHz) 1.16 (1H, m, Cy), 1.35 (2H, m, Cy), 1.52 (1H, m, Cy), 1.65 (2H, m, Cy), 1.85 (1H, m, Cy), 2.20 (1H, m, Cy), 2.54 (1H, t, Cy, $^3J_{HH}$ = 4.2), 2.65 (1H, t, Cy, $^3J_{HH}$ = 4.6), 3.56 (2H, d, CH_2, $^2J_{HH}$ = 6.0), 7.05-7.40 (15H, m, ArH), (1H, m, ArH). δ_C (125MHz, CDCl₃) 23.14 (1C, s, Cy), 23.42 (1C, s, Cy), 25.18 (1C, d, Cy, $^2J_{CP}$ = 8.1), 29.79 (1C, s, Cy), 35.97 (1C, s, CH_2), 39.42 (1C, d, Cy, $^2J_{CP}$ = 15.0), 44.74 (1C, d, Cy, $^2J_{CP}$ = 16.7), 126.89 (1C, s, Ph), 128.06 (1C, s, Ph), 128.53 (2C, s, Ph), 128.87 (1C, s, Ph), 129.06 (1C, s, Ph), 130.60 (1C, s, Ph), 130.67 (1C, s, Ph), 131.67 (1C, s, Ph), 131.80 (1C, s, Ph), 133.13 (2C, d, Ph, $^2J_{CP}$ = 19.0), 134.15 (2C, d, Ph, $^2J_{CP}$ = 20.2), 136.51 (1C, d, Ph, $^2J_{CP}$ = 16.7), 137.38 (1C, d, Ph, $^2J_{CP}$ = 14.4), 138.79 (1C, s, Ph). δ_P (CDCl₃, 121MHz) –11.7.
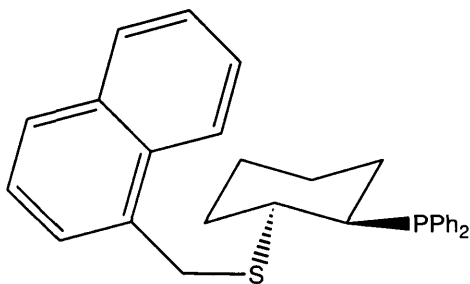
Preparation of C₁₁H₉SC₆H₁₀PPh₂ L¹1-MN. Diphenyl phosphine (1.57 g, 8.43 mmol) was diluted with dry, degassed THF (30 ml) whilst stirring under argon. The solution was then cooled to 0°C using an ice bath, followed by the addition of n-BuLi (2.5 M,

1.47 ml, 8.45 mmol) drop-wise turning the solution bright yellow. Cyclohexene sulphide (0.96 g, 8.43 mmol) was dissolved in dry THF (20 ml) and added to the reaction drop-wise at 0°C whilst stirring under argon. To this schlenk a solution of 1-chloromethyl naphthalene (1.49 g, 8.47 mmol) was added drop-wise turning the solution colourless. Removal of the solvent left a white crystalline solid. Yield 2.22 g (60%). δ_H (CDCl$_3$, 400MHz) 1.17 (1H, m, Cy), 1.34 (2H, m, Cy), 1.56 (1H, m, Cy), 1.67 (2H, m, Cy), 1.86 (1H, m, Cy), 2.22 (1H, m, Cy), 2.56 (1H, t, Cy, $^3J_{HH}$ = 4.4), 2.70 (1H, t, Cy, $^3J_{HH}$ = 4.4), 3.95 (2H, d, CH_2, $^2J_{HH}$ = 2.6), 6.93-7.74 (18H, m, ArH), 8.01 (1H, d, ArH, $^2J_{HH}$ = 8.4). δ_C (125MHz, CDCl$_3$) 23.26 (1C, s, Cy), 23.50 (1C, s, Cy), 25.29 (1C, s, Cy), 29.96 (1C, s, Cy), 33.87 (1C, s, CH_2), 39.61 (1C, s, Cy), 45.52 (1C, s, Cy), 124.35 (1C, s, Ph), 125.38 (1C, s, Ph), 125.91 (1C, s, Ph), 126.19 (1C, s, Ph), 126.92 (1C, s, Ph), 128.03 (1C, s, Ph), 128.40 (1C, s, Ph), 128.50 (1C, s, Ph), 128.58 (1C, s, Ph), 128.67 (1C, s, Ph), 128.88 (1C, s, Ph), 129.11 (1C, s, Ph), 131.78 (1C, s, Ph), 131.91 (1C, s, Ph), 132.98 (1C, s, Ph), 133.22 (1C, s, Ph), 134.12 (1C, s, Ph), 134.40 (1C, s, Ph), 136.35 (1C, s, Ph), 136.57 (1C, s, Ph), 137.41 (1C, s, Ph), 137.61 (1C, s, Ph). δ_P (CDCl$_3$, 121MHz) –11.8.
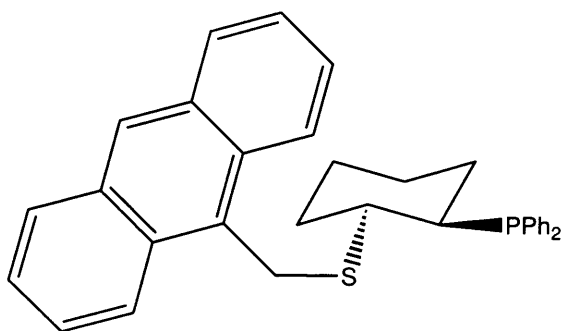
Preparation of C$_{15}$H$_{11}$SC$_6$H$_{10}$PPh$_2$ L^{1}9-MAN. Diphenyl phosphine (1.64 g, 8.79 mmol) was diluted with dry, degassed THF (30 ml) whilst stirring under argon. The solution was then cooled to 0°C using an ice bath, followed by the addition of n-BuLi (2.5 M, 1.53 ml, 8.83 mmol) drop-wise turning the solution bright yellow. Cyclohexene sulphide (1.01 g, 8.85 mmol) was dissolved in anhydrous THF (20 ml) and added to the reaction drop-wise at 0°C whilst stirring under argon. To this schlenk a solution of 9-chloromethyl anthracene (2.02 g, 8.90 mmol) dissolved in THF (30ml) was added drop-wise turning the solution colourless. Removal of the solvent left a white solid. Yield 3.40 g (79%). δ_H (CDCl$_3$, 400MHz) 1.14 (1H, m, Cy), 1.31 (2H, m, Cy), 1.56 (2H, m, Cy), 1.62 (1H, m, Cy), 2.21 (2H, m, Cy), 2.54 (1H, t, Cy, $^3J_{HH}$ = 4.1), 2.68 (1H, t, Cy,

$^3J_{HP}$ = 4.4), 3.93 (2H, d, CH_2, $^2J_{HP}$ = 2.6), 6.94-7.73 (18H, m, ArH), 8.00 (1H, d, ArH, $^2J_{HH}$ = 8.4). δ_P (CDCl$_3$, 121MHz) –11.8.
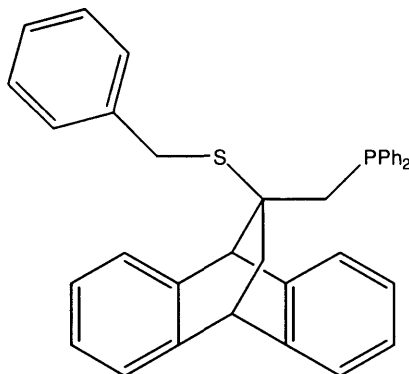
Preparation of C$_7$H$_7$SC$_{17}$H$_{14}$PPh$_2$ L^{2}Bn. Potassium diphenylphosphide (2M, 4.38ml, 8.76 mmol) was diluted with anhydrous THF (30 ml) giving a deep orange solution. Thiirane **6** (1.00 g, 8.76 mmol) was dissolved in anhydrous THF (20 ml) and added to the reaction drop-wise at 0°C whilst stirring under argon to give a green solution. After one hour a white precipitate had formed which was filtered and washed with THF (3x 30ml) and finally THF was added (30 ml) to give a suspension. To this schlenk benzyl chloride (1.11g, 8.76 mmol) was added drop-wise and the solution stirred for a further 12 hours. The potassium salt reacts to for the desired phosphino-thioether which dissolves in the THF to give a colourless solution. Removal of the solvent left a white solid. Yield 3.50 g (76%). δ_H (CDCl$_3$, 400MHz) 1.82 (1H, dd, CH_2, $^2J_{HH}$ = 2.8, $^2J_{HH}$ = 13.3), 1.94 (1H, dd, CH_2, $^2J_{HH}$ = 2.6, $^2J_{HH}$ = 13.3) 2.25 (1H, dd, CH_2, $^3J_{HP}$ = 4.2, $^2J_{HH}$ = 14.9), 2.49 (1H, dd, CH_2, $^3J_{HP}$ = 3.3, $^2J_{HH}$ = 14.9), 2.97 (1H, d, CH_2, $^2J_{HH}$ = 11.0), 3.39 (1H, d, CH_2, $^2J_{HH}$ = 11.0), 4.14 (1H, t, CH, $^3J_{HH}$ = 2.6) 4.44 (1H, s, CH) 6.72 (2H, m, ArH), 6.98-7.39 (11H, m, ArH). δ_C (125MHz, CDCl$_3$) 32.23 (1C, s, CH), 41.51 (1C, d, C, $^2J_{CP}$ = 11.3), 42.12 (1C, d, CH$_2$, $^2J_{CP}$ = 8.8), 43.42 (1C, s, CH), 52.29 (1C, d, CH$_2$, $^2J_{CP}$ = 17.6), 53.50 (1C, d, CH$_2$, $^2J_{CP}$ = 6.3) 122.32 (1C, s, ArC), 122.41 (1C, s, ArC), 124.06 (1C, s, ArC), 124.35 (1C, s, ArC), 124.51 (1C, s, ArC), 124.74 (1C, s, ArC), 124.83 (1C, s, ArC), 125.32 (1C, s, ArC), 125.56 (1C, s, ArC), 125.93 (1C, s, ArC), 126.62 (1C, s, ArC), 126.97 (1C, s, ArC), 127.14 (1C, s, ArC), 127.14 (1C, s, ArC), 127.24 (1C, s, ArC), 127.29 (1C, s, ArC) 127.37 (1C, s, ArC), 127.43 (1C, s, ArC), 127.51 (1C, s, ArC), 127.69 (1C, s, ArC), 128.12 (1C, s, ArC), 131.41 (1C, s, ArC) 131.56 (1C, s, ArC), 132.74 (1C, s, ArC), 132.90 (1C, s, ArC), 135.74 (1C, s, ArC), 138.84 (1C, s, ArC), 140.17 (1C, s, ArC), 141.04 (1C, s, ArC), 142.15 (1C, s, ArC). δ_P (CDCl$_3$, 121MHz) –23.7

Preparation of C₁₁H₉SC₁₇H₁₄PPh₂ L²1-MN. Potassium diphenylphosphide (2M, 8.89ml, 17.78 mmol) was diluted with anhydrous THF (30 ml) giving a deep orange solution. Thiirane **6** (2.03 g, 17.78 mmol) was dissolved in anhydrous THF (20 ml) and added to the reaction drop-wise at 0°C whilst stirring under argon to give a green solution. After one hour a white precipitate had formed which was filtered and washed with THF (3x 30ml) and finally THF was added (30 ml) to give a suspension. To this schlenk 1-chloromethyl naphthalene (3.14g, 17.78 mmol) was added drop-wise turning the solution colourless over a period of 12 hours. Removal of the solvent left a white crystalline solid. Yield 7.08 g (69%). δ_H (CDCl₃, 400MHz) 1.82 (1H, dd, CH_2, $^2J_{HH}$ = 2.7, $^2J_{HH}$ = 13.7), 1.94 (1H, dd, CH_2, $^2J_{HH}$ = 2.6, $^2J_{HH}$ = 13.3) 2.32 (1H, dd, CH_2, $^3J_{HP}$ = 4.3, $^2J_{HH}$ = 15.0), 2.53 (1H, dd, CH_2, $^3J_{HP}$ = 2.8, $^2J_{HH}$ = 15.0), 3.55 (1H, d, CH_2, $^2J_{HH}$ = 11.2), 3.92 (1H, d, CH_2, $^2J_{HH}$ = 11.2), 4.12 (1H, t, CH, $^3J_{HH}$ = 2.4) 4.46 (1H, s, CH) 6.76 (1H, d, ArH, $^2J_{HH}$ = 6.3), 6.95-7.80 (11H, m, ArH) 8.04 (1H, d, ArH, $^2J_{HH}$ = 6.3). ^{13}C NMR (125MHz, CDCl₃) 31.44 (1C, s, CH), 42.76 (1C, d, C, $^2J_{CP}$ = 6.2), 43.05 (1C, d, CH_2, $^2J_{CP}$ = 18.0), 43.42 (1C, s, CH), 44.68 (1C, s, CH_2), 53.90 (1C, s, CH_2) 122.32 (1C, s, ArC), 122.41 (1C, s, ArC), 124.06 (1C, s, ArC), 124.35 (1C, s, ArC), 124.51 (1C, s, ArC), 124.74 (1C, s, ArC), 124.83 (1C, s, ArC), 125.32 (1C, s, ArC), 125.56 (1C, s, ArC), 125.93 (1C, s, ArC), 126.62 (1C, s, ArC), 126.97 (1C, s, ArC), 127.14 (1C, s, ArC), 127.14 (1C, s, ArC), 127.24 (1C, s, ArC), 127.29 (1C, s, ArC) 127.37 (1C, s, ArC), 127.43 (1C, s, ArC), 127.51 (1C, s, ArC), 127.69 (1C, s, ArC), 128.12 (1C, s, ArC), 131.41 (1C, s, ArC) 131.56 (1C, s, ArC), 132.74 (1C, s, ArC), 132.90 (1C, s, ArC), 135.74 (1C, s, ArC), 138.84 (1C, s, ArC), 140.17 (1C, s, ArC), 141.04 (1C, s, ArC), 142.15 (1C, s, ArC). δ_P (CDCl₃, 121MHz) –24.1
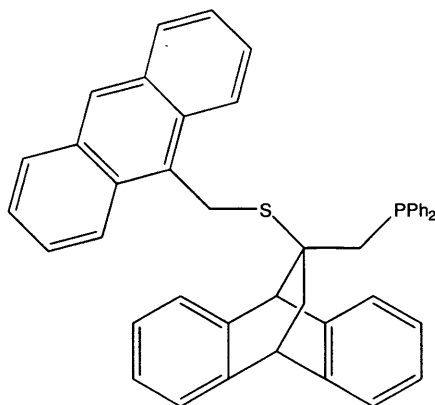
Preparation of $C_{15}H_{11}SC_{17}H_{14}PPh_2$ **L^29-MAN.** Potassium diphenylphosphide (2M, 6.88ml, 13.75 mmol) was diluted with anhydrous THF (30 ml) giving a deep orange solution. Thiirane **6** (1.57 g, 13.75 mmol) was dissolved in anhydrous THF (20 ml) and added to the reaction drop-wise at 0°C whilst stirring under argon to give a green solution. After one hour a white precipitate had formed which was filtered and washed with THF (3 x 30ml) and finally THF was added (30 ml) to give a suspension. To this schlenk a solution of 9-chloromethyl anthracene (3.12g, 13.75 mmol) dissolved in anhydrous thf (20 ml) was added drop-wise turning the solution colourless and stirred for two hours. Removal of the solvent left a white solid. Yield 12.13 g (71%). δ_H (CDCl$_3$, 400MHz) 2.02 (2H, m, CH_2), 2.70 (1H, d, CH_2, $^2J_{HH}$ = 15.1), 2.80 (1H, dd, CH_2, $^3J_{HP}$ = 5.0, $^2J_{HH}$ = 15.1) 4.27 (1H, t, CH, $^3J_{HH}$ = 2.4), 4.39 (1H, d, CH_2, $^2J_{HH}$ = 10.8), 4.58 (1H, d, CH_2, $^2J_{HH}$ = 10.9), 4.64 (1H, s, CH), 7.25 (2H, d, ArH, $^2J_{HH}$ = 7.3), 7.20-7.71 (20H, m, ArH), 8.00-8.42 (7H, m, ArH). δ_C ^{13}C NMR (125MHz, CDCl$_3$) 25.77 (1C, d, CH_2, $^2J_{CP}$ = 3.7), 37.94 (1C, s, CH), 40.70 (1C, d, C, $^2J_{CP}$ = 7.3), 43.53 (1C, s, CH), 53.11 (1C, d, CH_2, $^2J_{CP}$ = 15.8), 54.30 (1C, d, CH_2, $^2J_{CP}$ = 4.9), 122.32 (1C, s, ArC), 122.53 (1C, d, ArC, $^2J_{CP}$ = 7.3), 123.79 (1C, s, ArC), 123.90 (1C, s, ArC), 124.16 (1C, s, ArC), 124.32 (1C, d, ArC, $^2J_{CP}$ = 19.5), 124.75 (2C, s, ArC), 124.91 (1C, d, ArC, $^2J_{CP}$ = 9.7), 125.17 (1C, d, ArC, $^2J_{CP}$ = 12.1), 125.84 (1C, s, ArC), 126.18 (1C, s, ArC), 126.73 (1C, s, ArC), 127.26 (1C, s, ArC), 127.36 (1C, d, ArC, $^2J_{CP}$ = 6.1), 127.55 (1C, d, ArC, $^2J_{CP}$ = 6.09), 127.69 (1C, s, ArC), 127.89 (2C, s, ArC), 128.22 (1C, s, ArC) 129.23 (1C, s, ArC), 130.37 (2C, s, ArC), 131.56 (2C, d, ArC, $^2J_{CP}$ = 18.3), 132.51 (2C, d, ArC, $^2J_{CP}$ = 19.5), 138.46 (1C, d, ArC, $^2J_{CP}$ = 14.6), 139.15 (1C, d, ArC, $^2J_{CP}$ = 12.2), 140.47 (1C, s, ArC), 141.06 (1C, d, ArC, $^2J_{CP}$ = 12.2), 142.48 (1C, s, ArC). δ_P (CDCl$_3$, 121MHz) -24.7

Chapter 3 Conformationally confined phosphinothiolate complexes

3.1 M(L^1)$_2$ complexes

The most common type of co-ordination compounds formed between phosphinothiolate ligands and the group 10 metals are bis-chelating complexes of the type [M(P-S)$_2$]. Most bis-chelating complexes reported so far adopt a *trans* arrangement around the metal centre due to the bulky nature of the diphenylphosphino- group. However, there are a few examples even with nickel, the smallest metal of the triad, where *cis* geometry is preferred. We performed a number of experiments to synthesise palladium and nickel bis-chelate complexes using ligand L^{1}H. The synthetic route adopted was similar to those proposed in the literature. Below shows the synthetic step used in the synthesis of nickel (II) bis-2-(diphenylphosphino)cyclohexanethiol **7** (Scheme 3-1).
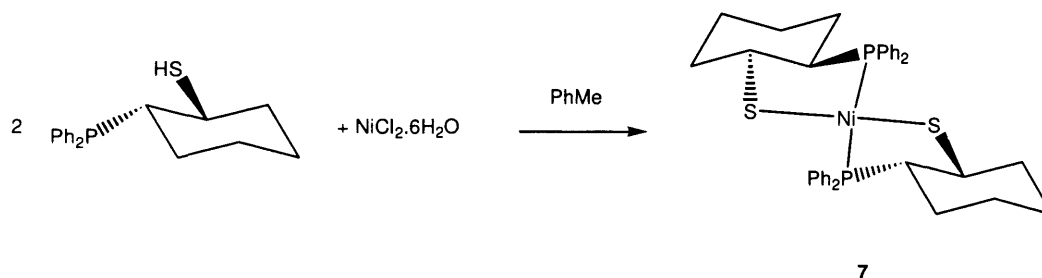
Scheme 3-1: Synthesis of nickel (II) bis-2-(diphenylphosphino)cyclohexanethiol **7**

Examples of bis-chelate complexes with one unresolved chiral centre forming two bis-chelate complexes have been reported [50]. In keeping with the stereoisomer analysis of compound *trans*-Ni(L^1)$_2$ **7**, the preferred geometry of the chiral chelate ring depends on the orientation of the chiral carbons of the cyclohexane backbone. As discussed in the previous chapter two enantiomers are formed during the ring opening of cyclohexene sulphide with the two chiral centres being either (*R*, *R*) or (*S*, *S*). Figure 3-1 shows the possible combinations of stereoisomers which we would expect to observe in the synthesis of such complexes. All reactions are monitored using NMR spectroscopy which cannot distinguish between enantiomers, therefore we would expect to see four diastereoisomers in NMR analysis.

cis - (R, R) (S, S)
meso

diastereomers

cis - (R, R) (R, R)
rac

enantiomers

cis - (S, S) (S, S)
rac

trans - (R, R) (S, S)
meso

diastereomers

trans - (R, R) (R, R)
rac

enantiomers

trans - (S, S) (S, S)
rac
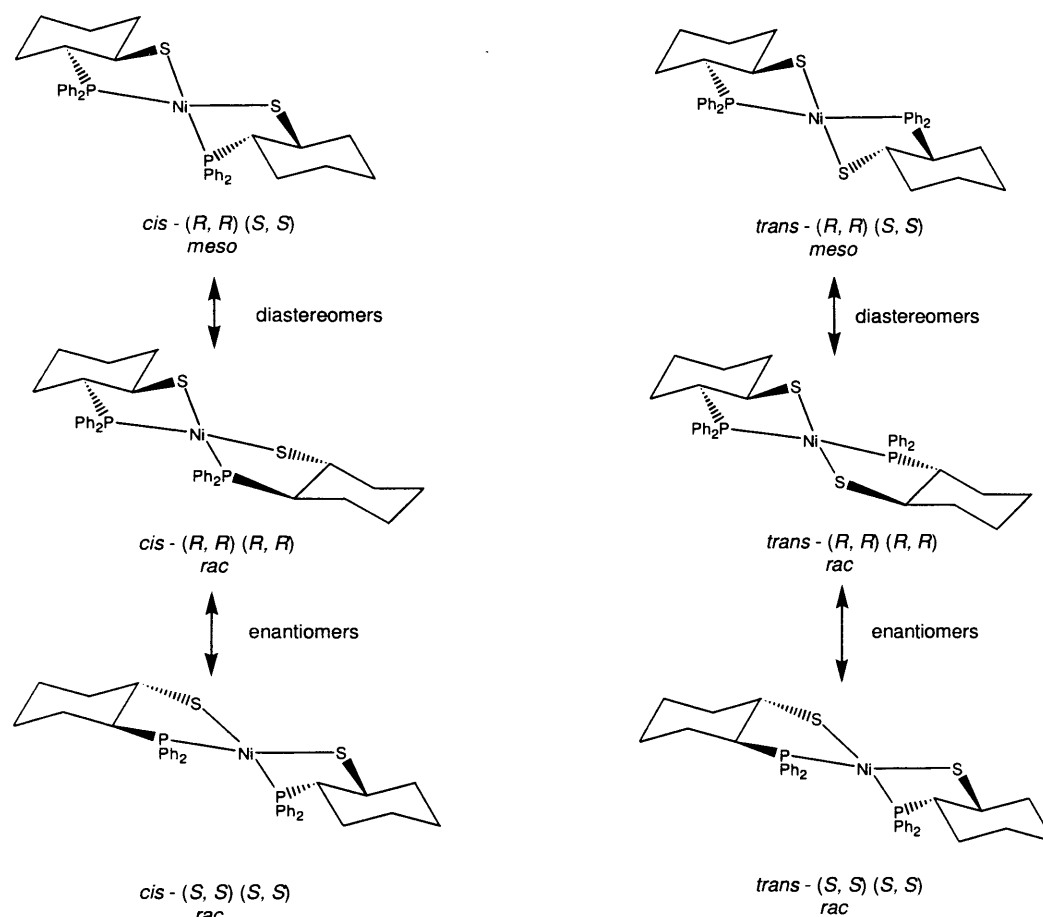
Figure 3-1: Conformational analysis for complex Ni(L^1)$_2$ **7**

The nickel centred bis-chelate complex was synthesised by reacting one equivalent of NiCl$_2$.H$_2$O and two equivalents of racemic L^{1}H in toluene. On addition of the ligand the solution turned a dark green colour, ^{31}P NMR spectroscopy was used to determine the end point of the reaction, showing the formation of a peak in the positive region of the spectrum and the disappearance of that of the free ligand at δ_P -6.3. Using the racemic ligand mixture it was initially presumed that four products would be observed for the *meso* and *rac* forms of both the *cis* and *trans* isomers. However, in the phosphorus NMR spectrum we observed only one peak, at δ_P 63.2, showing that even in solution the complex adopts a single conformation. The ^{1}H NMR spectrum of *trans*-Ni(L^1)$_2$ **7** shows there to be equivalent proton environments for the two ligands in the complex with ten saturated protons between δ_H 0.79-2.24. Green block crystals of *trans*-Ni(L^1)$_2$ **7** suitable for X-ray analysis were obtained by slow diffusion of petroleum ether into a CH$_2$Cl$_2$ solution. An ORTEP view of bis[2-(diphenylphosphino)cycylohexanethiol] nickel (II) **7** is shown in **Figure 3-2** and

71

confirmed a square planar *trans rac* isomer was isolated in the solid state. We report the first structural characterisation of a nickel (II) bidentate phosphinothiolate complex. An example of a tridentate complex formed by Laguna [80] is the closest reference for comparing bond lengths and angles.
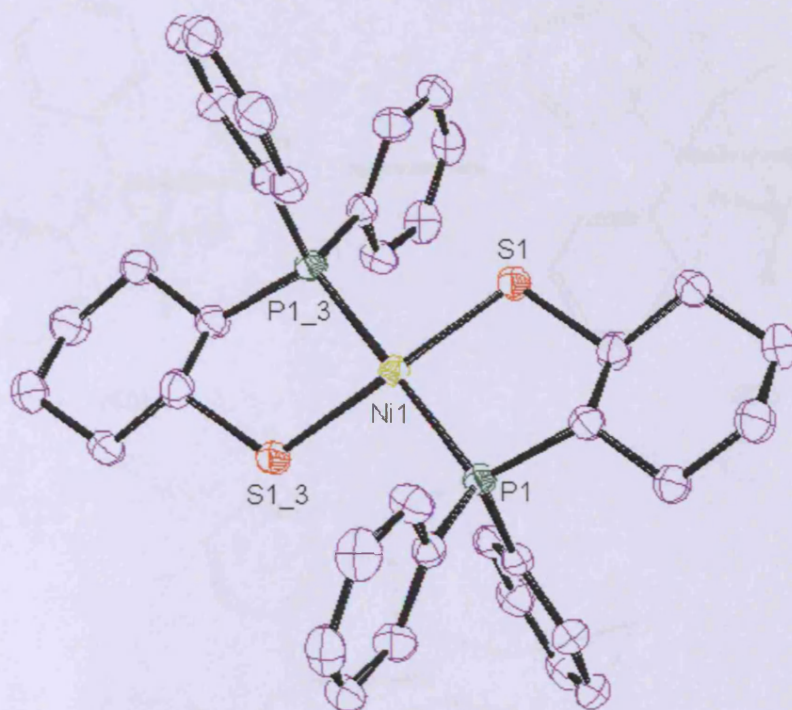
Figure 3-2: ORTEP view of *trans*-Ni(**L**^{1})$_2$ **7**. Hydrogen atoms are omitted for clarity. Thermal ellipsoids are drawn at 50% probability.

The ORTEP view shows the *trans* arrangement and δ skew conformation of the two ligands around the metal centre. The structure shows a *meso* orientation with the chiral carbons showing a *trans*-(*S, R*) arrangement. Conformations of δ and λ are pictured below (**Figure 3-3**) giving an example of a phosphinothiol complex with a single chiral centre. This example shows how the λ conformation would unfavourably arrange the bulky R group in closer proximity to the diphenylphosphino- group. Although only the *S*(δ) and *S*(λ) conformers are pictured below, the relation between *R*(λ) and *R*(δ) is completely analogous. The **L**^{1} ligand is slightly different because it contains two stereogenic centres and has a connected backbone. In order for the ligand moieties to be on the correct geometry for coordination they must be situated

equatorially on the cyclohexane backbone. If adopting the λ conformation one of the coordinating ligands would be placed in an axial position therefore breaking a metal-ligand bond. Finally a diagram of the favoured δ conformation of L^1 is shown with the ligand donors taking an equatorial position.

$S(\delta)$ $S(\lambda)$

7
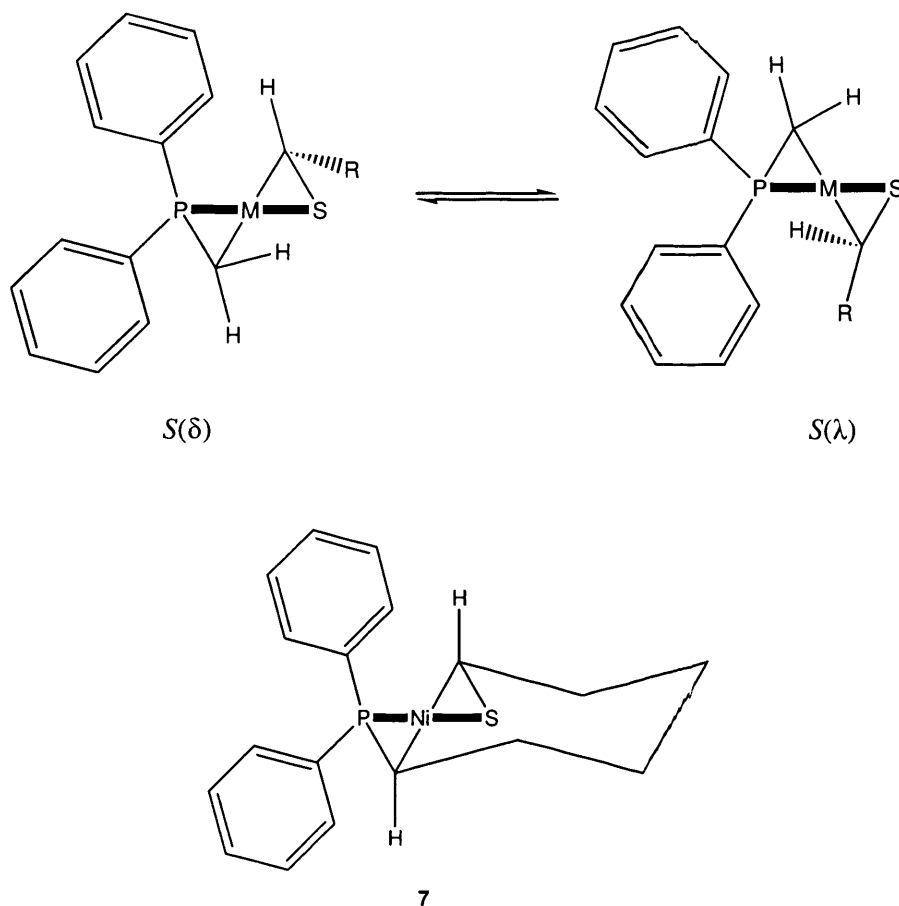
Figure 3-3: Skew conformations showing both the favourable (δ) and unfavourable (λ) conformations for a phosphinothiol complex S isomer.

Crystallographic data obtained for *trans*-Ni$(L^1)_2$ **7** giving selected bond lengths and angles is shown in **Table 3-1**. The Ni-P bonds at 2.1708(7) Å are slightly longer to the tridentate complex with the 1, 2-bis(diphenylphosphanyl)-ethane ligand, PhP(C$_6$H$_4$S)$_2$ [80]. The chelate angles at 88.99(3)° are the first reported and have no nickel (II) complexes to compare. The metal plane is an exact square planar with the P(1)-Ni(1)-P(2) and S(1)-Ni(1)-S(2) bond angles measuring 180.00(4)°. According to the crystallographic data the complex does not contain any points of symmetry due to the different stereogenic centres of each ligand backbone being R and S.

73

Ni(1)-P(2)	2.1708(7)	-	Ni(1)-P(1)	2.1708(7)
Ni(1)-S(1)	2.1713(7)		Ni(1)-S(2)	2.1713(7)
P(1)-C(13)	1.818(3)		S(1)-C(1)	1.836(3)
P(2)-Ni(1)-P(1)	180.00(4)		P(2)-Ni(1)-S(1)	91.01(3)
P(1)-Ni(1)-S(1)	88.99(3)		P(2)-Ni(1)-S(2)	88.99(3)
P(1)-Ni(1)-S(2)	91.01(3)		S(1)-Ni(1)-S(2)	180.00(4)

Table 3-1: Selected bond lengths (Å) and angles (°) of *trans*-Ni(L^1)$_2$ **7**

The majority of P, S bis-chelate complexes reported in the literature are palladium (II) complexes due to their ease of formation and available precursors [113], [114]. As we have explained previously a combination of the HSBA theory and the chelate effect makes palladium an ideal candidate for the formation of stable phosphinothiol complexes. Palladium bis-chelate **8** was synthesied in the form of Pd(L^1)$_2$ using the same synthetic methodology of *trans*-Ni(L^1)$_2$ **7**. Again it was assumed that two diastereoisomers of the *trans* and *cis* form would be observed in any spectroscopic monitoring. On addition of two equivalents of the racemic free ligand L^{1}H to a CH$_2$Cl$_2$ solution of palladium bis-benzonitrile dichloride at room temperature an orange solution was formed, the reaction progress was then monitored by ^{31}P NMR spectroscopy. After one hour the reaction was complete with formation of two singlets in the positive region of the ^{31}P NMR spectrum.

trans-8   *cis*-8
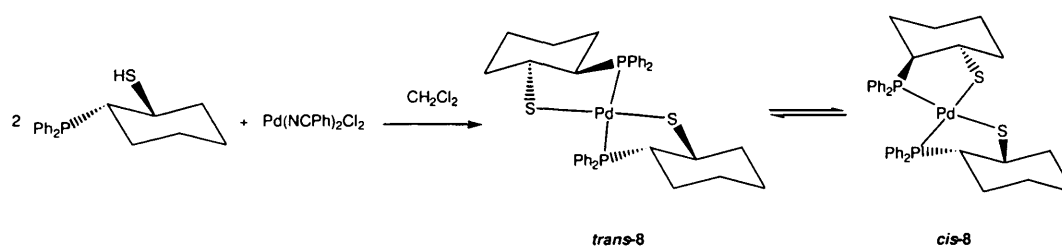
Scheme 3-2: Reaction scheme for the synthesis of complexes *cis/trans*-Pd(L^1)$_2$ **8**

Dissolved in a solution of deuterated chloroform ^{31}P {^{1}H} NMR analysis showed two singlets at δ$_P$ 62.6 and δ$_P$ 59.9, with an intensity ratio of 4:1, which suggested that the bis-chelate complex was present in both *trans* and *cis* forms (**Figure 3-4**). NMR spectroscopy proved to be the best tool to analyse the isomeric mixtures, due to the *cis-trans* interconversion equilibria being relatively slow. Slow crystallisation

in CH_2Cl_2 / Et_2O afforded pure cis-[Pd(L^1)$_2$], this homogeneous crystalline material had a single resonance at δ_P 59.9 in chloroform, and its cis-P,P geometry was finally established by X-ray diffraction. When re-dissolved in a chloroform solution cis-[Pd(L^1)$_2$] undergoes slow isomerisation, and in 24 hours at room temperature the pattern of two singlet resonances of the original $trans$ / cis equilibrium mixture is observed again. The more soluble $trans$-[Pd(L^1)$_2$] was isolated by slow diffusion of $CHCl_3$ / Et_2O which afforded both the $trans$ and cis forms. The $trans$-Pd(L^1)$_2$ crystals were in the shape of yellow blocks and could be separated. The ^{31}P NMR shows a singlet at δ_P 62.6 before any chemical isomerism can take place, which falls in the region where other $trans$ palladium bis-phosphinothiol complexes have been isolated [50], [52], [72]. The observed behaviour is explained by the existence of two distinct equilibria. Using d^4-methanol an increase in the ratio of the cis isomer was observed compared to those dissolved in chloroform and benzene, as seen in **Figure 3-5**. This preference of solvent of cis-Pd(L^1)$_2$ **8** can be attributed to the dipole moment which is induced by vibrations of the Pd-P and Pd-S bonds. The $trans$-Pd(L^1)$_2$ **8** complex is a symmetrical compound therefore no dipole moment is induced and prefers to be dissolved in non-polar solvents.

In general, slow crystallisation causes the formation of crystals of the less soluble form, which in turn should displace the isomerisation equilibrium accordingly. In non-polar solvents, equilibrium mixtures crystallise in the form of the more polar cis-Pd(L^1)$_2$ **8** exclusively. When a polar solvent is used the opposite is observed and the $trans$-Pd(L^1)$_2$ **8** crystallises preferentially. In aged solutions, the isomerisation equilibrium mixture shown in the above figures is always observed for each of the solutions.
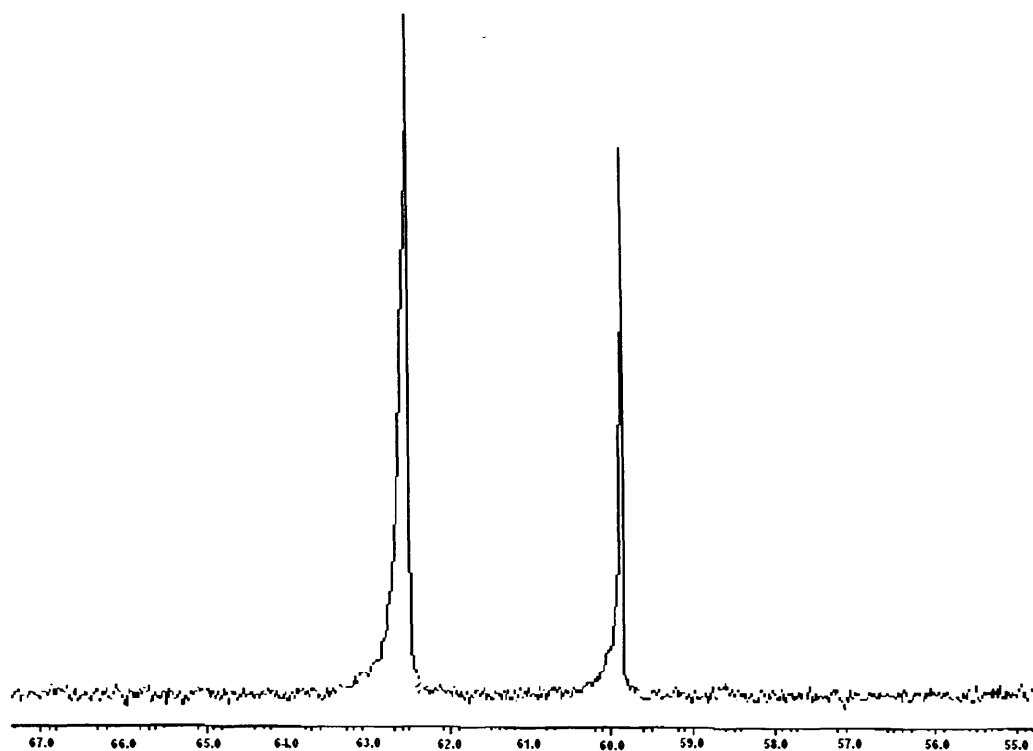
Figure 3-4: ^{31}P NMR spectrum of equilibria of *cis* / *trans*-Pd(L^1)$_2$ **8** dissolved in CDCl$_3$
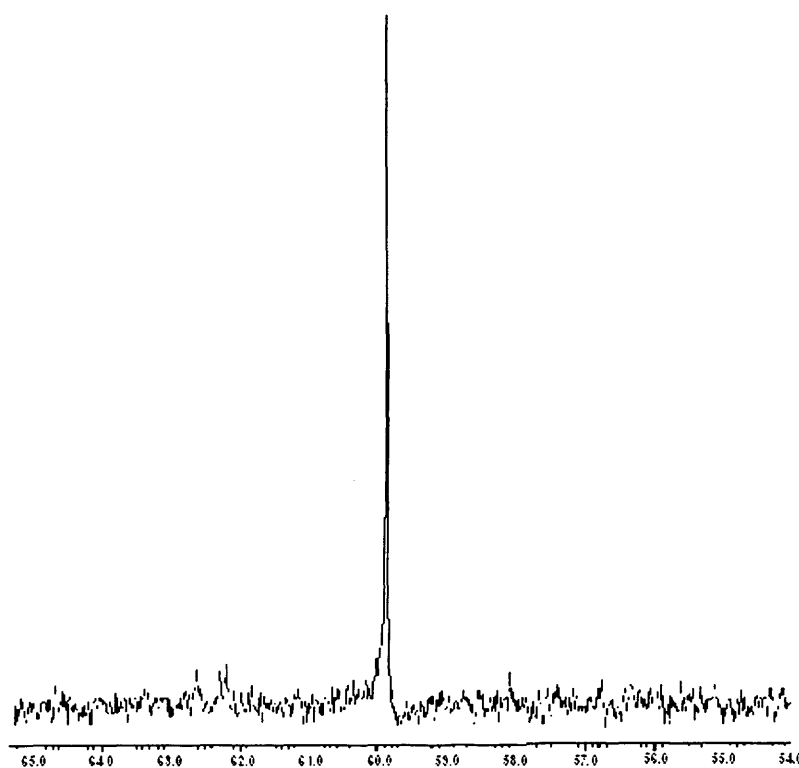
Figure 3-5: ^{31}P NMR spectrum of equilibria of *cis* / *trans*- Pd(L^1)$_2$ **8** dissolved in CD$_3$OD

76

Complexes *cis* / *trans*-Pd(L^1)$_2$ **8** were also isolated by the reaction of Pd(PPh$_3$)$_4$ with two equivalents of **L^{1}H**. The reaction is thought to proceed via the oxidative addition of **L^{1}H** to palladium (0) and form an unstable intermediate hydride complex which reacts further with free **L^{1}H** to form complex the equilibrium mixture of *cis* / *trans*-Pd(L^1)$_2$ **8** (**Scheme 3-3**). The same reactivity has been previously observed with the phosphinothiol ligands dppet and dpppt [71].
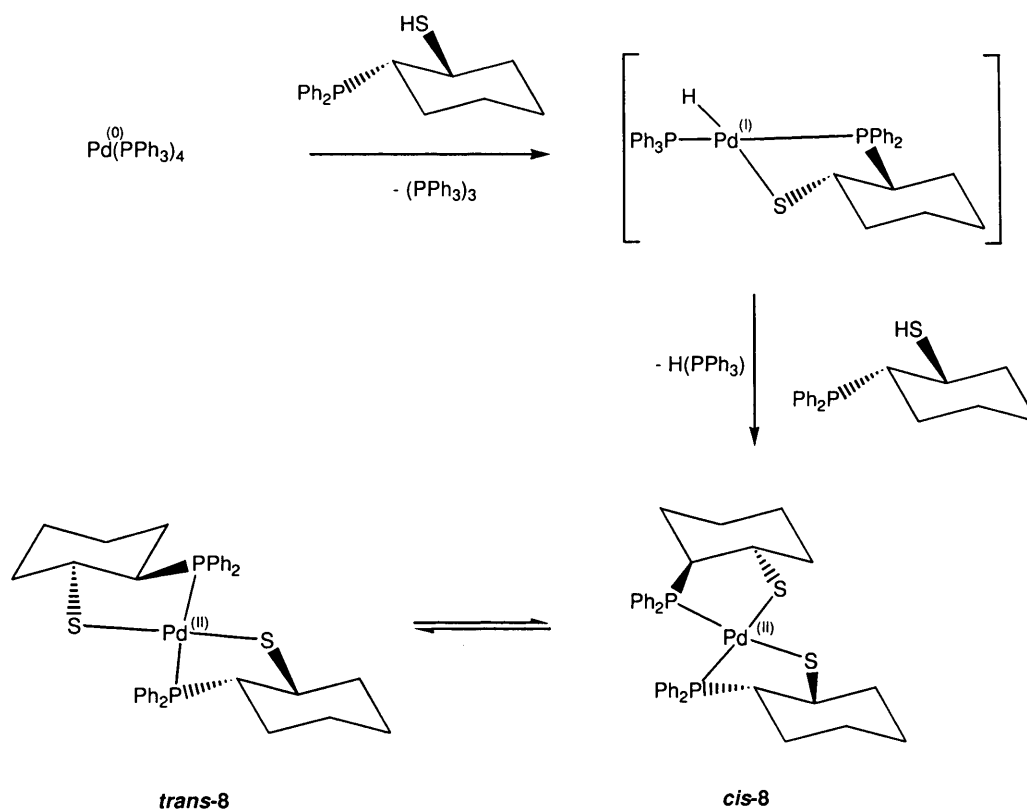
Scheme 3-3: Proposed chelate assisted oxidative addition of a phosphinothiol L^{1}H

After isolating the *cis*-Pd(L^1)$_2$ **8** isomer through re-crystallisation the solid was dissolved in deuterated d^4 methanol for ^{1}H NMR analysis. The NMR spectrum of *cis*-Pd(L^1)$_2$ **8** resulted in the observation of the single stereoisomer. The spectrum shows ten protons in the saturated hydrocarbon region representing the cyclohexyl backbone and ten protons in the aromatic region for the phenyl protons which means ligand protons are in an equivalent environment in the liquid phase.

In the literature only one *cis*-phosphinothiolato complex has been isolated and reported by Real [69] and Canseco-González [79], here we report the second such complex being isolated and make direct comparisons of their crystal structures. Similarly they talk about the chemical equilibrium of a bis-(2-diphenylphosphino-benzenethiol)

palladium (II) complex and its isomerisation in different polarity solvents. Slow crystallisation from CHCl₃/petroleum ether afforded the less soluble *cis* isomer in the shape of yellow needles, as later confirmed by X-ray diffraction. In **Figure 3-6** the ORTEP view of the *cis*-Pd(**L**¹)₂ **8** complex shows the phenyl phosphine groups in a near parallel position. It is also a good representation of the C_2 symmetry seen down the centre of the complex which can be confirmed by all NMR spectra. Unlike *trans*-Ni(**L**¹)₂ **7** the chiral backbone of the *cis*-Pd(**L**¹)₂ **8** complex adopts a *rac* orientation with all the chiral carbons being *trans*-(*S, S*).
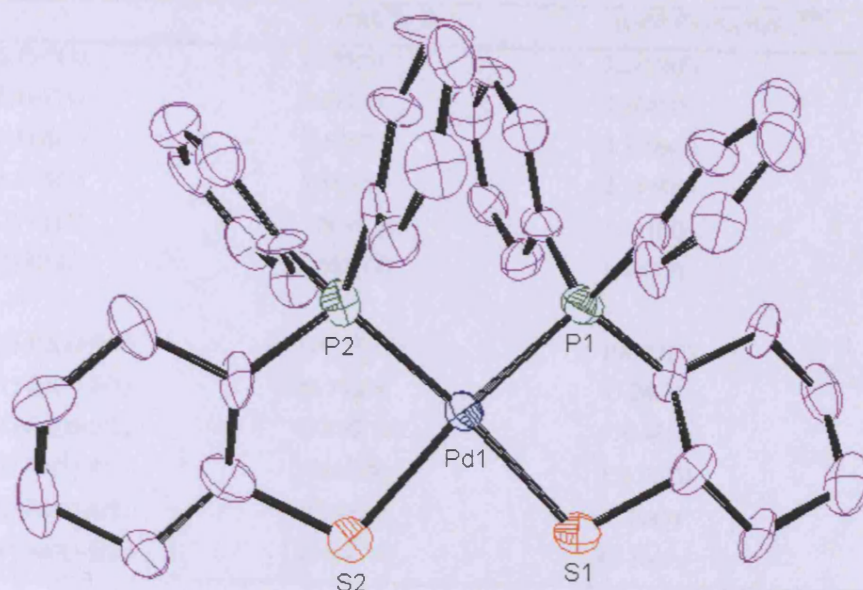
Figure 3-6: Crystal structure of *cis*-Pd(**L**¹)₂ **8.** Hydrogen atoms are omitted for clarity. Thermal ellipsoids are drawn at 50% probability

Crystallographic data obtained for *cis*-Pd(**L**¹)₂ **8** and *cis*-Pd(Ph₂PC₆H₄S)₂ are listed in **Table 3-2** showing the selected bond lengths and angles. The metal-ligand bonds of *cis*-Pd(**L**¹)₂ **8** accommodate the extra strain induced by the bulky diphenylphosphino groups by opening the P(1)-Pd(1)-P(2) angle to 100.57°(17), closing the S1-Pd-S2 angle to 85.85(18)°, and arranging the interfering phenyl rings parallel to each other. This straining of the ligand bite angles is almost identical to that of *cis*-bis-2-(diphenylphosphino)benzenethiol palladium (II) complex where the angles differ less than 0.7°. This shows that the steric bulk of the backbone plays a significant role determining whether *cis* geometry is preferred. One would expect to see a greater bite

78

angle difference between the two complexes due to the carbons on the chelate ring being of different hybridisation states. The chelate carbons of cis-Pd(Ph$_2$PC$_6$H$_4$S)$_2$ being sp^2 compared to the carbons of cis-[Pd(L^1)$_2$] being sp^3, steric repulsion must be an over-riding factor.

Two opposite forces determine the *cis / trans* structural preference of [M(L^1)$_2$] complexes, repulsive steric interactions clearly favouring the *trans* isomers while electronic factors should favour the *cis* isomers. These electronic factors can be attributed to the *trans* effect where the thiolato group has a higher *trans* effect to that of the diphenylphosphino group placing the second chelating ligand in a *cis* geometry.

	cis-Pd(L^1)$_2$ **8**	cis-Pd(Ph$_2$PC$_6$H$_4$S)$_2$[69]
Pd(1)-P(2)	2.271(5)	2.2802(8)
Pd(1)-P(1)	2.274(5)	2.2845(8)
Pd(1)-S(1)	2.298(5)	2.3209(8)
Pd(1)-S(2)	2.317(5)	2.3194(9)
S(2)-C(19)	1.808(19)	1.761(3)
P(1)-C(1)	1.833(17)	1.820(3)
P(2)-Pd(1)-P(1)	100.57(17)	100.57(3)
P(1)-Pd(1)-S(1)	86.74(19)	87.24(3)
P(1)-Pd(1)-S(2)	170.48(19)	170.48(3)
P(2)-Pd(1)-S(1)	171.00(2)	171.05(3)
P(2)-Pd(1)-S(2)	87.39(19)	87.06(3)
S(1)-Pd(1)-S(2)	85.85(17)	85.16(3)

Table 3-2: Selected bond lengths (Å) and angles (°) of cis-Pd(L^1)$_2$ **8** and cis-Pd(Ph$_2$PC$_6$H$_4$S)$_2$

In the literature there is a number of palladium phosphinothiol bis-chelate complexes only isolated in the *trans* geometry [53], [45]. Only a small number of complexes have been structurally characterised using X-ray diffraction methods, shown in **Table 3-3** which will be used to make direct structural comparisons. Palladium bis-chelate *trans*-Pd(L^1)$_2$ **8** was isolated by crystallisation from CHCl$_3$/petroleum ether in the shape of a yellow block shaped crystals. These crystals were then dissolved in CDCl$_3$ for NMR analysis for comparison to that of the *cis* complex. Similarities can be seen in the ^{1}H NMR which is expected with no changes to the chemical environment of any of the corresponding protons. The only anticipated chemical shift changes would be in the aromatic region of the spectrum. With the overlapping of signals in this region it

is impossible to distinguish between any changes in signals between the *cis / trans-*
Pd(L^1)$_2$ **8** complexes. The block shape crystals were isolated using the previously
described techniques and were confirmed to be that of the *trans-*Pd(L^1)$_2$ **8** complex by
X-ray diffraction analysis. In **Figure 3-7** an ORTEP view of the *trans-*Pd(L^1)$_2$ **8**
complex shows the *trans* arrangement and δ skew conformation of the two ligands
around the metal centre analogous to the characteristics seen in *trans-*Ni(L^1)$_2$ **7**.
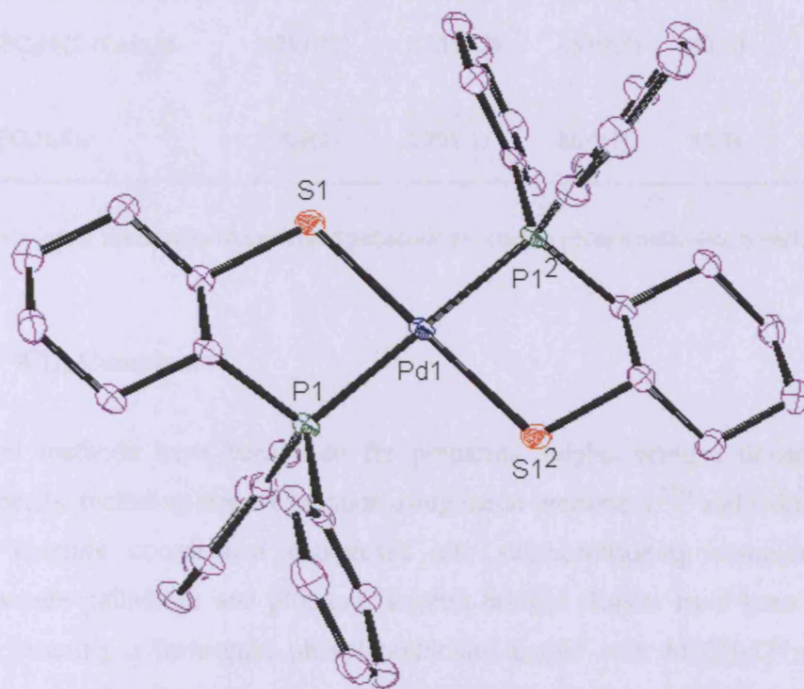
Figure 3-7: Crystal structure of *trans–*Pd(L^1)$_2$ **8**. Hydrogen atoms are omitted for clarity. Thermal
ellipsoids are drawn at 50% probability

Studying the data shown in **Table 3-3** comparisons can be made with previously
prepared *trans* palladium bis-phosphinothiol complexes. The Pd-S bond lengths of both
cis and *trans-*Pd(L^1)$_2$ **8** are within the expected region, similar to that seen before in
analogous complexes [50], [53], [79]. The more significant find is that we can report the
chelate angle of the *trans-*Pd(L^1)$_2$ **8** is the smallest seen at 85.739(19)° for a bis-
chelating palladium phosphinothiolate complex.

Complex	d(M-S) [Å]	d(M-P) [Å]	P-Pd-S [°]	^{31}P NMR	Ref
cis-Pd(Ph$_2$PC$_6$H$_4$S)$_2$	2.2802(8)	2.2802(8)	87.24(3)	48.01	[69]
	2.2845(8)	2.2845(8)	87.06(3)		
cis-Pd(L^1)$_2$	2.298(5)	2.271(5)	86.74(19)	59.90	8
	2.317(5)	2.274(5)	87.39(19)		
trans-Pd(L^1)$_2$	2.3173(5)	2.2971(5)	85.739(19)	62.64	8
trans-Pd(Ph$_2$PC$_2$H$_3$(CH$_2$OCH$_2$Ph)$_2$	2.319(2)	2.282(2)	86.96(7)	50.56	[50]
trans-Pd{Ph$_2$PC$_2$H$_3$[2-(CMe$_2$)5-MeC$_6$H$_8$S}$_2$	2.287(12)	2.335(13)	86.08(5)	50.10	[52]
trans-Pd(Ph$_2$PC$_6$H$_4$S)$_2$	2.308(2)	2.291(1)	86.6(1)	53.74	[72]

Table 3-3: Data for all structurally characterised palladium bis-chelate phosphinothiolato complexes

3.2 [M(L^1)Cl]$_2$ Complexes

Several methods have been used for preparing sulphur-bridged dimers of d^8 transition metals, including direct formation using metal precursors [53] and indirectly by converting existing coordinated complexes into sulphur-bridging complexes [71]. Examples where palladium and platinum sulphur-bridged dimers have been formed directly by reacting a ferrocenyl phosphinothiolato ligand with M(CH$_3$CN)$_2$Cl$_2$ [51]. Another example of a direct formation is seen in the formation of [Pd(dpppt)Cl]$_2$ by reacting Pd(PPh$_3$)$_2$Cl$_2$ and dppptH without formation of the expected triphenylphosphine complex [Pd(dpppt)(PPh$_3$)Cl] [71]. Sulphur bridged dimers have also been obtained by cleavage of the S-C thioether bond, the complex [Pd{PCy$_2$CH$_2$CH(CH$_3$)S}Cl]$_2$ was obtained according to this method [99]. The nickel dimer [Ni(L^1)Cl]$_2$ 9 was isolated as a deep red solid after reacting equimolar amounts of NiCl$_2$.6H$_2$O and L^{1}H in a dichloromethane solution (Scheme 3-4).
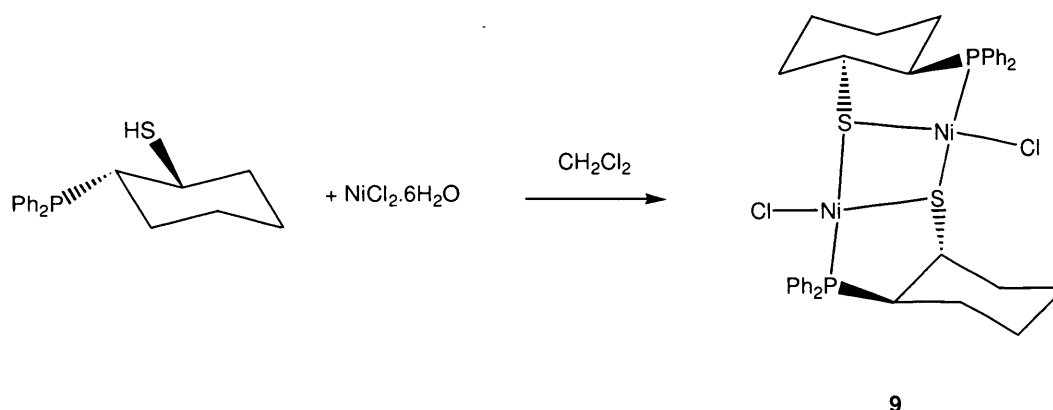
Scheme 3-4: Reaction scheme for the direct synthesis of [Ni(L^1)Cl]$_2$ **9**

Thiolato ligands are well known for forming sulphur-bridged species in the absence of other suitable ligands. Although the chloride may also act as a bridging ligand the bridging ability of the sulphur is over-riding, as evidence of this has been previously reported [89]. Starting from racemic **L^{1}H** the ^{31}P{^{1}H} spectrum of [Ni(L^1)Cl]$_2$ **9** shows one singlet at δ_P 42.3 instead of the expected two singlets due to the diasteromeric *meso* and *rac* isomers of [Ni(L^1)Cl]$_2$ **9**. Single crystals of [Ni(L^1)Cl]$_2$ **9** were grown by the slow diffusion of diethyl ether into a solution of CH$_2$Cl$_2$. Using these crystals, crystallographic data was obtained by X-ray diffraction confirming the complexes dimeric structure as shown in **Figure 3-8**, where the 5-membered chelates adopt an *S*(δ) skew confirmation. The nickels are bridged by thiolates, and the chloride atoms take up non-bridging positions at the end of each dimer unit. The ORTEP view shows [Ni(L^1)Cl]$_2$ to be a *rac* orientation with the ligands being of (*R*, *R*) stereochemistry.
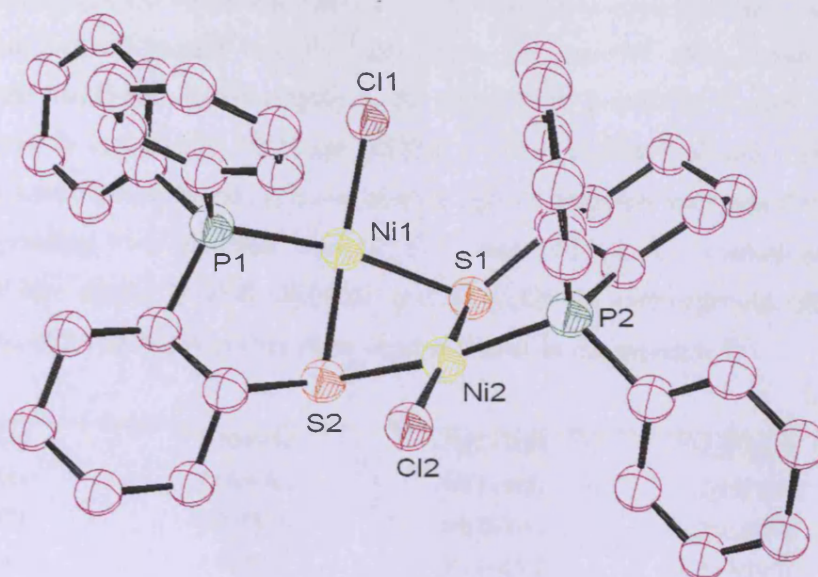
Figure 3-8: Crystal structure of [Ni(**L¹**)Cl]₂ **9**. Hydrogen atoms are omitted for clarity. Thermal ellipsoids are drawn at 50% probability

Selected bond lengths and angles of dimer [Ni(**L¹**)Cl]₂ **9** are presented in **Table 3-4**. From the ORTEP view the complex geometry around the two metal centres is a distorted square planar and the molecule is bent about the *S-S* axis adopting a 'butterfly' core structure with *syn* orientation of the sulphur substituents. For μ–SR⁻ complexes both *syn* and *anti* orientations of the sulphur substituents have been observed [51]. The preference for a *syn* orientation of the μ–SR⁻ substituent for complex [Ni(**L¹**)Cl]₂ **9** is likely to arise from the prevailing skew conformation that places the cyclohexyl substituents of the metallacycle in the sterically favoured pseudoequitorial position. The dihedral angle defined by the two NiS₂ planes in complex **9** is 111.32(6)° and is one of the smallest reported so far. The S-Ni-S angles are 79.34(2)° and 79.81(2)° respectively and are at the lower end of the literature range of 80-86° [112]. For similar complexes the rather small S-Ni-S angles and *syn* orientation of the sulphur substituents have been attributed to the repulsive interaction between the lone pairs on the sulphur atom and metal *d*-electrons [112]. After studying the nickel thiolate bond lengths we can report differences in their bond lengths owing to the *trans* influence. The *trans* influence uses a series of functional group to class ligands relative *trans* influence of which the substituents in complex **9** are present being Cl < PR₃, SR₂. The *trans* influence is particularly seen in square planar complexes the ligands *trans* to each other can affect relative bond energies and lengths. This can be seen in complex **9** where the Ni(1)-S(1)

and Ni(2)-S(2) are affected by the greater *trans* influence of -PPh$_2$ compared to Ni(1)-S(2) and Ni(2)-S(1) which are *trans* to -Cl. The degree of *trans* influence can be seen in the relative bond lengths with the greater *trans* influence of -PPh$_2$ causing the Ni(1)-S(2) and Ni(2)-S(1) bond lengths to be stretched to 2.2353(6) Å and 2.2184(6) Å compared to that of Ni(1)-S(1) and Ni(2)-S(2) being 2.1694(6) Å and 2.1651(7) Å. A similar trend was observed for the analogous thiolate complex [Ni(dppet)Cl]$_2$, where the corresponding Ni-S distances were 2.230(3) and 2.164(3) Å , respectively [116]. The chelate bite angles, P-Ni-S, 88.39(6)° and 88.96(6)° are unexceptional and the Ni-Ni distance of 2.7882(4) Å is very close to what is seen in the literature [53].

Ni(1)-P(1)	2.1680(6)	Ni(2)-P(2)	2.1520(6)
Ni(1)-S(1)	2.1694(6)	Ni(2)-S(2)	2.1651(7)
Ni(1)-S(2)	2.2353(6)	Ni(2)-S(1)	2.2184(6)
Ni(1)-Cl(1)	2.1779(7)	Ni(2)-Cl(2)	2.1803(7)
P(1)-C(6)	1.840(2)	P(2)-C(24)	1.853(2)
S(1)-C(1)	1.836(2)	S(2)-C(19)	1.842(2)
P(1)-Ni(1)-S(1)	88.34(2)	P(2)-Ni(2)-S(2)	89.28(2)
P(1)-Ni(1)-S(2)	165.95(3)	P(2)-Ni(2)-S(1)	168.05(3)
P(1)-Ni(1)-Cl(1)	93.47(3)	P(2)-Ni(2)-Cl(2)	92.13(3)
Cl(1)-Ni(1)-S(2)	98.42(3)	Cl(2)-Ni(2)-S(2)	98.65(2)
S(1)-Ni(1)-Cl(1)	176.01(3)	S(1)-Ni(2)-Cl(2)	177.86(3)
S(1)-Ni(1)-S(2)	79.34(2)	S(2)-Ni(2)-S(1)	79.81(2)

Table 3-4: Selected bond lengths (Å) and angles (°) of [Ni(L^1)Cl]$_2$ **9**

Attempts were then made to prepare the palladium dimer complex analogous to that of [Ni(L^1)Cl]$_2$ **9**. The first attempt was by means of a direct addition of one equivalent of the ligand L^{1}H to a CH$_2$Cl$_2$ solution of palladium bisbenzonitrile dichloride. The reaction produced two peaks in the phosphorus NMR and was later found to be the *cis* / *trans* equilibrium of the bis-chelates. Attempts were then made to form the dimer complex indirectly by reacting one equivalent of palladium bisbenzonitrile chloride with a toluene solution of the mixture *cis* / *trans*-Pd(L^1)$_2$ **8** at 120°C. Again the dimer product was not isolated leaving the final route of forming the dimer by initially synthesising the thioether complex palladium 2-(diphenylphosphino)cyclohexanethiomethyl and demethylating to produce the corresponding palladium dimer complex. Failure to produce the dimer in this reaction led us to the conclusion that the rigid backbone of the ligand stops the thiol from

orientating itself into a position that can accommodate the tri-coordinated bridging sulphur. There is evidence that phosphinothiolate ligands only form square planar complexes, they are usually seen in ligands that have a constrained backbone not allowing the sulphur to sit in a pyramidal arrangement [51]. For this particular ligand the cyclohexyl backbone forces the sulphur into a position that favours the formation of the bis-chelate complex.

3.3 Bis[palladium 2-(diphenylphosphino)cyclohexanethiol chloride] 10

The synthesis of 2-(diphenylphosphino)ethanethiol (Hdppet) has been well documented [42]. Coordination of such a ligand with a number of late transition metals has been studied, including the synthesis of palladium (II) complexes [71]. From the literature review on phosphinothiol complexes (Scheme 3-5) we discovered that synthesis of a palladium (II) chloride dimer using ligand Hdppet had not been reported. Our aim was to synthesis the [Pd(dppet)Cl]$_2$ complex using an alternative method to that used in the direct formation of [Ni(L^1)Cl]$_2$ 9. Initially the bis(2-diphenylphosphino)ethanethiolate) palladium (II) complex was formed using a previously published method by Brugat [71]. The complex was then recrystallised for purification, and reacted with one equivalent of palladium bis-benzonitrile dichloride in a solution of toluene. The solution was heated to 110°C and stirred overnight (Scheme 3-5).
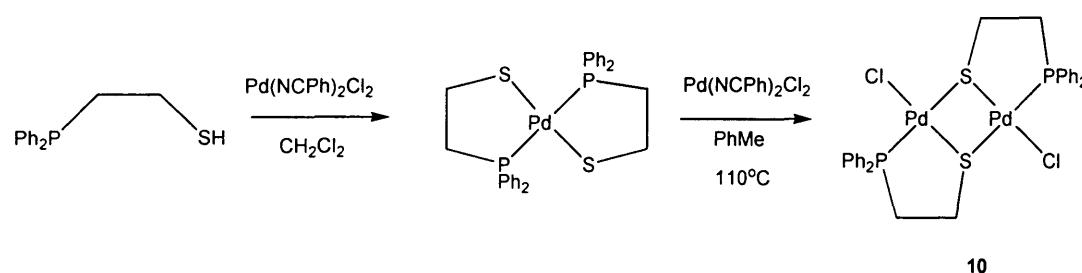
Scheme 3-5: Two-step process for the synthesis of bis[palladium 2-(diphenylphosphino)ethanethiol chloride] 10

The reaction progress was monitored by ^{31}P NMR spectroscopy following the expected disappearance of the signal corresponding to the bis-chelate at δ_P 64.2 followed by the appearance of the desired product at δ_P 59.3. Crystals suitable for X-ray diffraction analysis were grown by the slow diffusion of diethyl ether into a solution of

CH$_2$Cl$_2$. From these crystals crystallographic data was obtained by X-ray diffraction confirming the complexes dimeric structure as shown in **Figure 3-9**.
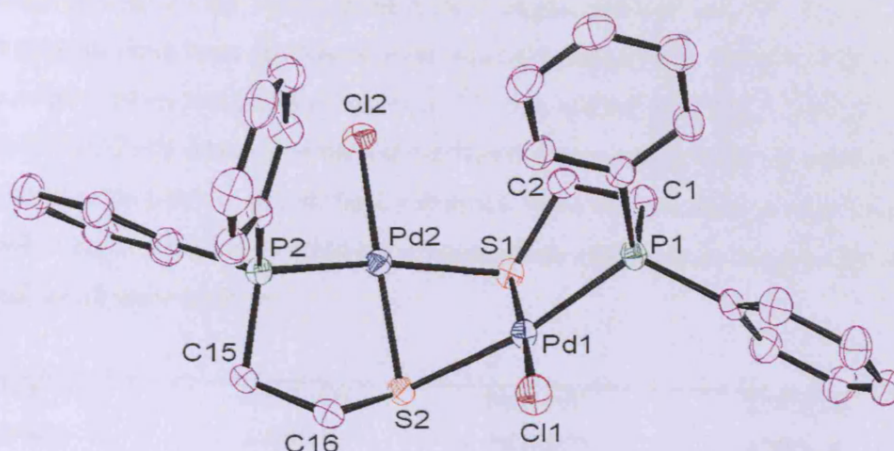
Figure 3-9: Crystal structure of [Pd(Ph$_2$PCH$_2$CH$_2$S)Cl]$_2$ **10**. Hydrogen atoms are omitted for clarity. Thermal ellipsoids are drawn at 50% probability

After studying the crystallographic data we can ascertain that the [Pd(dppet)Cl]$_2$ complex does not hold any points of symmetry. The complex does prefer to adopt an (δ) skew confirmation in the solid state which orientates the protons of the backbone away from the sterically bulky diphenylphosphino groups (**Figure 3-10**). With both sides of the ligand being sterically equivalent we would assume that both conformations would be formed in solution being energetically equivalent.
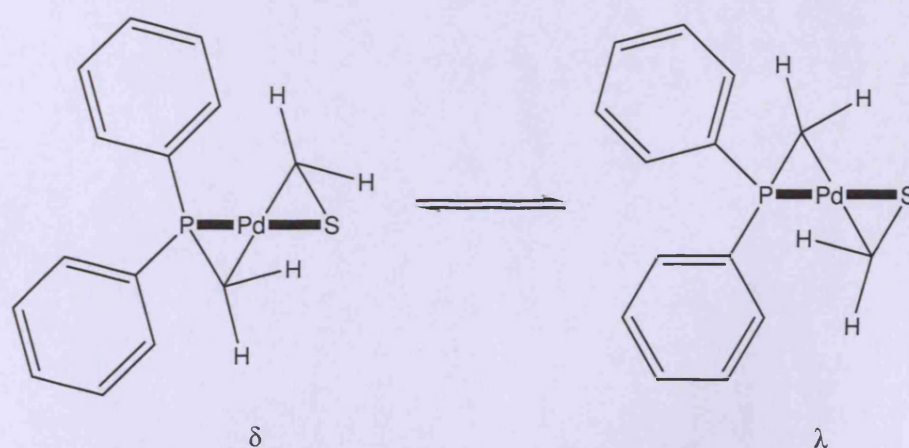
Figure 3-10: Skew conformations showing both the (δ) and (λ) conformations for [Pd(dppet)Cl]$_2$ **10**

86

Crystallographic data obtained for **10** are listed in **Table 3-5** showing selected bond lengths and angles. The dihedral angle defined by the two PdS_2 planes in complex **10** is 128.63(5)° at the high end of dihedral angles. The S-Pd-S angles are 80.99(5)° and 80.69(5)° respectively and are at the lower end of the literature range of 80-88° [112]. For similar complexes the rather small S-Pd-S angles and *syn* orientation of the sulphur substituents have been attributed to the repulsive interaction between the lone pairs on the sulphur atom and metal *d*-electrons [112]. The chelate bite angles, P-Pd-S, 87.62(5)° and 86.71(5)° are unexceptional and the Pd-Pd distance of 3.010(5) Å shows that a Pd-Pd bond cannot be made over such a distance. With the two metal centres based on the dihedral angle there are no vacant *d*-orbitals which can orientate into a position where a metal-metal bond can form.

Pd(1)-P(1)	2.2353(13)	Pd(2)-P(2)	2.2477(14)
Pd(1)-S(1)	2.2901(13)	Pd(2)-S(2)	2.2895(14)
Pd(1)-S(2)	2.3749(13)	Pd(2)-S(1)	2.3895(13)
Pd(1)-Cl(1)	2.3287(13)	Pd(2)-Cl(2)	2.3405(14)
P(1)-C(1)	1.836(5)	P(2)-C(15)	1.836(5)
S(1)-C(2)	1.839(5)	S(2)-C(16)	1.828(5)
P(1)-Pd(1)-S(1)	87.62(5)	P(2)-Pd(2)-S(2)	86.71(5)
P(1)-Pd(1)-Cl(1)	92.67(5)	P(2)-Pd(2)-Cl(2)	96.40(5)
S(2)-Pd(1)-Cl(1)	98.35(5)	S(1)-Pd(2)-Cl(2)	96.67(5)
S(1)-Pd(1)-S(2)	80.99(5)	S(1)-Pd(2)-S(2)	80.69(5)
P(1)-Pd(1)-S(2)	167.33(5)	P(2)-Pd(2)-S(1)	163.61(5)
S(1)-Pd(1)-Cl(1)	176.45(5)	S(2)-Pd(2)-Cl(2)	176.11(5)

Table 3-5: Selected bond lengths (Å) and angles (°) of [Pd(dppet)Cl]$_2$ **10**

3.4 Palladium (II) bis(diphenylphosphino)cyclohexanethiol palladium (II) dichloride 11

The work of Roundhill [98] reported the interconversion of *o*-(diphenylphosphino)thioanisole to the dimer complex diiodobis[(diphenylphosphino)benzenethiolato]dipalladium (II) shown in **Scheme 3-6**. They reported that the dimer was synthesised through the demethylation of [PdI₂(*o*-MeSC₆H₄PPh₂)]. The species was identified using spectroscopic evidence obtained after heating [PdI₂(*o*-MeSC₆H₄PPh₂)] in DMF solvent. To re-coordinate and reform the starting phosphinothioether complex the dimer was dissolved in DMF, and reacted with methyl iodide and an excess of iodide.
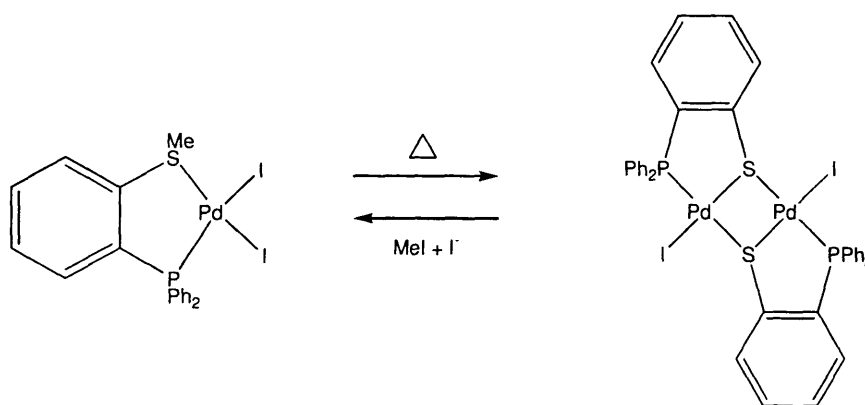
Scheme 3-6: Formation of a palladium dimer via an indirect thermal conversion

The progress of the reactions was monitored using UV-Vis spectroscopy with each coordinated species giving its own distinct absorbance. After previous unsuccessful attempts to synthesise the corresponding bis-(diphenylphosphino)cyclohexane thiol dichloride dipalladium (II) complex this similar synthetic route was utilised.

The mixture of *cis* / *trans*-Pd(L^1)$_2$ **8** dissolved in toluene was reacted with cyclohexyl chloride at elevated temperatures (70°C) overnight (**Scheme 3-7**). With bis-chelate complex **8** existing in a *cis* / *trans* equilibrium we expected the disappearance of both the chelate signals in the ^{31}P NMR spectrum. After a period of 3 hours the reaction was proceeding with a signal seen in the ^{31}P NMR spectrum at δ_P 45.0, completion of the reaction was observed after stirring overnight. With one singlet in the ^{31}P NMR spectrum, *trans*-Pd(L^{1}Cy)$_2$ was proposed with the observation of cyclohexane protons in the saturated region of the ^{1}H NMR spectrum. Attempts to isolate the intermediate proved unsuccessful, therefore the reaction was continued in attempt to isolate the final product. The final synthetic step involved heating the intermediate to 110°C in a solution of toluene and adding one equivalent of palladium bis-benzonitrile chloride. Over a period of 24 hours the solution formed a dark orange colour and ^{31}P NMR spectroscopy shown a new signal at δ_P 63.2.
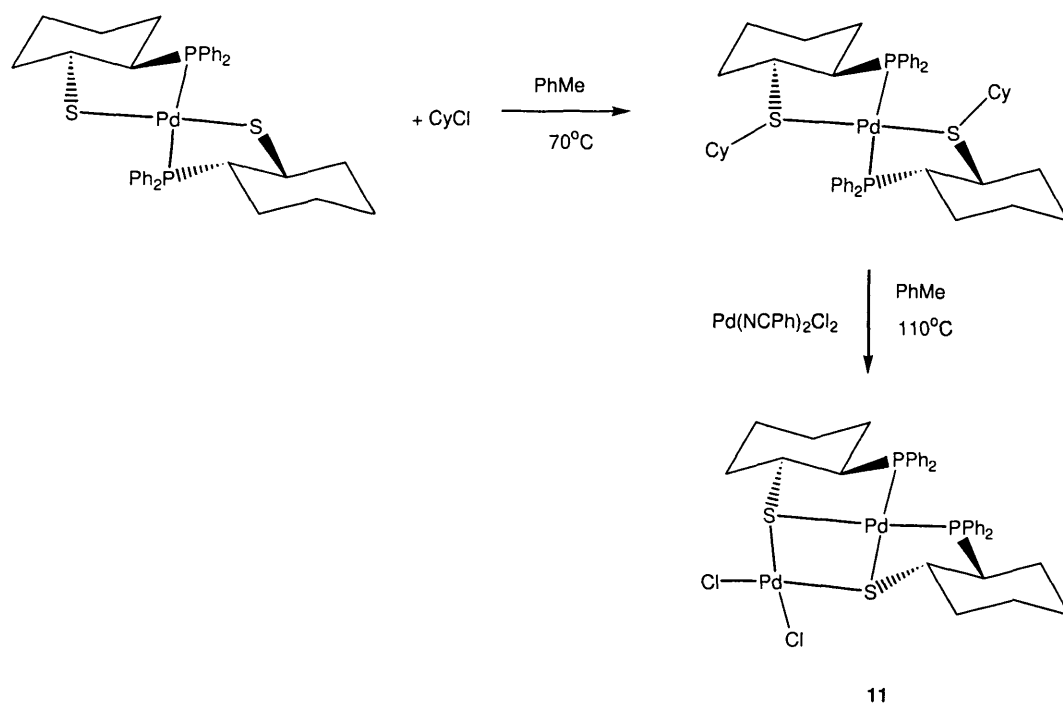
Scheme 3-7: Formation of *cis*-bis(diphenylphosphino)cyclohexanethiol dichloride palladium (II) complex [*cis*-Pd(L^1)$_2$PdCl$_2$] **11**

The complex was the isolated by the slow diffusion of diethyl ether into a solution of chloroform, forming single crystals that were suitable for X-ray diffraction analysis. An ORTEP view of complex **11** is shown in **Figure 3-11**, and confirms a palladium dimer complex is formed with an unexpected geometry. The resulting complex is *cis* coordinated with sulphur bridging and chloride non-bridging end groups situated on one of the palladium metal centres. Using the crystal data we can confirm that the *meso* stereoisomer is formed with the chiral carbons adopting a (*R*, *S*) orientation therefore no enantiomeric mixtures are present.
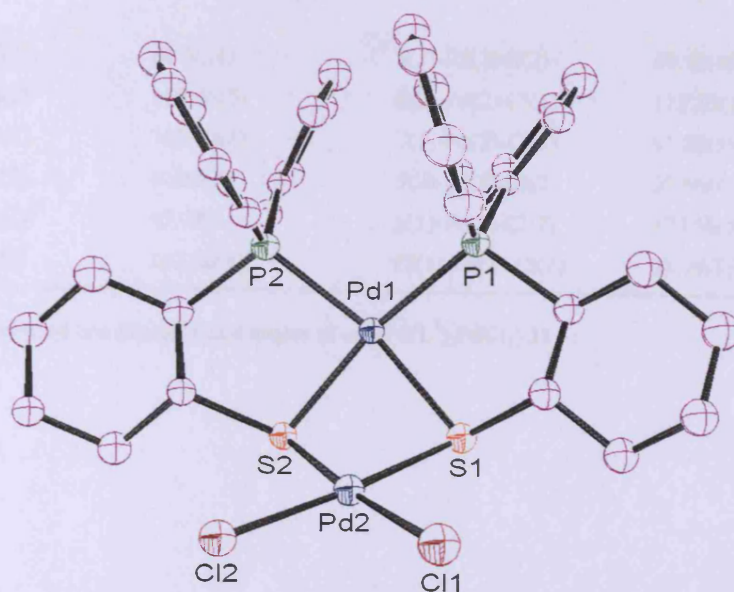
Figure 3-11: Crystal structure of Pd(**L^1**)$_2$PdCl$_2$ **11**. Hydrogen atoms are omitted for clarity. Thermal ellipsoids are drawn at 50% probability

The dihedral angle defined by the two PdS$_2$ planes in complex **11** is 133.01(4)°
is one of the largest reported so far. Selected bond angles and lengths of complex *cis*-
Pd(L^1)$_2$PdCl$_2$ **11** are shown in **Table 3-6**. The most notable information gathered from
this data is found in the variation of Pd-S bond lengths giving evidence of the *trans*
influence similar to that seen in complex **9**.

Pd(1)-P(1)	2.2811(12)	Pd(2)-S(2)	2.3063(12)
Pd(1)-P(2)	2.2804(12)	Pd(2)-S(1)	2.3157(13)
Pd(1)-S(1)	2.3089(11)	Pd(2)-Cl(1)	2.3290(12)
Pd(1)-S(2)	2.3177(12)	Pd(2)-Cl(2)	2.3301(13)
P(1)-Pd(1)-S(1)	88.30(4)	S(1)-Pd(2)-S(2)	80.96(4)
P(1)-Pd(1)-S(2)	168.06(5)	S(2)-Pd(2)-Cl(1)	172.85(5)
P(2)-Pd(1)-S(1)	168.12(4)	S(1)-Pd(2)-Cl(1)	91.88(5)
S(1)-Pd(1)-S(2)	80.87(4)	S(2)-Pd(2)-Cl(2)	92.66(4)
P(2)-Pd(1)-S(2)	87.78(4)	S(1)-Pd(2)-Cl(2)	173.58(5)
P(1)-Pd(1)-P(2)	102.66(4)	Cl(1)-Pd(2)-Cl(2)	94.49(5)

Table 3-6: Selected bond lengths and angles of *cis*-[Pd(L^1)$_2$PdCl$_2$] **11**

Below is a list of phosphinothiol complexes that allow palladium dimer complexation and their respective sulphur coordination bond angles (**Table 3-7**). In the formation of palladium dimer complexes the sulphur must have to some extent a degree of flexibility. From the data gathered one can see the range of bond angle which the sulphur must accommodate coordination, the simple ethylene backbone of [Pd(dppet)Cl]$_2$ exerts the least strain on the sulphur coordination with the smallest M-S-C bond angle. Compared to the largest backbone of the ferrocenyl complex which imparts an opening of the M-S-C bond angle to 113.08°, this is over ten degrees more than a simple ethylene backbone. For our ligand which has a conformationally confined backbone which limits the amount of movement in the backbone of the ligand and therefore does not accommodate the formation of a sulphur bridging dimer complex.

Complex	M-S-C (°)	[M(L)Cl]$_2$ formation	M-S-C (°)	Ref
Pd(dppet)$_2$	Not available	[Pd(dppet)Cl]$_2$	102.43, 104.39	**10**
Pd(Ph$_2$PC$_6$H$_4$S)$_2$		[Pd(Ph$_2$PC$_6$H$_4$S)I]$_2$	106.35, 104.88	[98]
Pd(Cy$_2$PC$_2$H$_3$MeS)$_2$		[Pd(Cy$_2$PC$_2$H$_3$MeS)Cl]$_2$	104.56, 102.74	[89]
Pd(Ph$_2$PC$_2$H$_3$EtS)$_2$	104.65 106.75	[Pd(Ph$_2$PC$_2$H$_3$EtS)Cl]$_2$	103.61, 105.14	[53]
Pd(Ph$_2$PCpFeCpS)		[Pd(CpFePh$_2$PC$_5$H$_3$CHMeS)Cl]$_2$	109.23, 108.84	[49]
Pd(Ph$_2$PCpFeCpS)		[Pd(Ph$_2$PCpFeCpS)N(tBu)]$_2$	113.08, 111.13	[49]
trans-Pd(L^1)$_2$	105.96 105.96	Not formed	Not Formed	**8**
Pd(Ph$_2$PC$_2$H$_3$CH$_2$OCH$_2$Ph	107.6(3) 105.3(2)	Not formed	Not Formed	[50]
Pd[Ph$_2$PC$_2$H$_3$C$_6$H$_3$Me(t-Bu)S]	107.4(2) 102.4(2)	Not formed	Not Formed	[52]

Table 3-7: Review of ligand and their formation of palladium dimer complexes

Formation of complex **11** gives further evidence that the backbone of the ligand influences the readiness of the formation of palladium dimer complexes. As we can see from the data below (**Table 3-8**) the factors that influence the formation of a standard dimer complex are not dependant on bond lengths. Preference for ligand L^1 to form the cis-Pd(L^1)$_2$ complex instead of a standard dimer can be attributed to the bite angles of the ligand which are relatively fixed by the ligand backbone. In the case of cis-Pd(L^1)$_2$ **8** the bite angles fit perfectly for a cis-bis-chelate and replicates the orientation of cis-Pd(Ph$_2$PC$_6$H$_4$S)$_2$[69] as discussed previously. The nickel complex Ni(L^1)$_2$ **7** shows how the cis geometry is not formed with a total preference of the $meso$ $trans$-Ni(L^1)$_2$ bis-chelate. This means there is no preference of the cis geometry and allows the standard rac dimer to be synthesised. A combination of ligand bite angle and the preference of conformationally confined stereoisomers attributes to the preferred synthesis of the $meso$-$trans$, rac-cis bis-chelates or rac-dimer complexes. The formation of cis-bis-chelates is unusual and in the case of ligand L^1 the conformational confined backbone gives such preference to the formation of the rac cis-Pd(L^1)$_2$ geometry that the rac-dimer cannot be synthesised.

No.	Complex	M-P (Å)	M-S (Å)	P-M-S (°)	M-S-C (°)	Stereoisomer
7	$trans$-Ni(L^1)$_2$	2.1708(7)	2.1713(7)	91.01(3)	106.82(10)	$meso$
8	$trans$-Pd(L^1)$_2$	2.2971(5)	2.3173(5)	85.74(19)	105.96(7)	$meso$
8	cis-Pd(L^1)$_2$	2.271(5)	2.298(5)	86.74(19)	105.5(5)	rac
		2.274(5)	2.317(5)	87.39(19)	105.3(5)	
9	[Ni(L^1)Cl]$_2$	2.1680(6)	2.1694(6)	88.34(2)	105.90(7)	rac
		2.1520(6)	2.2353(6)	89.28(2)	111.65(8)	
			2.1651(7)		107.21(8)	
			2.2184(6)		115.37(8)	
10	[Pd(SC$_2$H$_4$PPh$_2$)Cl]$_2$	2.2353(13)	2.2901(13)	87.62(5)	111.25(18)	No chiral
		2.2477(14)	2.2895(14)	86.71(5)	102.43(17)	centre
					111.36(18)	
					104.39(18)	
11	cis-Pd(L^1)$_2$PdCl$_2$	2.2811(12)	2.3157(13)	87.39(19)	110.94(17)	$meso$
		2.2804(12)	2.3177(12)	86.74(19)	102.65(16)	
			2.3063(12)		113.16(16)	
			2.3089(11)		103.21(15)	

Table 3-8: Structural comparison of selected bond lengths (Å) and angles (°) of complexes synthesised

3.5 Experimental
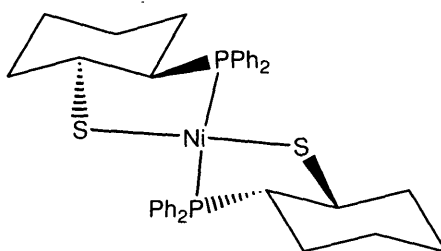
Preparation of *trans*-Ni(SC₆H₁₀PPh₂)₂ 7. NiCl₂.6H₂O (0.13 g, 0.547 mmol) and $\mathbf{L^1H}$ (0.16 g, 0.547 mmol) were dissolved in anhydrous PhMe (30 ml) whilst stirring under argon. The reaction mixture was then stirred at room temperature for 2 hours. *trans*-Ni($\mathbf{L^1}$)₂ **7** was isolated from slow diffusion of petroleum ether into a dichloromethane solution. This method afforded green block type crystals suitable for X-ray diffraction. Yield 0.23g (63%).δ_H (CDCl₃, 400MHz) 0.79 (2H, m, Cy), 1.04 (1H, m, Cy), 1.23 (1H, m, Cy), 1.48 (2H, m, Cy), 1.81 (2H, m, Cy), 2.05 (1H, m, Cy), 2.27 (1H, m, Cy), 7.16-7.62 (15H, m, Ar*H*), 7.82 (2H, m, Ar*H*), 7.95 (1H, m, Ar*H*). δ_P (CDCl₃, 121MHz) 63.2.
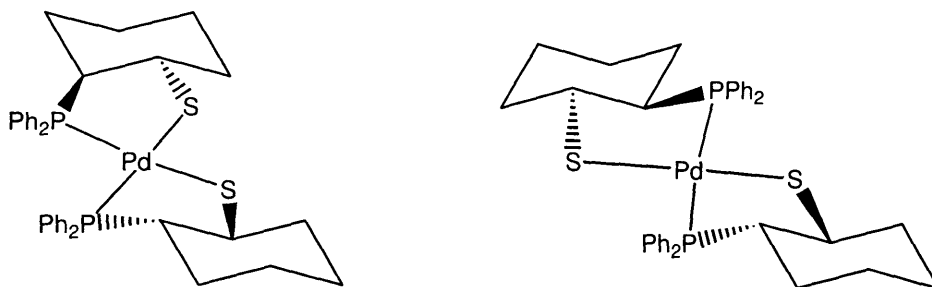
Preparation of Pd(SC₆H₁₀PPh₂)₂ *cis / trans*-8. PdCl₂(NCPh)₂ (0.27 g, 0.705 mmol) and $\mathbf{L^1H}$ (0.21 g, 0.705 mmol) were dissolved in anhydrous CH₂Cl₂ (30 ml) whilst stirring under argon. The reaction mixture was then stirred at room temperature for 2 hours. Yield 0.36g (72%) *cis*-Pd($\mathbf{L^1}$)₂ **8** was isolated from slow diffusion of petroleum ether into a dichloromethane solution. This method afforded yellow needle type crystals suitable for X-ray diffraction. *trans*-Pd($\mathbf{L^1}$)₂ **8** was isolated from slow diffusion of diethyl ether into a solution of chloroform. This method afforded yellow block type crystals suitable for X-ray diffraction.

***rac- cis*–Pd($\mathbf{L^1}$)₂ 8.** δ_H (CDCl₃, 400MHz) 0.81 (2H, m, Cy), 0.92 (1H, m, Cy), 1.30 (1H, m, Cy), 1.48 (3H, m, Cy), 1.95 (1H, m, Cy), 2.13 (1H, m, Cy), 2.29 (1H, m, Cy),

7.00 (4H, t, $^3J_{HH}$ = 6.7 o-ArH), 7.08 (1H, m, p-ArH), 7.20 (2H, t, $^3J_{HH}$ = 6.6), 7.32 (1H, m, ArH), 7.50 (2H, t, $^3J_{HH}$ = 9.4). δ_C (125 MHz, CDCl$_3$) 29.71 (1C, s, Cy), 37.85 (1C, s, Cy), 41.12 (1C, s, Cy), 42.50 (1C, s, Cy), 57.75 (1C, s, Cy), 58.03 (1C, s, Cy), 127.89 (1C, m, Ph), 128.15 (1C, t, Ph, $^3J_{CP}$ = 3.7), 128.58 (1C, t, Ph, $^3J_{CP}$ = 3.7), 129.75 (1C, t, Ph, $^3J_{CP}$ = 9.7), 130.29 (1C, s, Ph), 131.01 (1C, s, Ph), 131.85 (1C, t, Ph, $^3J_{CP}$ = 4.9), 132.08 (1C, t, Ph, $^3J_{CP}$ = 4.9), 136.26 (1C, t, Ph, $^3J_{CP}$ = 7.6). δ_P (CDCl$_3$, 121MHz) 59.9.

***meso*- *trans*-Pd(L^1)$_2$ 8.** δ_H (CDCl$_3$, 400MHz) 0.75 (1H, m, Cy), 0.87 (1H, m, Cy), 1.15 (1H, m, Cy), 1.58 (2H, m, Cy), 1.72 (1H, m, Cy), 1.88 (1H, m, Cy), 2.09 (1H, m, Cy), 2.36 (2H, d, Cy), 4.07 (1H, d, Cy, $^2J_{HH}$ = 13.6), 4.94 (1H, d, Cy, $^2J_{HH}$ = 13.6) 7.14-7.73 (15H, m, ArH). δ_C (125 MHz, CDCl$_3$) 24.58 (1C, s, Cy), 25.10 (1C, s, Cy), 26.50 (1C, s, Cy), 36.07 (1C, s, Cy), 40.84 (1C, s, Cy), 43.26 (1C, s, Cy), 128.21 (1C, s, Ph), 128.34 (1C, s, Ph), 128.40 (1C, s, Ph), 129.29 (1C, s, Ph), 129.54 (1C, s, Ph), 131.17 (1C, s, Ph), 131.26 (1C, s, Ph), 132.34 (1C, s, Ph), 135.52 (1C, s, Ph), 135.65 (1C, s, Ph), 136.92 (1C, s, Ph), 139.16 (1C, s, Ph). δ_P (CDCl$_3$, 121MHz) 62.6.
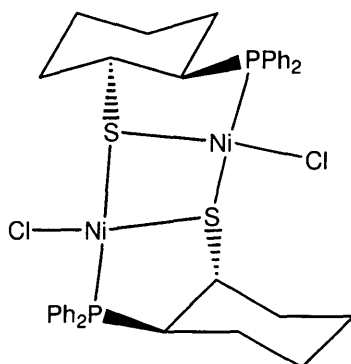
Preparation of [Ni(SC$_6$H$_{10}$PPh$_2$)Cl]$_2$ 9. NiCl$_2$.6H$_2$O (0.15 g, 0.651 mmol) and L^{1}H (0.20 g, 0.651 mmol) were dissolved in anhydrous CH$_2$Cl$_2$ (30 ml) whilst stirring under argon. The reaction mixture was then stirred at room temperature for 2 hours. Removal of the solvent left a red solid. [Ni(L^1)Cl]$_2$ 9 was isolated from slow diffusion of diethyl ether into a dichloromethane solution. This method afforded dark red block type crystals suitable for X-ray diffraction. Yield 0.29 g (57%). δ_H (CDCl$_3$, 400MHz) 0.75 (1H, m, Cy), 0.87 (1H, m, Cy), 1.15 (1H, m, Cy), 1.58 (2H, m, Cy), 1.72 (1H, m, Cy), 1.88 (1H, m, Cy), 2.09 (1H, m, Cy), 2.36 (2H, d, Cy), 4.07 (1H, d, Cy, $^2J_{HH}$ = 13.6), 4.94 (1H, d, Cy, $^2J_{HH}$ = 13.6) 7.14-7.73 (15H, m, ArH). δ_P (CDCl$_3$, 121MHz) 42.3.

λ

Preparation of [Pd(SC₂H₄PPh₂)Cl]₂ 10.
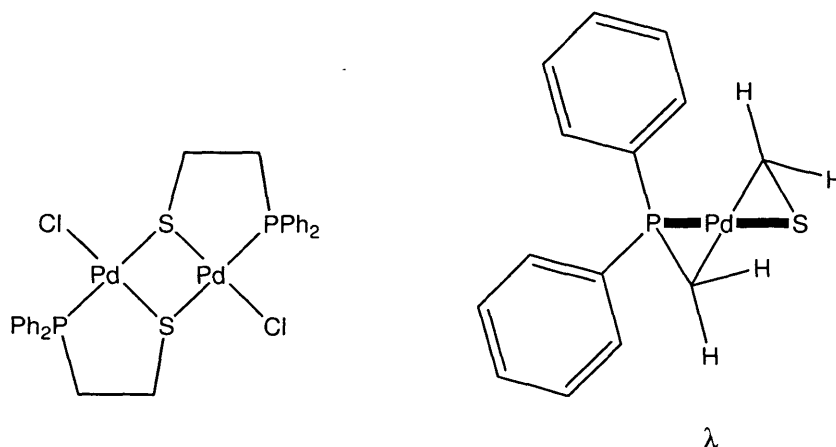
Preparation of [Pd(SC₂H₄PPh₂)Cl]₂ 10. Pd(NCPh)₂Cl₂ (0.20 g, 0.51 mmol) and dppet (0.25 g, 1.02 mmol) were dissolved in anhydrous CH₂Cl₂ (30 ml) whilst stirring under argon. The reaction mixture was then stirred at room temperature for 2 hours. Removal of the solvent left a red solid. The solid was then dissolved in a solution of toluene (30 ml) along with Pd(NCPh)₂Cl₂ (0.20 g, 0.51 mmol) and heated to 110°C with constant stirring for 24 hours. The solvent was removed leaving a dark red solid. [Pd(dppet)Cl]₂ 10 was isolated from slow diffusion of diethyl ether into a dichloromethane solution. This method afforded dark red block type crystals suitable for X-ray diffraction. Yield 0.38 g (48%). δ_H (CDCl₃, 400MHz) 2.86 (4H, m, CH₂), 2.97 (4H, m, CH₂), 7.48 (12H, m, Ph), 7.89 (8H, m, Ph). δ_P (CDCl₃, 121MHz) 59.3.

Preparation of cis-Pd(SC₆H₁₀PPh₂)₂PdCl₂ 11.
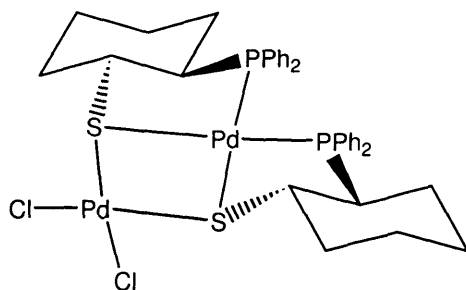
Preparation of cis-Pd(SC₆H₁₀PPh₂)₂PdCl₂ 11. Pd(L¹)₂ (0.21 g, 0.298 mmol) and cyclohexyl chloride (0.08 g, 0.61 mmol) were dissolved in anhydrous toluene (30 ml) whilst stirring. The reaction mixture was then stirred at 70°C for 24 hours in a sealed pressure tube. Pd(NCPh)₂Cl₂ (0.12g, 0.31 mmol) was then added to the reaction and the solution was stirred at 110°C for a further 24 hours in a sealed pressure tube. Removal of the solvent left a red solid. Pd(L¹)₂PdCl₂ 11 was isolated from slow diffusion of

diethyl ether into a chloroform solution. This method afforded dark red needle shaped crystals suitable for X-ray diffraction. Yield 0.084 g (32%). δ_P (CDCl$_3$, 121MHz) 63.2.

Chapter 4 Sterically hindered phosphinothiolate complexes

4.1 Palladium phosphinosulfinato complexes

In the previous chapter we have concentrated on a ligand based on a simple commercially available substrate. This route of synthesis in turn forms a relatively small, conformationally confined backbone due to the fixed steric properties. In this chapter the focus will switch to using a higher molecular weight substrate (L^2H) with more freedom around the functional groups. Coordinating this ligand with palladium has formed metal complexes which can be structurally compared to those synthesied in the previous chapter.

Phosphinothiolate complexes can be oxidised stepwise to the corresponding sulfenato (-RSO) and sulfinato (-RSO$_2$) analogues with suitable oxidising agents [120], [132], [133]. The redox chemistry of thiols plays key roles in many biological processes [124]. The important biochemical oxidations of cysteine include its conversion to disulfides (cystine) and the formation of oxy acids such as cysteine sulfenic acid, cysteine sulfinic acid (CSA), hypotaurine, cysteic acid and taurine [125]. In this chapter we report the spontaneous oxidation of ligand L^2H during complexation to form a sulfinato complex.

As part of our structural studies concerned with chiral phosphinothiolate and phosphinothioether ligands we considered thiol L^2H as a potential auxiliary. Here, we report the synthesis of new bulky chiral phosphinothiol monomeric, oligomeric and sulfinato palladium (II) complexes.

4.2 Co-ordination of 9, 10-ethanoanthracene-2-diphenylphosphino-1-ethanethiol, 9-10-dihydro L^2H

Our initial studies for the coordination chemistry of the dihydro-anthracene ligand L^2H have focused on the preparation of palladium (II) complexes, due to the 'soft' acid and base properties of the metal precursor and ligand respectively. Phosphinothiolate ligands form bis-chelate and sulphur-bridged dimeric complexes with group 10 metals as we have observed in the previous chapter. But we have also observed that the backbone of the ligand can influence the geometries of the metal complexes formed. Here we study what influences the sterically diverse ligand (L^2H) has on standard coordination reactions. The first complex to be synthesised was that of the palladium bis-chelate following the synthetic method outlined in the previous chapter.

98

Accordingly, the reaction of two equivalents of phosphinothiol L^2H with PdCl$_2$(NCPh)$_2$ in anhydrous degassed THF was carried out (**Scheme 4-1**). The ^{31}P NMR spectrum of the below reaction showed the presence of two signals, resonating at δ_P 50.0 and δ_P 48.0 respectively with equal intensity for both fresh and aged solutions. The complex Pd(L^2)$_2$ was isolated first, after fractional crystallisation by the slow diffusion of diethyl ether into a THF solution (δ_P 50.0). To our surprise the second compound isolated, with δ_P 48.0, was the bis-sulfinato (-SO$_2$R) complex, **13**, according to spectroscopic and crystallographic data. Reactions were carried out in anaerobic conditions with the only oxygen source being THF. Thus far we have not ascertained the source of this oxidation and can only report our findings. The same reaction was repeated several times always forming complexes Pd(L^2)$_2$ **12** and Pd(L^{2}O$_2$)$_2$ **13** in equimolar ratios.
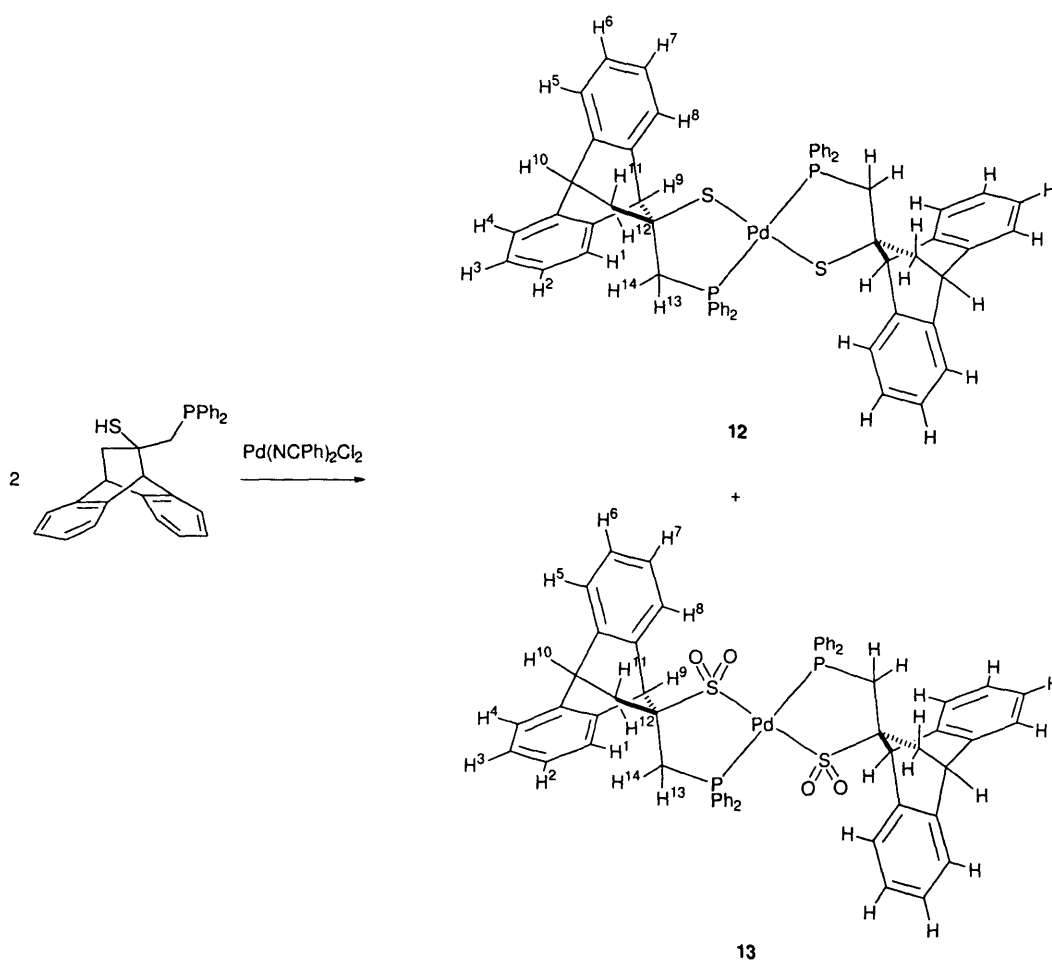
Scheme 4-1: Reaction scheme for the formation of Pd(L^2)$_2$ **12** and oxidised Pd(L^{2}O$_2$)$_2$ **13**

Deliberate oxidation of S-bound thiolates to sulfenates and sulfinates can be achieved using a variety of oxidants such as hydrogen peroxide and hexaquacobalt(III) [128]. Spontaneous oxidation of metal-thiolates however has rarely been reported. The only case of serendipitous S-oxidation we have come across is that of a nickel bis-sulfonato complex, isolated during the synthesis of the parent complex Ni(dsdm), dsdm = N,N'-dimethyl-N,N'-bis(mercaptoethyl)ethylenediamine. As was the case with the Ni(dsdm) complex, the bis-thiolato complex 12 is air-stable indefinitely both in the solid state and in solution with no S-oxidation products observed, thus leading us to conclude that it is the presence of other reactants during the formation of 13 that cause the redox chemistry to occur. A complex containing a combination of oxidised and non-oxidised ligand, $[Pd(L^2)(L^2O_2)]$, was not observed. Factors which lead to stable bis-thiolato and bis–sulfinato complexes *vs.* disproportionation products are not well understood.

Both complexes are isolated in equimolar amounts and combine to give a reasonable overall yield of 76%. Each of the complexes are isolated and purified due to their differing solubility in polar solvents (Acetonitrile). Starting with the racemic ligand L^2H both *rac* and *meso* complexes were expected to form in equimolar amounts. However, only the *meso* isomers of 12 and 13 are observed according to the NMR and crystallographic data obtained, possibly due to the steric requirements of the bulky dihydro-anthracene backbone. In the case of the geometry it is controlled by the bulk of the $-PPh_2$ groups, as the *trans*-P,P arrangement is sterically more stable than the *cis*-P,P configuration, which places the bulky groups close to each other. It would seem that the steric interactions of the two $-PPh_2$ groups is not the only cause for the fact that the *cis* isomer of 12 and 13 are not observed, as the phenyl groups can rotate to accommodate each other in a *cis* isomer. We suggest that it is because of the bulky ligand interference that the phenyl groups cannot adopt a conformation compatible with the *cis* geometry, forcing 12 and 13 to exist only in the *trans*-P, P form with high geometrical rigidity. The ^1H NMR spectrum of complex 12 reveals a dramatic upfield shift for the aromatic protons of the [2.2.2] dibenzobicyclic unit when compared to the free ligand. This is particularly true for the aromatic protons H^1 and H^8 located on the substituted side of the ethylene bridge resonating at δ_H 4.89 and 6.11, respectively (numbering scheme shown in **Scheme 4-1**). The neighbouring protons H^2 and H^7 show a smaller downfield shift at 6.45 and 6.55, respectively. In contrast, resonances for the aromatic protons on the non substituted side of the bicyclic, $H^{3/6}$ and $H^{4/5}$, appear in the normal aromatic range, at δ_H 6.80 and δ_H 6.96, respectively.

The infrared spectrum of **13** contains three strong bands at 1049, 1099 and 1214 cm^{-1} which can be assigned to $\nu(SO)$ stretches. These bands are very close to the ones reported by Darensbourg for a related bis-sulfinato Pd(N$_2$S$_2$) complex [123]. The ^{1}H NMR spectrum of Pd(L^{2}O$_2$)$_2$ shows a downfield shift of protons affected by the oxidation of the sulphur. The protons most influenced are those at the bridgehead position nearest the sulphur, H^9, resonating at δ_H 4.18 and the aromatic protons H^1 and H^8, at δ_H 5.48 and δ_H 7.10, respectively. COSY NMR spectra for compounds **12** and **13** were recorded in deuterated chloroform. The data was used to identify the backbone protons H$^{11, 12}$ and H$^{13, 14}$, which are both neighbouring the ligand chiral carbon and have complex couplings. Protons H$^{11, 12}$ can be identified by their correlation to bridgehead proton H^{10} which protons H$^{13, 14}$ do not contain such correlation. The spectrum for **12** identifys δ_H 2.27 and 2.40 being protons H$^{11, 12}$ and δ_H 2.47 and 2.90 corresponding to H$^{13, 14}$. Compound **13** shows a slight increase of sepataion between protons H$^{11, 12}$ (δ_H = 2.21 and 2.42) and a decrese of the separation between H$^{13, 14}$ (δ_H = 2.62 and 2.74). Electrospray mass spectroscopy analyses were carried out for both complexes. Apart from the parent ions, stepwise loss of oxygen is observed for the sulfinato complex showing that at least under mass spectrometry conditions the sulfenato and sulfinato/sulfenato intermediates are formed.

Red block crystals of the *meso* isomer **12** suitable for X-ray analysis were obtained after cooling a concentrated chloroform solution at -5°C. Crystallographic data was collected for bis-chelate complex **12** and the corresponding ORTEP is shown in **Figure 4-1**. Of note is the envelope conformation of the five-membered chelate ring which places the bridgehead proton of the dibenzobicyclic unit in an axial position with the methylene group pointing away from the coordination plane. This is the usual conformation observed for the chelate ring in the solid state structures of L^2 complexes.
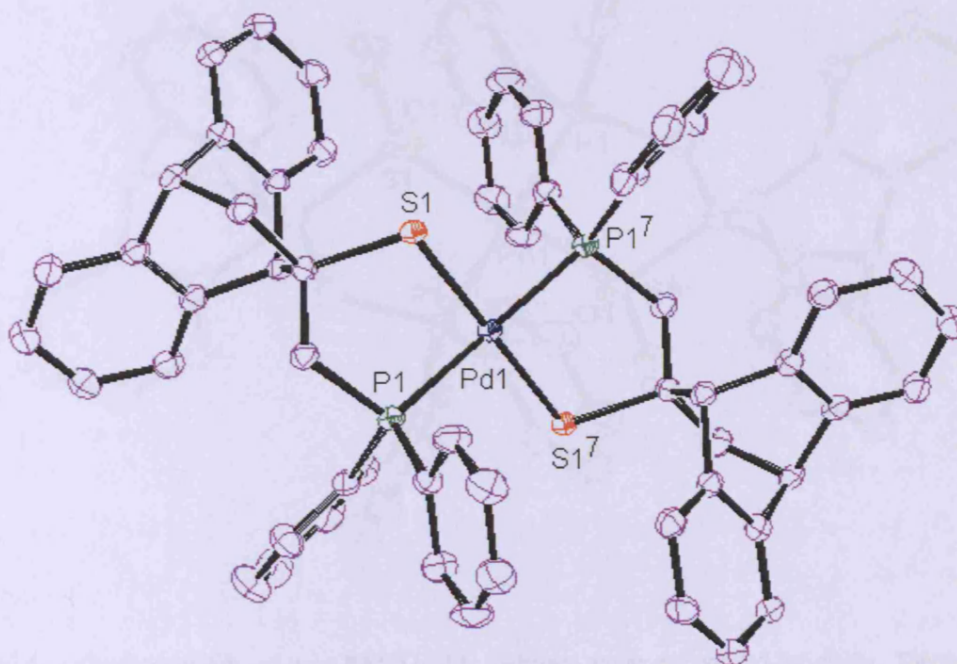
Figure 4-1: Crystal structure of *trans*-Pd(L^2)$_2$ **12**. Hydrogen atoms have been omitted for clarity. Thermal ellipsoids are drawn at 50% probability

Yellow block shaped crystals of the *meso* isomer of **13** suitable for X-ray diffraction analysis were obtained from the slow diffusion of diethyl ether into a solution of THF. The structure of the *meso* isomer of **13** is the first example of a palladium-phosphinosulfinato complex reported. Of note is the tetrahedral arrangement of sulphur which closes the bite angle of the chelate from 86.30(7)° to 83.59(3)°.
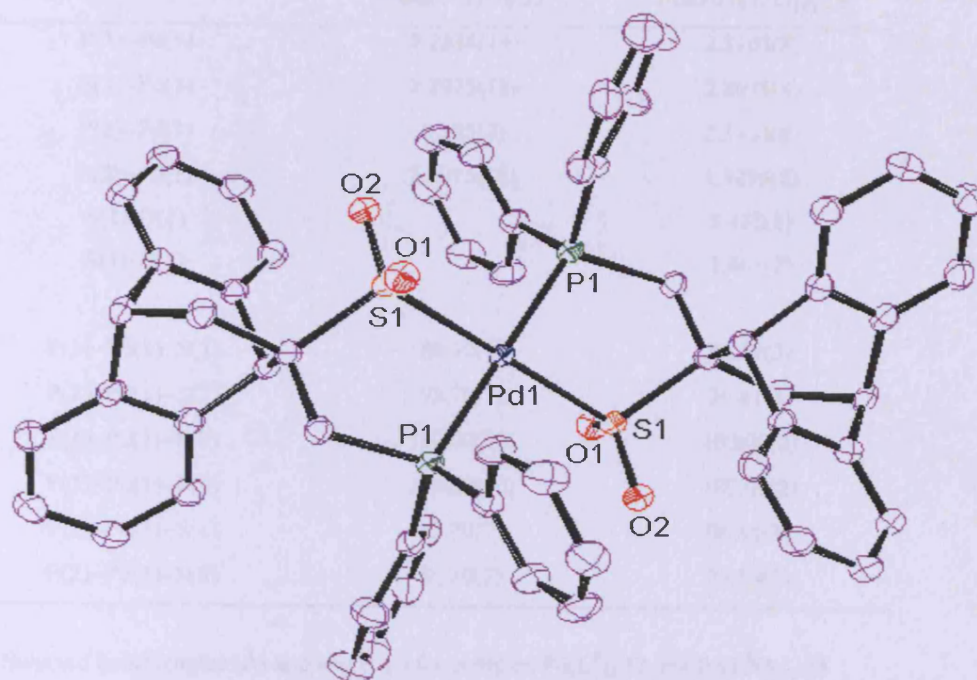
Figure 4-2: Crystal structure of *trans*-Pd(L^{2}O$_2$)$_2$**13.** Hydrogen atoms are omitted for clarity. Thermal ellipsoids are drawn at 50% probability

Crystallographic data of the two complexes are given in **Table 4-1** showing selected bond lengths and angles. Upon oxidation of the sulphur, the Pd-S bond slightly lengthens from 2.2975(18) Å in complex **13** to 2.3095(8) Å in the sulfinato complex [123], [127]. Lengthening of the Pd-P bond from 2.2848(19) in **12** to 2.3103(8) Å in complex **13** is also observed, as a result of the steric influences of the addition of two oxygen and greater electron donation of the sulphur donor [120].

	trans-Pd(L²)₂ 12	trans-Pd(L²O₂)₂ 13
P(1)–Pd(1)	2.2848(19)	2.3103(8)
S(1)–Pd(1)	2.2975(18)	2.3095(8)
P(2)–Pd(1)	2.285(2)	2.3103(8)
S(2)–Pd(1)	2.2975(18)	2.3095(8)
S(1)-O(1)		1.473(2)
S(1)-O(1)		1.461(2)
P(1)–Pd(1)–S(1)	86.30(7)	83.59(3)
P(1)–Pd(1)–S(2)	93.70(7)	96.41(3)
S(1)–Pd(1)–S(2)	180.00(10)	180.00(2)
P(1)–Pd(1)–P(2)	180.00(10)	180.00(2)
P(2)–Pd(1)–S(1)	93.70(7)	96.41(3)
P(2)–Pd(1)–S(2)	86.30(7)	83.59(3)

Table 4-1: Selected bond lengths (Å) and angles (°) for complex Pd(L²)₂ 12 and Pd(L²O₂)₂ 13

Next we studied the chemical oxidation of complex **12** in order to isolate S-oxygenate intermediates. Using re-crystallised complex **12** dissolved in degassed acetonitrile, excess hydrogen peroxide was added at room temperature. Within one hour the bis-chelate had completely oxidised to sulfinato complex **13**. The bis-chelate complex **12** is air stable and does not oxidise in solution like analogous complexes [120], [124]. Furthermore no mixture of sulphoxide palladium was observed giving only the fully oxidised disulfonate complex using excess hydrogen peroxide. Pd(L²)₂ cleanly oxidises in the presence of excess hydrogen peroxide to the fully oxygenated complex **13** without any sulfenate intermediates observed. In an attempt to form a partially reduced intermediate, the thiolate complex was reacted with one equivalent of H₂O₂.urea adduct. ³¹P NMR revealed a mixture of products. Integration of the peaks showed relatively equal amounts of unreacted bis-chelate **12** (δ_P 50.0), fully oxidised sulfinato **13** (δ_P 48.0) and a new peak at δ_P 46.0 attributed to the bis-sulfenato Pd(L²O)₂ complex.

4.3 Preparation and isolation of polymetallic complexes using L^2H

Several attempts were made to obtain the dimeric palladium complex, $[Pd(L^2)Cl]_2$, by mixing equimolar amounts of the ligand L^2H and $Pd(PhCN)_2Cl_2$ in anhydrous degassed THF (**Scheme 4-2**). ^{31}P NMR spectra of the dissolved materials consistently showed the presence of two distinct complexes giving rise to a sharp singlet at $\delta_P\,40.4$ (dimer **14**) and a set of doublets at $\delta_P\,39.9$ and $\delta_P\,46.9$, $^2J_{PP} = 11.1$ Hz. After prolonged standing of the mixture the set of doublets disappears from the ^{31}P NMR spectrum and a new singlet is observed at $\delta_P\,50.0$ corresponding to the bis-chelate complex, **12**. It was possible to establish the identity of the species giving rise to the set of doublets in ^{31}P NMR (complex **15**) from single crystal X-ray diffraction studies.
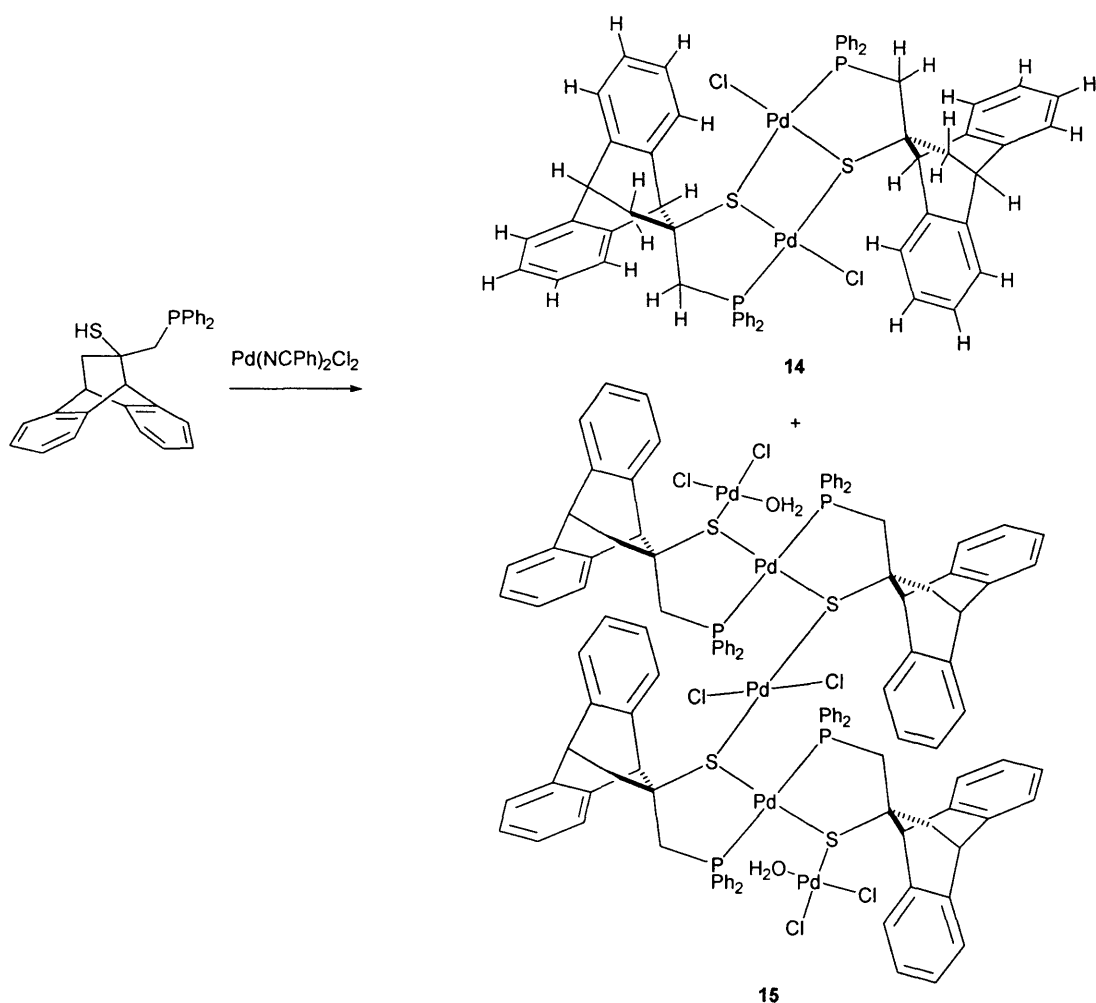
Scheme 4-2: Reaction scheme for the formation of $[PdL^2Cl]_2$ **14** and $PdCl_2[PdCl_2(H_2O)\text{-}Pd(L^2)_2]_2$ **15**

Single crystals of **15** were isolated by slow diffusion of diethyl ether into a solution of chloroform. Orange block shaped crystals of **15** were used for X-ray diffraction analysis producing an ORTEP view shown in **Figure 4-3**. Complex **15** has an unexpected pentameric structure with two $PdCl_2(H_2O)$-$Pd(L^2)_2$ units linked by a $PdCl_2$ fragment. The ORTEP view identifies the two sets of doublets in the ^{31}P NMR spectrum corresponding to the two phosphorus environments in the complex with *cis* stereochemistry. There are several unusual features observed in the $Pd(L^2)_2$ subunits of **15**, most likely the result of the steric demands of the bulky dibenzobicyclic substituents and *cis* orientation of the PPh_2 groups that deserve further comment. Deviation from square planarity as defined by the tetrahedral twist, the angle of the intersection between PdP_2 and PdS_2 planes, is 12.73°. A tetrahedral distortion of the metal core of the $Pd(L^2)_2$ subunits is observed as evidenced from the average value of 169.6° for the *trans* S-Pd-P angles.
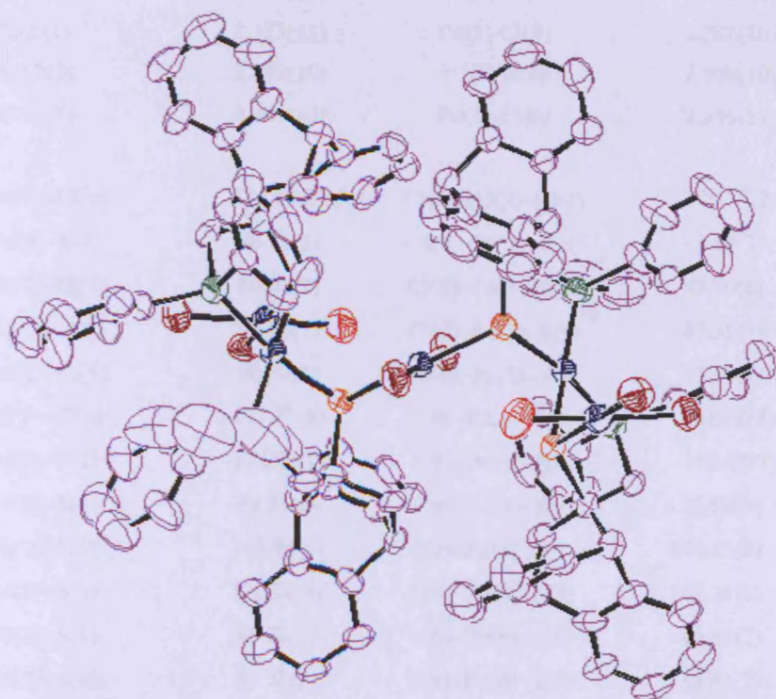
Figure 4-3: Crystal structure of $PdCl_2$-{$Pd(L^2)_2$-[$PdCl_2(H_2O)$]}$_2$ **15**. Hydrogen atoms have been omitted for clarity. Thermal ellipsoids are drawn at 50% probability

Crystallographic data in **Table 4-2** shows selected bond lengths and angles. Both Pd(L^2)$_2$ subunits form the *meso* isomer, which in combination with the requirement to place one dibenzobicyclic unit above the coordination plane and the other below the plane in order to minimise steric repulsions, places the methylene group of the dibenzobicyclic unit of *S*-L^2 in a pseudoaxial position and the chelate adopts a distorted δ-skew conformation. This is the only example in the solid state structures of L^2 complexes where the methylene group faces the chelate ring, in all other structures L^2 adopts an almost perfect envelope conformation with the bridgehead proton in an axial position.

Pd(1)–Cl(2)	2.288(10)	Pd(3)-S(6)	2.340(10)
Pd(1)–S(1)	2.315(11)	Pd(3)-S(3)	2.341(10)
Pd(1)–Cl(1)	2.328(10)	Pd(4)-P(9)	2.274(10)
Pd(1)–P(3)	2.281(10)	Pd(4)-P(6)	2.285(10)
Pd(2)-P(1)	2.284(10)	Pd(4)-S(6)	2.327(10)
Pd(2)-S(3)	2.317(10)	Pd(5)-O(2)	2.080(10)
Pd(2)-S(1)	2.323(11)	Pd(5)-Cl(5)	2.289(10)
Pd(3)-Cl(3)	2.299(10)	Pd(5)-S(9)	2.308(10)
Pd(3)-Cl(4)	2.304(10)	Pd(5)-Cl(6)	2.339(11)
O(1)–Pd(1)–Cl(2)	176.33(8)	Cl(3)–Pd(3)–Cl(4)	179.37(7)
O(1)–Pd(1)–S(1)	86.18(7)	Cl(3)–Pd(3)–S(6)	91.87(7)
O(1)–Pd(1)–Cl(1)	86.02(7)	Cl(3)–Pd(3)–S(3)	87.00(6)
Cl(2)–Pd(1)–S(1)	97.03(7)	Cl(4)–Pd(3)–S(6)	87.56(7)
Cl(2)–Pd(1)–Cl(1)	90.90(6)	Cl(4)–Pd(3)–S(3)	93.56(7)
S(1)–Pd(1)–Cl(1)	171.23(8)	S(6)–Pd(3)–S(3)	178.86(8)
P(3)–Pd(2)–P(1)	102.04(7)	P(9)–Pd(4)–P(6)	102.04(7)
P(3)–Pd(2)–S(3)	86.54(6)	P(9)–Pd(4)–S(9)	86.64(7)
P(3)–Pd(2)–S(1)	168.93(8)	P(9)–Pd(4)–S(6)	170.85(8)
P(1)–Pd(2)–S(3)	170.18(8)	P(6)–Pd(4)–S(9)	168.39(8)
P(1)–Pd(2)–S(1)	86.22(7)	P(6)–Pd(4)–S(6)	86.31(7)
S(3)–Pd(2)–S(1)	85.92(7)	S(9)–Pd(4)–S(6)	85.63(7)

Table 4-2: Selected bond lengths (Å) and angles (°) for PdCl$_2$-{Pd(L^2)$_2$-[PdCl$_2$(H$_2$O)]}$_2$ **15**

For structural comparison reasons we include another interesting complex isolated as a by-product from the reaction coordination of phosphinothioether $L^2$1-MN (**Chapter 5**). During the coordination of $L^2$1-MN small traces of the phosphinothiol L^2H were present causing the formation of trimer $[Pd(L^2)Cl]_3$ **16**. Attempts were made to form the complex directly but proved unsuccessful, the presence of the phosphinothioether ligand is required to form the trimer as part of a complex mixture. This unexpected by-product was isolated and can be used as an example of another bridging thiolate complex. Block shaped crystals of the homochiral trimer were obtained after slow diffusion of ether into a dichloromethane and used for X-ray diffraction analysis producing an ORTEP view shown in **Figure 4-4**.
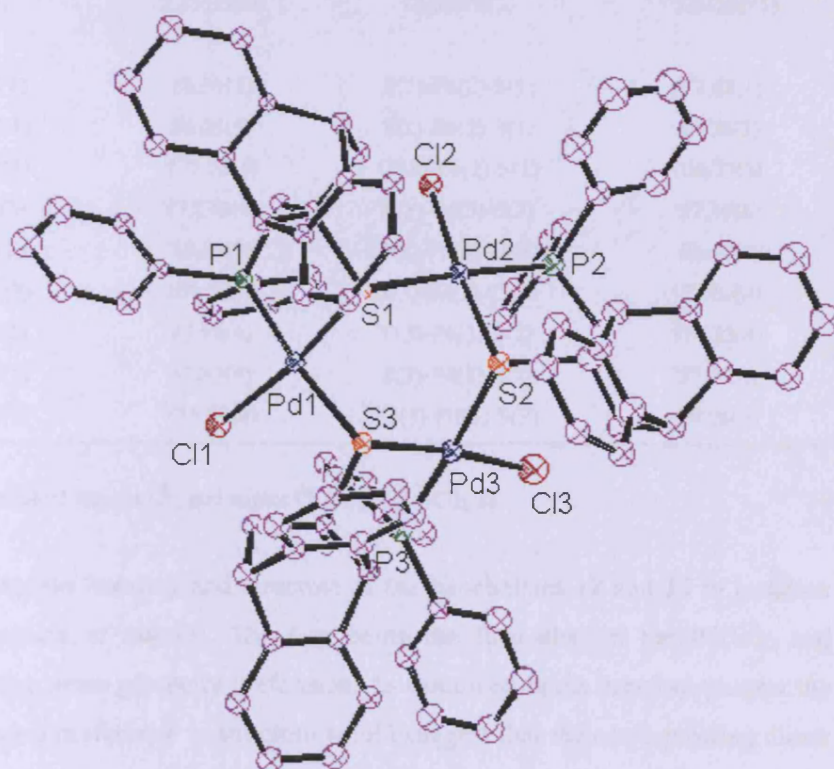
Figure 4-4: Crystal structure of $[Pd(L^2)Cl]_3$ **16**. Hydrogen atoms have been omitted for clarity. Thermal ellipsoids are drawn at 50% probability

Trimer **16** has an unusual six-membered $[Pd-S]_3$ core adopting a chair conformation and it is the only one in the L^2 complex series that the *rac* isomer is formed. It possesses near C_3 symmetry with the rotation axis passing through the middle of the six-membered core. The five-membered chelate ring of L^2 in **16** adopts an envelope conformation, with the methylene group of the dibenzobicyclic unit occupying

a pseudo-equatorial position. This is the first complex using L^2 where evidence of the *trans* influence can be seen. All Pd-S bond which are *trans* to metal chloride bonds have bond lengths of 2.2803(10), 2.2877(10) and 2.3065(10) for bonds Pd(1)-S(1), Pd(2)-S(2) and Pd(3)-S(3) respectively. Due to the dipenylphosphino group having a greater *trans* influence Pd-S bond lengths *trans* to them are lengthened: Pd(1)-S(3), Pd(2)-S(1) and Pd(3)-S(2) having bond lengths of 2.3843(10), 2.3822(10) and 2.3908(11) respectively.

Cl(1)-Pd(1)	2.3576(10)	Pd(2)-P(2)	2.2323(11)
Pd(1)-P(1)	2.2336(10)	Pd(2)-S(2)	2.2877(10)
Pd(1)-S(1)	2.2803(10)	S(2)-Pd(3)	2.3908(11)
Pd(1)-S(3)	2.3843(10)	P(3)-Pd(3)	2.2370(11)
S(1)-Pd(2)	2.3822(10)	S(3)-Pd(3)	2.3065(10)
Cl(2)-Pd(2)	2.3511(10)	Cl(3)-Pd(3)	2.3421(11)
P(1)-Pd(1)-S(1)	86.96(4)	P(2)-Pd(2)-S(1)	172.68(4)
P(1)-Pd(1)-Cl(1)	86.05(4)	S(2)-Pd(2)-S(1)	85.96(3)
S(1)-Pd(1)-Cl(1)	172.23(4)	Cl(2)-Pd(2)-S(1)	100.73(3)
P(1)-Pd(1)-S(3)	172.43(4)	P(3)-Pd(3)-S(3)	87.39(4)
S(1)-Pd(1)-S(3)	85.51(3)	P(3)-Pd(3)-Cl(3)	86.42(4)
Cl(1)-Pd(1)-S(3)	101.52(4)	S(3)-Pd(3)-Cl(3)	173.60(4)
P(2)-Pd(2)-S(2)	87.98(4)	P(3)-Pd(3)-S(2)	174.33(4)
P(2)-Pd(2)-Cl(2)	85.33(4)	S(3)-Pd(3)-S(2)	87.09(4)
S(2)-Pd(2)-Cl(2)	173.31(4)	Cl(3)-Pd(3)-S(2)	99.06(4)

Table 4-3: Selected bond lengths (Å) and angles (°) for [Pd(L^2)Cl]$_3$ **16**

Evaluating the bonding and structure of the bis-chelates **12** and **13** in isolation there are two points of interest. The first being the formation of the Pd(L^2)$_2$ and Pd(L^2O_2)$_2$ taking a *trans* geometry preference. As discussed in the previous chapter the formation of such a preference in structure would suggest that the corresponding dimer would be synthesised containing the opposite *rac* stereoisomer. Re-crystallisation of the dimer complex was unsuccessful, but formation of the trimer gives similar structural information for what could be expected for the dimer. The ligands of the trimer all prefer to position in an (*S*) orientation giving the expected *rac* stereoisomer. Compared to the conformationally confined backbone of L^1 we would anticipate that the freedom around the chiral backbone would allow the formation of the *cis* geometry. From the results obtained we can conclude that the formation of a *cis*-geometry bis-chelate is based on the steric bulk of the ligand backbone. With evidence that the only two reported *cis* geometry bis-chelates have almost identical steric properties. However the

increase in freedom around the chiral axis does allow sulphur to coordinate and form bridging complexes of trimeric and pentameric complexes as demonstrated in this chapter and summarised in **Table 4-4**.

No.	Complex	Geometry	M-P (Å)	M-S (Å)	P-M-S (°)	Stereoisomer
12	*trans*-Pd(L^2)$_2$	Monomer	2.2719(10)	2.3250(10)	85.57(4)	*meso*
13	*trans*-Pd(L^{2}O$_2$)$_2$	Monomer	2.3103(8)	2.3095(8)	83.59(3) 86.54(7)	*meso*
15	PdCl$_2$-{Pd(L^2)$_2$-[PdCl$_2$(H$_2$O)]}$_2$	Pentimer	2.281(10)	2.341(10)		*meso*
16	[Pd(L^2)Cl]$_3$	Trimer	2.2336(10)	2.2803(10)	86.96(4)	*rac*

Table 4-4 Structural comparison of selected bond lengths (Å) and angles (°) of complexes synthesised

The second point of interest comes from the formation of oxidised sulfinato complex Pd(L^{2}O$_2$)$_2$ **13**. During complexation, stoichiometric amounts of oxygen are coordinated to form a palladium sulfinato complex Pd(L^{2}O$_2$)$_2$ **13**. The mechanism of this oxidation may need further study to establish documented evidence for the synthesis and oxygen origin. One observation that can be highlighted is the formation of complex **15** which contains coordinated water and two bis-chelate fragments. The complex is formed by reacting one equivalent of metal precursor to ligand L^{2}H. Addition of another equivalent of ligand L^{2}H affords the bis-chelate and sulfinato mixture, the oxygenated species is already present in the intermediate stage in the form of coordinated water. During the synthesis of ligand L^1 no oxygenated species have been isolated, this leads us to the assumption that one of the seven steps of synthesis could produce a by-product which causes the coordination of water during the formation of complex **15**. Thus far no such by-products have been isolated and further study would be needed to fully validate the reaction mechanism. In summary ligand L^2 has unique properties that can oxidise sulphur upon complexation using water bound to a palladium intermediate. Similar ligand properties have not been reported in the literature and appear to be unique to this ligand.

4.4 Experimental
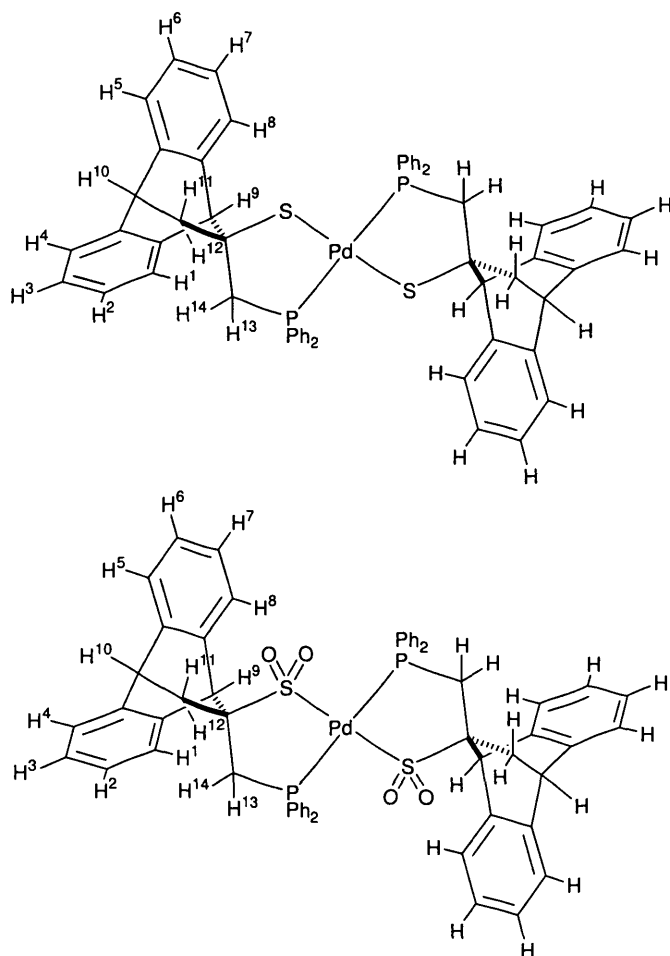
Preparation of Pd(L²)₂ 12 and Pd(L²O₂)₂ 13. PdCl₂(NCPh)₂ (0.160 g, 0.418 mmol) and L²H (0.226 g, 0.517 mmol) were dissolved in anhydrous degassed CH₂Cl₂ (15 ml) whilst stirring under argon. The reaction mixture was then stirred for 2 hours at room temperature the solvent was evaporated leaving a dark red solid. *trans*-Pd(L²)₂ 12 was isolated from cooling a concentrated chloroform solution to -5°C. This method afforded red block type crystals suitable for X-ray diffraction. *trans*-Pd(L²O₂)₂ 13 was isolated from slow diffusion of diethyl ether into a solution of THF. This method afforded yellow block type crystals suitable for X-ray diffraction.

meso- *trans*-Pd(L²)₂ 12. Yield 0.314 g (38%). COSY ¹H NMR (CDCl₃, 400MHz) 2.27 (1H, dd, H¹¹, $^2J_{HH}$ = 2.8 $^3J_{HH}$ = 13.1), 2.40 (1H, dd, H¹², $^2J_{HH}$ = 2.4 $^3J_{HH}$ = 13.0), 2.47

(1H, dt, H^{13}, $^2J_{HH}$ = 13.9 $^3J_{HH}$ = 4.8), 2.90 (1H, dt, H^{14}, $^2J_{HH}$ = 13.9 $^3J_{HH}$ = 4.8), 3.60 (1H, s, H^9), 4.03 (1H, t, H^{10}), 4.89 (1H, d, H^1, $^2J_{HH}$ = 7.3), 6.11 (1H, d, H^8, $^2J_{HH}$ = 7.2), 6.45 (1H, t, H^2, $^3J_{HH}$ = 5.8), 6.80 (2H, m, ArH), 6.96 (2H, t, ArH, $^3J_{HH}$ = 7.9), 7.43 (6H, m, ArH), 7.74 (2H, m, H^{14}), 7.83 (2H, m, H^{15}). ^{13}C NMR (125MHz, CDCl$_3$) 44.20 (1C, s, CH), 45.33 (1C, t, CH$_2$, $^3J_{CP}$ = 6.2), 50.99 (1C, t, CH$_2$, $^3J_{CP}$ = 18.0), 56.61 (1C, t, C, $^3J_{CP}$ = 11.7), 58.09 (1C, s, CH), 121.36 (1C, s, ArC), 121.88 (1C, s, ArC), 123.57 (1C, s, ArC), 123.83 (1C, s, ArC), 123.94 (1C, s, ArC), 124.34 (1C, s, ArC), 125.40 (1C, s, ArC), 127.69 (1C, t, C$_m$, $^3J_{CP}$ = 4.9), 127.95 (1C, t, C'$_m$, $^3J_{CP}$ = 5.6), 128.52 (1C, s, C$_p$), 130.06 (1C, t, C$_i$, $^3J_{CP}$ = 22.5), 130.37 (1C, s, C'$_p$), 131.18 (1C, t, C$_o$, $^3J_{CP}$ = 5.6), 133.82 (1C, t, C'$_i$, $^3J_{CP}$ = 22.9), 135.16 (1C, t, C'$_o$, $^3J_{CP}$ = 8.4), 141.25 (1C, t, ArC, $^3J_{CP}$ = 4.1), 141.44 (1C, s, ArC). δ_P (CDCl$_3$, 121MHz) 50.0.

meso- *trans*-Pd(L^{2}O$_2$)$_2$ 13. Yield 0.122 g (39%). IR (KBr) 1049s, 1099s and 1214s cm$^-$ ^{1}. COSY ^{1}H NMR (CDCl$_3$, 400MHz) 2.21 (1H, dd, H^{11}, $^2J_{HH}$ = 2.4 $^3J_{HH}$ = 13.0), 2.42 (1H, dd, H^{12}, $^2J_{HH}$ = 2.3 $^3J_{HH}$ = 13.0), 2.62 (1H, dt, H^{13}, $^2J_{HP}$ = 13.8 $^3J_{HH}$ = 3.4), 2.75 (1H, dt, H^{14}, $^2J_{HP}$ = 13.9 $^3J_{HH}$ = 4.6), 4.18 (1H, s, H^9), 5.49 (1H, d, H^1, $^2J_{HH}$ = 7.3), 6.70 (1H, t, H^{10}, $^3J_{HH}$ = 7.4), 6.93 (1H, t, H^2, $^3J_{HH}$ = 7.3), 7.20 (4H, m, ArH), 7.47 (2H, q, ArH, $^4J_{HH}$ = 5.7), 7.59 (6H, m, ArH), 8.18 (2H, q, ArH, $^4J_{HH}$ = 5.9). ^{13}C NMR (125MHz, CDCl$_3$) 45.47 (1C, s, CH), 46.61 (1C, t, CH, $^3J_{CP}$ = 5.9), 50.95 (1C, t, CH$_2$, $^3J_{CP}$ = 18.2), 57.85 (1C, t, C, $^3J_{CP}$ = 11.8), 59.62 (1C, t, CH$_2$, $^3J_{CP}$ = 8.6), 123.10 (1C, s, ArC), 123.31 (1C, s, ArC), 123.58 (1C, s, ArC), 123.85 (1C, s, ArC), 125.20 (1C, s, ArC), 125.70 (1C, s, ArC), 126.08 (1C, s, ArC), 126.78 (1C, s, ArC), 128.36 (1C, t, C$_m$, $^3J_{CP}$ = 5.2), 128.84 (1C, t, C'$_m$, $^3J_{CP}$ = 5.2), 129.41 (1C, s, C$_p$), 131.26 (1C, s, C'$_p$), 131.80 (1C, t, C$_i$, $^3J_{CP}$ = 21.9), 132.36 (1C, t, C$_o$, $^3J_{CP}$ = 7.5), 134.19 (1C, t, C$_i$, $^3J_{CP}$ = 22.5), 136.25 (1C, t, C'$_o$, $^3J_{CP}$ = 7.8), 142.67 (1C, s, ArC), 142.87 (1C, s, ArC), 143.00 (1C, s, ArC), 143.42 (1C, s, ArC). δ_P (CDCl$_3$, 121MHz) 48.0.
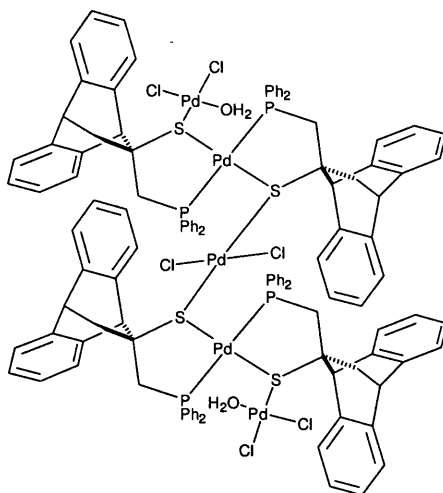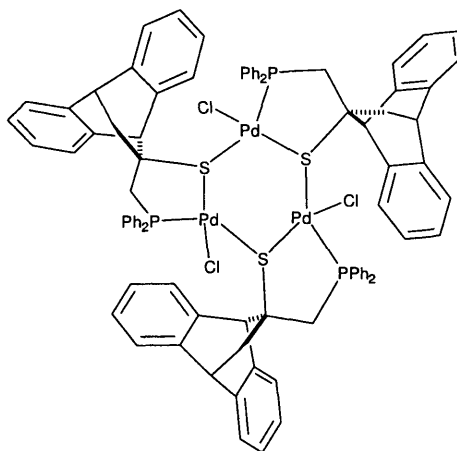
Preparation of PdCl₂[Pd(L²)₂Pd(H₂O)Cl₂]₂ 15. $PdCl_2(NCPh)_2$ (0.160 g, 0.418 mmol) and **L²H** (0.226 g, 0.517 mmol) were dissolved in anhydrous dichloromethane (15 ml) whilst stirring under argon. The reaction mixture was then stirred for 2 hours at room temperature the solvent was evaporated leaving a pale orange solid. Single yellow crystals were grown by slow diffusion of diethyl ether into a chloroform solution. **PdCl₂[Pd(L²)₂Pd(H₂O)Cl₂]₂ 15** was isolated from slow diffusion of diethyl ether into a solution of chloroform. This method afforded oragne block type crystals suitable for X-ray diffraction. Yield 0.114 g (26%). δ_P (CDCl₃, 121MHz) 39.9 (PPh₂, d, $^2J_{PP}$ = 11.1), 46.9 (PPh₂, d, $^2J_{PP}$ = 11.1).

113

Preparation of [Pd(L^2]$_3$ 16. PdCl$_2$(NCPh)$_2$ (0.160 g, 0.418 mmol) and **L^{2}1-MN** (0.226 g, 0.517 mmol) were dissolved in anhydrous dichloromethane (15 ml) whilst stirring under argon. The reaction mixture was then stirred for 2 hours at room temperature the solvent was evaporated leaving a pale orange solid. Single yellow crystals were grown by slow diffusion of diethyl ether into a chloroform solution. Yield 0.051 g (11%). ^{1}H NMR (CDCl$_3$, 400MHz) 2.08 (1H, dd, CH_2, $^2J_{HH}$ = 10.0 $^2J_{HH}$ = 14.5), 2.60 (1H, dd, CH_2, $^2J_{HH}$ = 2.5 $^3J_{HH}$ = 14.1), 2.68 (1H, dd, CH_2, $^2J_{HH}$ = 2.4 $^2J_{HP}$ = 14.1) , 4.09 (1H, s, CH), 4.25 (1H, t, CH, $^3J_{HH}$ = 2.4), 4.60 (1H, dd, CH_2, $^2J_{HH}$ = 10.2 $^2J_{HP}$ = 14.5), 4.96 (1H, d, ArH, $^2J_{HH}$ = 7.3), 6.50 (1H, m, ArH), 6.67 (1H, d, ArH, $^2J_{HH}$ = 7.4), 6.83 (2H, m, ArH), 7.00 (1H, t, ArH), 7.06 (1H, d, ArH, $^2J_{HH}$ = 7.14), 7.17 (2H, m, ArH) 7.30 (1H, m, ArH) 7.55-8.09 (7H, m, ArH). δ_P (CDCl$_3$, 121MHz) 50.1.

Chapter 5 Coordination of thioether ligands L^1R and L^2R

After the successful formation of a number of sterically diverse ligands in the Chapter 2 we report the synthesis and isolation of a number of novel phosphinothioether complexes using late transition metal precursors. Complexation reactions of this particular ligand could be followed by a number of spectroscopic methods. The first method being the presence and shift of the methylene proton signals in ^1H NMR spectra. The second being the disappearance of the negative signal in the ^{31}P NMR spectrum for the free ligand and the appearance of signals in the positive region for coordinated species (δ_P 40-70).

5.1 Coordination of phosphinothioether L^1Bn

The nickel benzyl thioether complex $Ni(L^1Bn)Br_2$ **17** was synthesised by the simple addition of equimolar amounts of the phosphinothioether ligand L^1Bn to a THF solution of nickel chloride followed by potassium bromide at room temperature (**Scheme 5-1**). After stirring the solution for two hours a sample was taken for ^{31}P NMR analysis. Disappearance of the signal for the free ligand gave evidence of coordination of the free ligand with a singlet at δ_P 60.0.
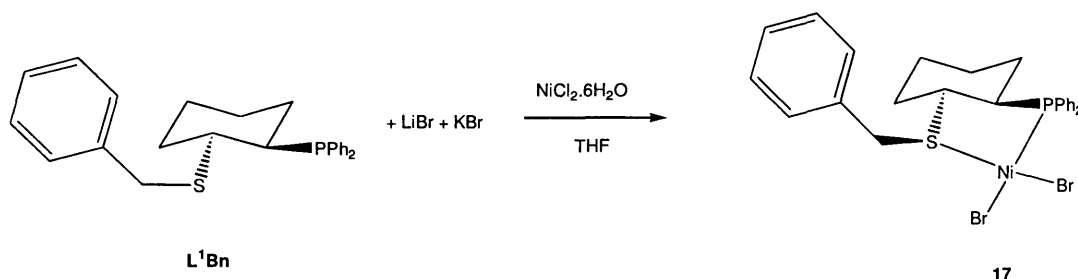
Scheme 5-1: Formation of phosphinothioether complex $Ni(L^1Bn)Br_2$ **17**

The complex was dried under vacuum to a purple powder, a sample analysed by low resolution electrospray mass spectrometry shows the major ion fragment at m/z 529.0, corresponding to the $Ni(L^1Bn)Br^+$ confirming the synthesis of complex **17**. In the formation of the phosphinothioether ligand L^1Bn, benzyl bromide was used as the aryl methyl halide precursor forming a by-product of lithium bromide. This by-product was present in the coordination reaction that proceeded. Initial formation of the nickel dichloride complex was then followed by a partial displacement reaction of the

115

coordinated chlorides by the more reactive bromides. Addition of excess potassium bromide completed the reaction.

An analogous reaction was performed using palladium bisbenzonitrile chloride as the metal precursor. Equimolar amounts of L^1Bn and metal precursor were mixed together in anhydrous THF followed by excess potassium bromide (**Scheme 5-2**). After mixing for 2 hours a sample was taken for ^{31}P NMR analysis. The disappearance of the signal for the free ligand gave an indication that a reaction had occurred with the appearance of a singlet at δ_P 65.9.
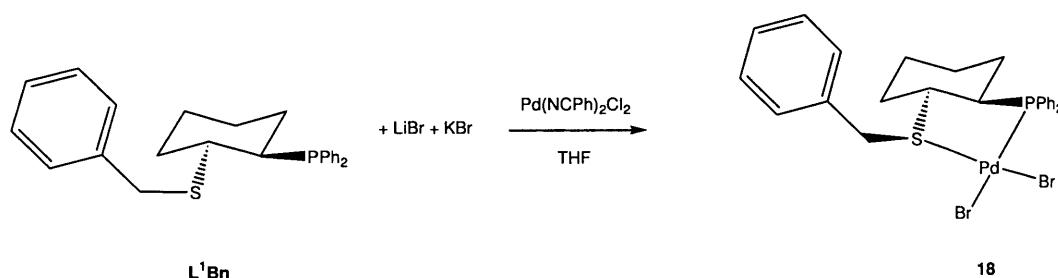
Scheme 5-2: Formation of phosphinothioether complex $Pd(L^1Bn)Br_2$ **18**

Removal of the solvent left an orange solid which was treated as air stable. The resulting material was then re-dissolved in a CH_2Cl_2 solution to filter off excess KBr and was allowed to recrystallise by the slow evaporation of solvent in an attempt to isolate the complex. This method produced a number of orange block shaped crystals, of high enough quality for X-ray diffraction analysis. Crystallographic data obtained shows the formation of the palladium dibromide $Pd(L^1Bn)Br_2$ **18** as seen in the ORTEP view (**Figure 5-1**). The main feature of this ORTEP view is the observation that the lone pair of sulphur adopts a position *trans* to the axial hydrogen on the backbone of the ligand, placing the thioether moiety and ligand backbone in a sterically favourable position. This observation is analogous to that of reported phosphino-thioether complexes reducing the number of complex conformations [89], [91], [93]. In the formation of enantiomerically pure complexes it can give good control for synthesising a range of phosphino-thioether complexes from the formation of one enantiomerically pure phosphinothiolate.
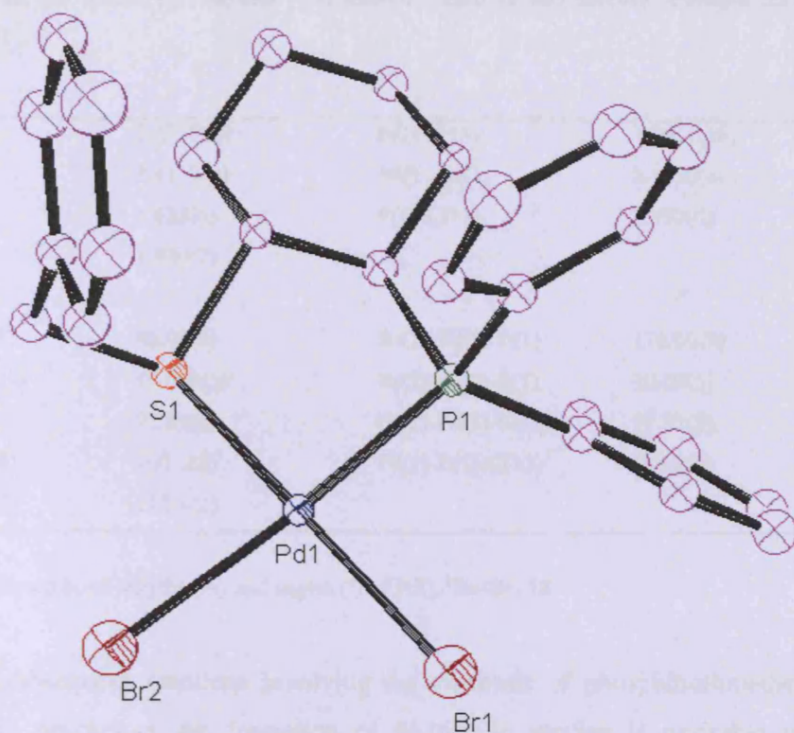
Figure 5-1: Crystal structure of Pd(**L^{1}Bn**)Br$_2$ **18**. Hydrogen atoms are omitted for clarity. Thermal ellipsoids are drawn at 50% probability

Crystallographic data is shown in **Table 5-1** shows selected bond angles and lengths form complex **18**. The formation of dibromide **18** does have advantages over the corresponding dichloride complex with the increased steric bulk giving decreased solubility and in this case greater ease of crystallisation, isolation and purification. The selected bond angles and lengths show the complex to be just off square planar with bond angles of S(1)-Pd(1)-Br(1) and P(1)-Pd(1)-Br(2) being 174.67(5)° and 176.00(5)° respectively. This is due to the S(1)-Pd(1)-P(1) bite angle of the chelate being 86.99(6)° pulling the geometry of the complex away from a perfect square planar arrangement. Studying the respective bond lengths they all appear to be in the longer regions expected for a phosphinothioether complex with the Pd-P and Pd-S being 2.2757(16) Å and 2.2461(16) Å, slightly longer than literature values [90], [89]. When studying the bond lengths of a square planar complex we would expect to see bond lengths consistent with the *trans influence* series, such as P(alkydiphenylphosphine) > P(triphenylphosphine) > S(terminal) > S(bridge) > Cl. According to the *trans influence* series, halides bonded *trans* to the diphenylphosphino moiety are affected more profoundly than those bonded *trans* to the thioether group. This theory is proven from the observation of halide bond

lengths being 2.4730(10) Å for Pd-Br(2) and 2.4177(9) Å for Pd-Br(1). This *trans influence* can be seen by similar palladium phosphinothioether complexes in the literature [89].

| Pd(1)-S(1)	2.2757(16)	Pd(1)-P(1)	2.2461(16)
Pd(1)-Br(1)	2.4177(9)	Pd(1)-Br(2)	2.4730(10)
S(1)-C(8)	1.823(6)	P(1)-C(13)	1.852(6)
S(1)-C(7)	1.839(7)		
P(1)-Pd(1)-S(1)	86.99(6)	Br(2)-Pd(1)-P(1)	176.00(5)
Br(1)-Pd(1)-S(1)	174.67(5)	Br(2)-Pd(1)-S(1)	90.09(5)
Br(1)-Pd-P(1)	91.24(5)	Br(2)-Pd(1)-Br(2)	91.91(5)
Pd(1)-S(1)-C(8)	106.3(2)	Pd(1)-P(1)-C(13)	105.8(2)
Pd(1)-S(1)-C(7)	112.8(2)		

Table 5-1: Selected bond lengths (Å) and angles (°) of Pd(L^{1}Bn)Br$_2$ **18**

For subsequent reactions involving the synthesis of phosphinothioethers from their thiolate precursors the formation of dichloride species is desirable to make structural comparisons to complexes in the literature. To remove the lithium halide from the remaining phosphinothioether ligand **L^{1}Bn** was dissolved in anhydrous, degassed CH$_2$Cl$_2$ followed by a water work-up. In subsequent reactions formation of phosphino-thioethers was achieved by using chlorinated aryl methyl halides which produced lithium chloride as the by-product and therefore not casing a secondary displacement reaction. Due to the substrates decreased reactivity, the ligand synthesis mixing time was extended.

Following the revised ligand synthesis a repeat of the complexation reactions for nickel and palladium were carried out. After dissolving **L^{1}Bn** in a degassed THF solution, the subsequent reaction with equimolar amounts nickel (II) chloride gave a purple solution (**Scheme 5-3**). ^{31}P {^{1}H} NMR spectrum of the solution showed a single sharp resonance at δ_P 50.0. Low resolution electrospray mass spectrometry of the reaction solution showed the presence of the major ion fragment [M-Cl]$^+$ at 483.1 confirming the synthesis of complex **19**.
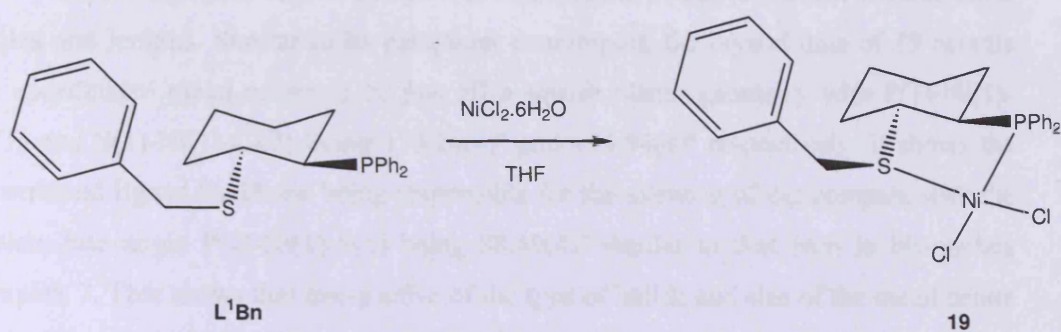
Scheme 5-3: Formation of phosphinothioether complex Ni(**L¹Bn**)Cl₂ **19**

Single crystals were then grown by slow diffusion of Et₂O into a solution of CH₂Cl₂. These purple block shaped crystals were of good enough quality for X-ray diffraction analysis. Crystallographic data shows an ORTEP view of complex **19** which can be seen in **Figure 5-2** validating the low resolution mass spectrometry analysis. We report the first structural characterisation of a nickel (II) phosphinothioether complex.
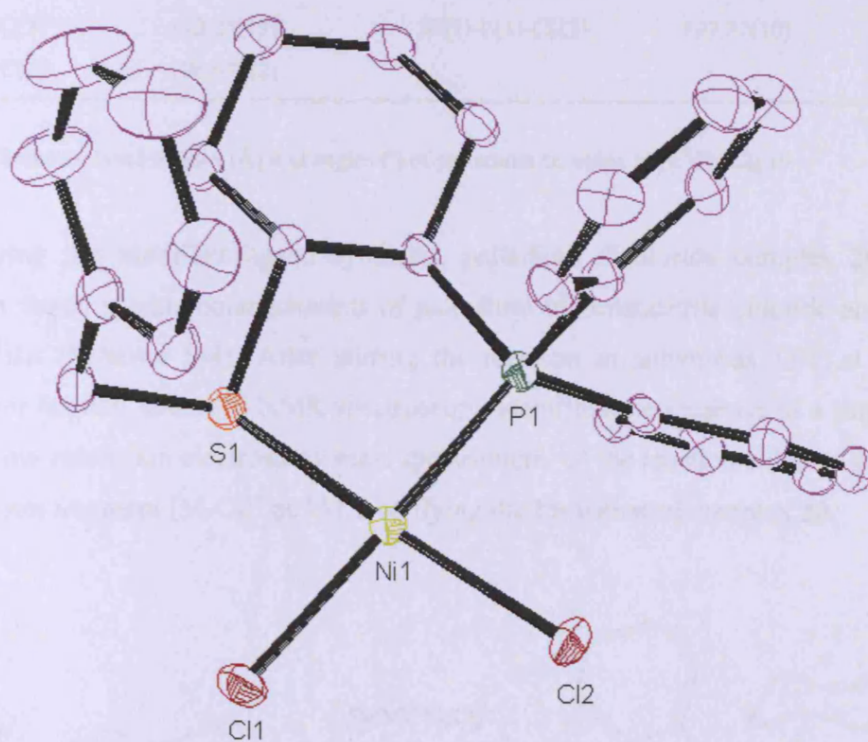

Figure 5-2: Crystal structure of Ni(**L¹Bn**)Cl₂ **19.** Hydrogen atoms are omitted for clarity. Thermal ellipsoids are drawn at 50% probability

Crystallographic data of complex **19** is displayed in **Table 5-2** and selected bond angles and lengths. Similar to its palladium counterpart, the crystal data of **19** reveals the coordinated metal centre to be just off a square planar geometry with P(1)-Ni(1)-Cl(1) and S(1)-Ni(1)-Cl(2) being 176.26(4)° and 174.94(4)° respectively. It shows the constrained ligand backbone being responsible for the skewing of the complex with the chelate bite angle P(1)-Ni(1)-S(1) being 88.49(4)° similar to that seen in bis-chelate complex **7**. This shows that irrespective of the type of halide and size of the metal centre the backbone of the ligand has a controlling force on the overall complex structure.

Ni(1)-S(1)	2.1771(10)	Ni(1)-P(1)	2.1607(14)
Ni(1)-Cl(2)	2.1851(10)	Ni(1)-Cl(1)	2.2212(8)
S(1)-C(8)	1.834(3)	P(1)-C(13)	1.851(4)
S(1)-C(7)	1.844(3)		
P(1)-Ni(1)-S(1)	88.49(4)	Cl(2)-Ni(1)-P(1)	87.41(4)
Cl(1)-Ni(1)-S(1)	91.07(3)	Cl(2)-Ni(1)-S(1)	174.94(4)
Cl(1)-Ni(1)-P(1)	176.26(4)	Cl(1)-Ni(1)-Cl(2)	93.21(4)
Ni(1)-S(1)-C(7)	113.25(13)	Ni(1)-P(1)-C(13)	107.87(10)
Ni(1)-S(1)-C(8)	106.07(12)		

Table 5-2: Selected bond lengths (Å) and angles (°) of palladium complex Ni(L¹Bn)Cl₂ **19**

Using the modified ligand synthesis, palladium dichloride complex **20** was formed by reacting equimolar amounts of palladium bisbenzonitrile chloride and free ligand **L¹Bn** (**Scheme 5-4**). After stirring the reaction in anhydrous THF at room temperature for two hours ³¹P NMR spectroscopy identified the presence of a singlet at δP 63.2. Low resolution electrospray mass spectrometry of the reaction solution showed the major ion fragment [M-Cl]⁺ at 537.1 verifying the formation of complex **20**.
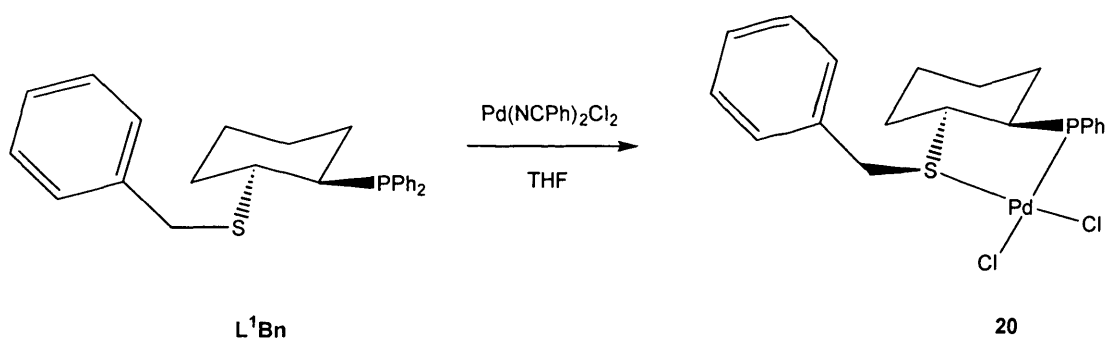
Scheme 5-4: Reaction scheme for the synthesis of Pd(L¹Bn)Cl₂ **20**

5.2 Coordination of phosphinothioether $L^1$1-MN

Through the successful complexation of L^1Bn to form the palladium (II) dichloride complex **20**, it was decided to use a similar synthetic method for ligand $L^1$1-MN and compare the complexes formed. Monitoring of complexation of this particular ligand was followed by the presence and shift of the thioether methylene protons in the ^1H NMR spectrum. Complexation was initiated by reacting previously formed ligand $L^1$1-MN with palladium bisbenzonitrile chloride to form the resulting palladium phosphinothioether dichloride **21** under anaerobic conditions (**Scheme 5-5**).
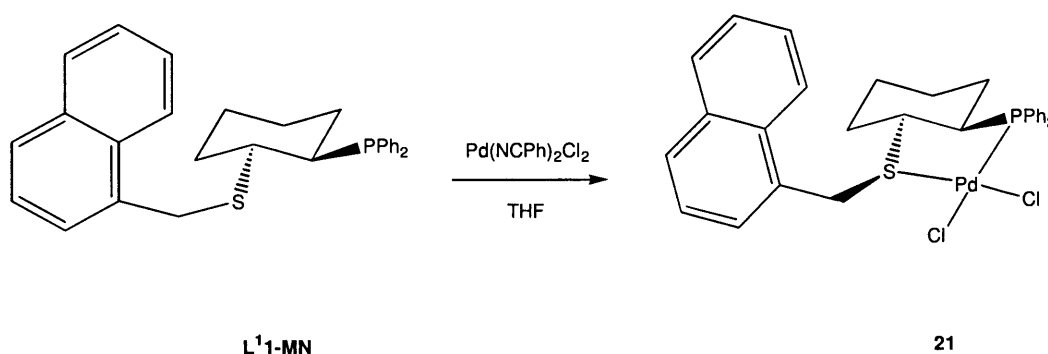
Scheme 5-5: Reaction scheme for the formation of Pd($L^1$1-MN)Cl$_2$ **21**

A THF solution of phosphinothioether $L^1$1-MN was added drop-wise to the dissolved palladium precursor, over the course of an hour the reaction solution changed from a deep orange colour to a bright yellow solution. Completion of the reaction resulted in a bright yellow precipitate crashing out of solution. ^{31}P NMR spectrum of the reaction solution shows completion of the reaction with the consumption of phosphinothioether ligand $L^1$1-MN. The precipitate was dissolved in CDCl$_3$ and a ^{31}P NMR spectrum of the solution shows two siganls at δ_P 68.5 and δ_P 67.7 of different intensity (5:1). ^1H NMR spectrum of the mixture shows the major product to be the palladium phosphinothioether complex **21** with the presence of the two methylene protons at δ_H 5.04 and 5.56 similar to that seen for complex **20**. Low resolution electrospray mass spectrometry of the mixture shown the presence of the major fragment being complex **21** missing one chloride [M-Cl]$^+$ at 581.0.

The mixture of compounds was separated by slow diffusion of diethyl ether into a CH$_2$Cl$_2$ solution. This process produced a number of high quality yellow block shaped crystals, of good enough quality for X-ray diffraction analysis. The result was somewhat of a surprise as the complex formed in small amounts was that of palladium thioether-ylide complex **22** (**Scheme 5-6**). The ^{31}P NMR spectrum of the free ligand **L^{1}1MN** did not suggest that there was a phosphonium salt present. Phosphonium salts can be easily identified in the ^{31}P NMR spectrum with signals around ~δ_P 60 and usually remain unreactive [120].
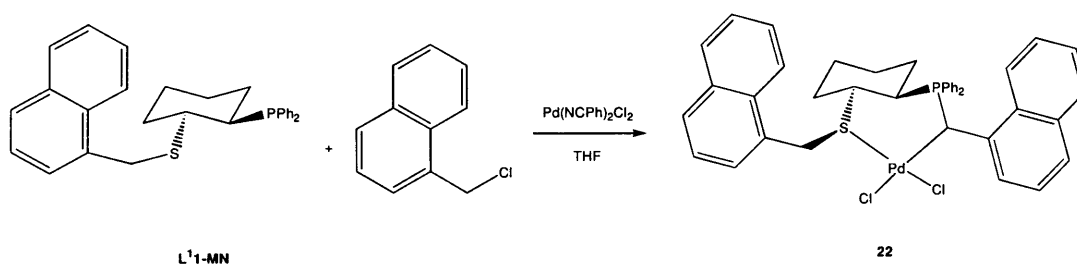
Scheme 5-6: Reaction scheme for the formation of Pd(1-MNL^{1}1-MN)Cl$_2$ **22**

In the literature there are no examples of S, C-chelating phosphonium-thioether ligands, the closest resembling complex is a palladium chiral chelating P, C complex synthesised by Zurawinski [136]. The synthesis of the complex uses (sulfinylmethyl)phosphonium salt [(S$_s$)-6H][PF$_6$] which is deprotonated using n-butyl lithium and regenerates the ylide which is in turn coordinated to a palladium (II) metal centre (**Scheme 5-7**). A presence of a base is required to deprotonate such ligands which are not present in the formation of complex **22**.
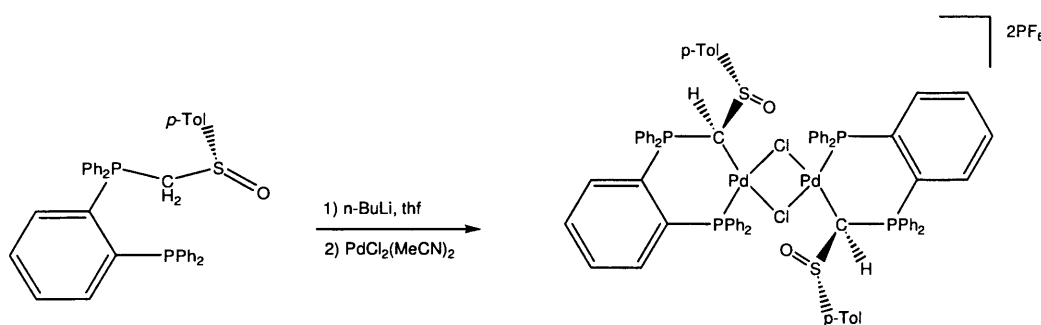
Scheme 5-7: Reaction scheme for the formation of a palladium ylide complex

For the synthesis of complex **22** to be possible, excess of aryl methyl halide must be present as the ylide does not form in preference to phosphinothioether **L^{1}1-MN**.

122

For the current reaction 1-methylchloro naphthalene is added directly using a syringe. In the proceeding reactions aryl methyl halides were diluted to give greater accuracy to ensure no ylide formation takes place unless required. Attempts to form crystals of the phosphinothioether complex **21** for X-ray analysis were unsuccessful with the ylide complex being more soluble in polar solvents.

An ORTEP view of complex **22** can be seen in **Figure 5-3** showing the first isolated palladium phosphinothioether dichloride species. Studying the crystal data for complex **22**, few comparisons can be made with the previously formed palladium phosphinothioether complexes as this is a different class of compound. The backbone of the ligand is extended to a six membered chelate, it would be expected that the metal plane would be even more skewed away from a square planar geometry, and that is what we see with S(1)-Pd(1)-Cl(2) and C(30)-Pd(1)-Cl(1) bond angles being 174.88(3)° and 175.66(11)° respectively.
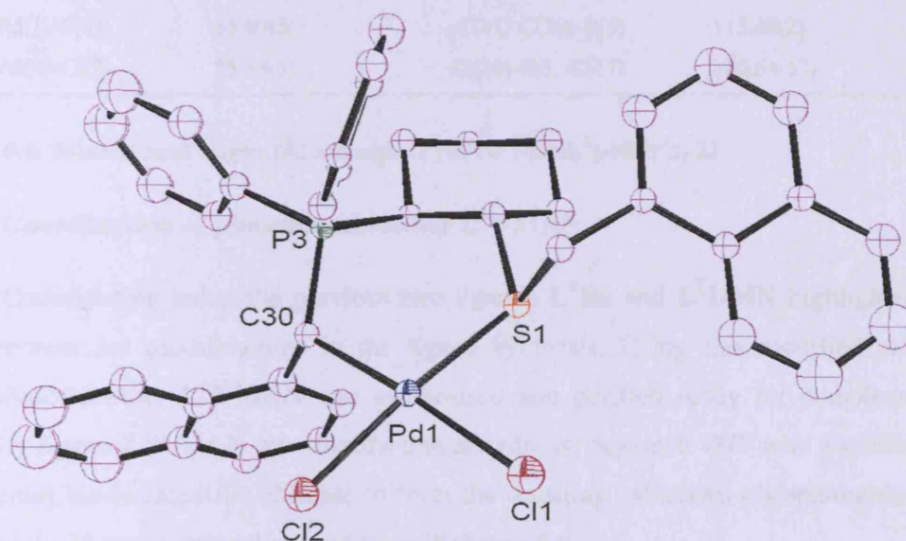
Figure 5-3: Crystal structure of Pd(1-MNL^{1}1-MN)Cl$_2$ **22**. Hydrogen atoms are omitted for clarity. Thermal ellipsoids are drawn at 50% probability

Crystallographic data in **Table 5-3** shows selected bond angles and lengths for Pd(1-MNL^{1}1-MN)Cl$_2$ **22**. Bond lengths of the metal centre show only slight differences to the literature with the Pd(1)-S(1) bond length of 2.2916(9)Å being in the slightly longer range to those in the literature for palladium phosphino-thioether complexes [89]. The palladium-carbon bond being 2.068(3)Å is in the range expected for a palladium phosphonium ylide complexes [130]. There is no evidence of a palladium phosphonium

123

ylide thiol complex in the literature, bond lengths are compared with mixed donor ylide complexes [131] and di-phosphonium complexes [132]. The synthesis of a nickel phosphonium ylide thiol complex has been reported [133]. The ORTEP view of the cyclohexyl backbone shows the chiral carbons of the adopting an (S, S) orientation, opposite to those seen in complexes 18 and 19. The cyclohexyl backbone prefers to be in the chair conformation when coordinating to metal centres when only one diastereoisomer is formed from a racemic ligand mixture.

| Pd(1)-Cl(2)	2.3355(10)	C(30)-P(3)	1.776(4)
Pd(1)-S(1)	2.2916(9)	P(3)-C(17)	1.836(4)
Pd(1)-C(30)	2.068(3)	S(1)-C(1)	1.852(4)
Pd(1)-Cl(1)	2.3958(9)	S(1)-C(12)	1.844(4)
C(30)-Pd(1)-S(1)	92.20(5)	Pd(1)-S(1)-C(12)	121.66(11)
Cl(2)-Pd(1)-S(1)	177.42(6)	Pd(1)-S(1)-C(1)	104.72(12)
Cl(2)-Pd(1)-C(30)	85.25(5)	Pd(1)-C(30)-P(3)	114.00(18)
Cl(1)-Pd(1)-C(30)	176.41(2)	Pd(1)-C(30)-C(31)	111.99(2)
Cl(1)-Pd(1)-S(1)	85.89(5)	C(31)-C(30)-P(3)	113.48(2)
Cl(2)-Pd(1)-Cl(2)	85.89(5)	C(30)-P(3)-C(17)	110.64(17)

Table 5-3: Selected bond lengths (Å) and angles (°) of Pd(1-MNL^{1}1-MN)Cl$_2$ **22**

5.3 Coordination of phosphinothioether L^{1}9-MAN

Coordination using the previous two ligands L^{1}Bn and L^{1}1-MN highlighted the requirement for modifications in the ligand synthesis. Using this modified process phosphinothioether L^{1}9-MAN was synthesised and purified ready for complexation. Initially ligand L^{1}9-MAN was dissolved in anhydrous, degassed THF with a solution of palladium bis-benzonitrile chloride to form the resulting palladium phosphinothioether dichloride **23** under anaerobic conditions (**Scheme 5-8**).
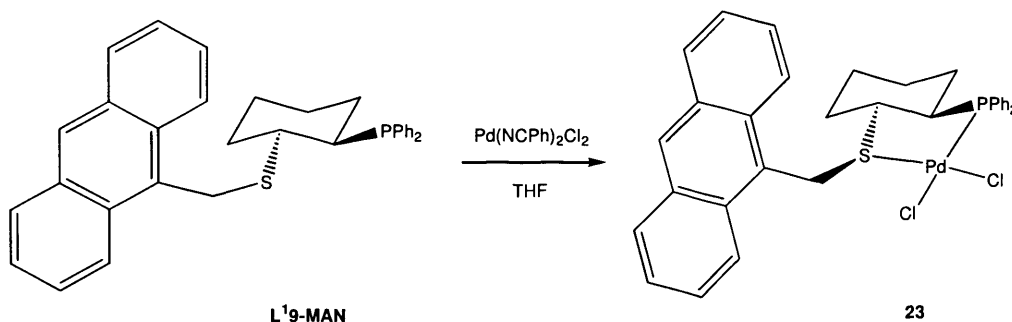
Scheme 5-8: Reaction scheme for the formation of Pd(L^{1}9-MAN)Cl$_2$ **23**

124

Evaporation of the solvent left an orange solid a sample was dissolved in CDCl$_3$ for ^{1}H NMR analysis. The spectrum reveals the only product present to be the palladium phosphinothioether complex **23** identified with the presence of the two methylene protons at δ_H 5.74 and δ_H 5.97 the largest shift downfield for any of the thioether complexes formed thus far. Single crystals were then grown by slow diffusion of Et$_2$O into a CH$_2$Cl$_2$ solution of **25**. These orange block shaped crystals were of good enough quality to run X-ray diffraction analysis and an ORTEP view of complex **23** can be seen in **Figure 5-4**.
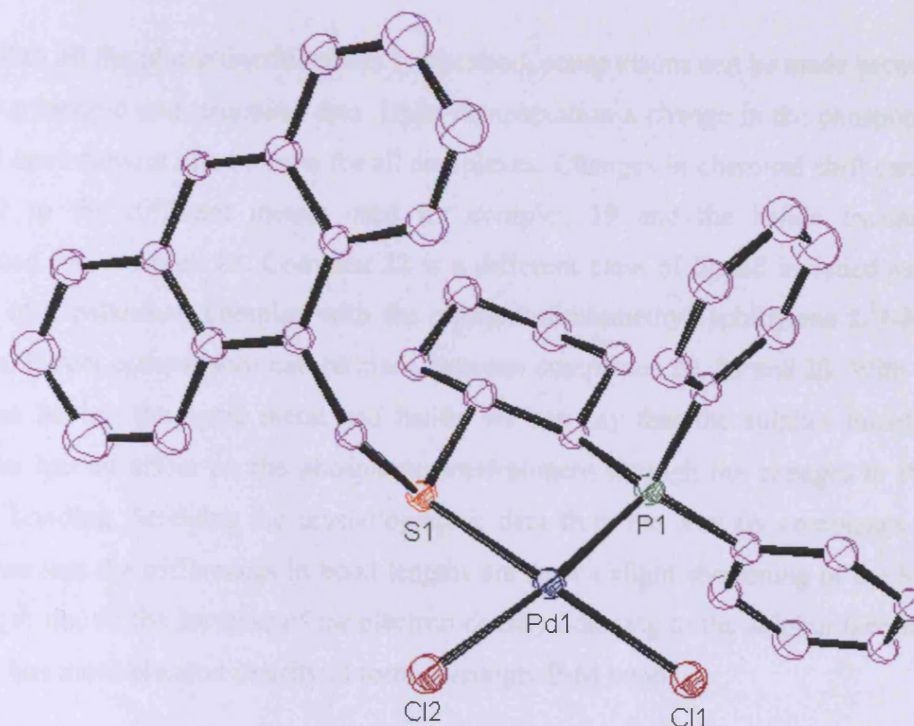
Figure 5-4: Crystal structure of Pd(**L^{1}9-MAN**)Cl$_2$ **23.** Hydrogen atoms are omitted for clarity. Thermal ellipsoids are drawn at 50% probability

Crystallographic data of complex **23** in **Table 5-4** shows selected bond angles and lengths. From the crystal data, comparisons can be made between the complexes that have been formed in earlier reactions. The ORTEP view also shows how the methyl anthracene thioether orientates itself away from the ligand backbone with a reduction in the P(1)-Pd(1)-S(1) bite angle by half a degree to 87.55(4)° compared to the less bulky benzyl thioether **18**. These values are still within the expected values seen in the literature [89].

Pd(1)-S(1)	2.2792(10)	Pd(1)-P(1)	2.2207(10)
Pd(1)-Cl(2)	2.3842(10)	Pd(1)-Cl(1)	2.3101(10)
S(1)-C(19)	1.851(4)	P(1)-C(13)	1.836(4)
S(1)-C(18)	1.846(4)		
P(1)-Pd(1)-S(1)	87.55(4)	Cl(2)-Pd(1)-P(1)	173.15(4)
Cl(1)-Pd(1)-S(1)	175.63(4)	Cl(2)-Pd(1)-S(1)	89.58(3)
Cl(1)-Pd(1)-P(1)	89.83(4)	Cl(2)-Pd(1)-Cl(2)	93.41(4)
Pd(1)-S(1)-C(19)	105.28(13)	Pd(1)-S(1)-C(18)	106.23(13)

Table 5-4: Selected bond lengths (Å) and angles (°) of Pd(L^{1}9-MAN)Cl$_2$ 23

With all the phosphinothioethers synthesised, comparisons can be made between their spectroscopic and structural data. Upon complexation a change in the phosphorus chemical environment can be seen for all complexes. Changes in chemical shift can be attributed to the different metals used for complex 19 and the halide exchange experienced for complex 18. Complex 22 is a different class of ligand included as an example of a palladium complex with the phosphino-thiomethylnaphthylene L^{1}1-MN backbone. Direct comparisons can be made between complexes 20, 21 and 23. With the complexes having the same metal and halide we can say that the sulphur thioether substituent has an effect on the phosphorus environment through the changes in P-M and S-M bonding. Studying the crystallographic data from the relevant complexes we can assume that the differences in bond lengths are seen a slight shortening of the M-P bond length due to the increase of the electron density donating to the sulphur therefore the metal has more electron density to form a stronger P-M bond.

Complex	S-M-P (°)	M-X(1)	M-X(2)	M-X length (Å)	Stereoisomer
Pd(L^{1}Bn)Br$_2$ 18	86.99(6)	2.4730(10)	2.4177(9)	2.24177(9)	(R, R)
				2.4730(10)	
Ni(L^{1}Bn)Cl$_2$ 19	88.79(4)	2.2212(8)	2.1851(10)	2.1851(10)	(R, R)
				2.2212(8)	
Pd(1-MNL^{1}1-MN)Cl$_2$ 22	100.39(11)	2.3958(9)	2.3355(10)	2.3355(10)	(S, S)
	(C-Pd-S)			2.3958(9)	
Pd(L^{1}9-MAN)Cl$_2$ 23	87.55(4)	2.3842(10)	2.3101(10)	2.3842(10)	(R, R)
				2,3101(10)	

Table 5-5: Comparison of phosphinothioether complexes synthesised

5.4 Synthesis of palladium phosphinothioether dichloride complexes using L²Bn, L²1-MN and L²9-MAN

After the study for producing phosphinothioether complexes using a relatively small conformationally confined ligand backbone we move our attention the second type of phospihnothioether ligands **L²R** with contrasting steric properties. We have formed a series of phosphinothioether complexes using the previously synthesised ligands for structural comparisons. All complexation reactions were performed using one equivalent of phosphino-thioether **L²R** dissolved in THF followed by drop-wise addition to a solution of palladium bis-benzonitrile dichloride (**Scheme 5-9**). All reactions gave similar visual indications with the formation of a yellow solution after two hours to indicate reaction completion.
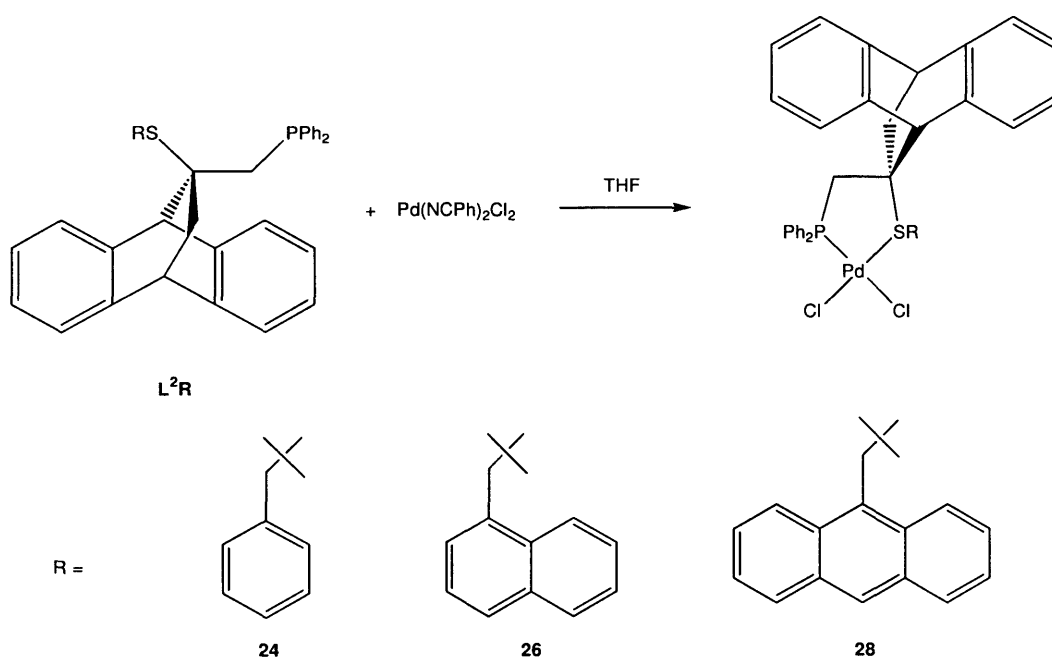
Scheme 5-9: Reaction scheme for the formation of phosphinothioether complexes Pd(L²R)Cl₂ (**24, 26, 28**)

Using the conformationally confined ligand **L¹R** single stereoisomers have been observed by spectroscopic analysis. From initial spectroscopic data we see the first indication of a mixture of stereoisomers and conformers from a single reaction. Phosphorus NMR data shown broad signals in the region of δP 40-50 for all materials confirming the formation of fluxional complexes. ¹H NMR gives an overall broad spectrum with only a small number of resolved signals in the aromatic region indicating

a change in ligand conformation or geometry. From this evidence it was assumed that more than one complex had formed for each phosphinothioether reaction.

Using different polarity solvents the same integration of signals in the phosphorus NMR spectrum was seen compared to those dissolved in deuterated chloroform. This would indicate that the complexes formed had similar dipole moments. All complexes were re-crystallised using diffusion techniques in attempt to isolate and identify the complexes formed. Only in the case of complex **24** were single crystals isolated suitable for X-ray diffraction analysis. The resulting data is displayed below along with an ORTEP view showing the isolation of phosphinothioether **24** (**Figure 5-5**).
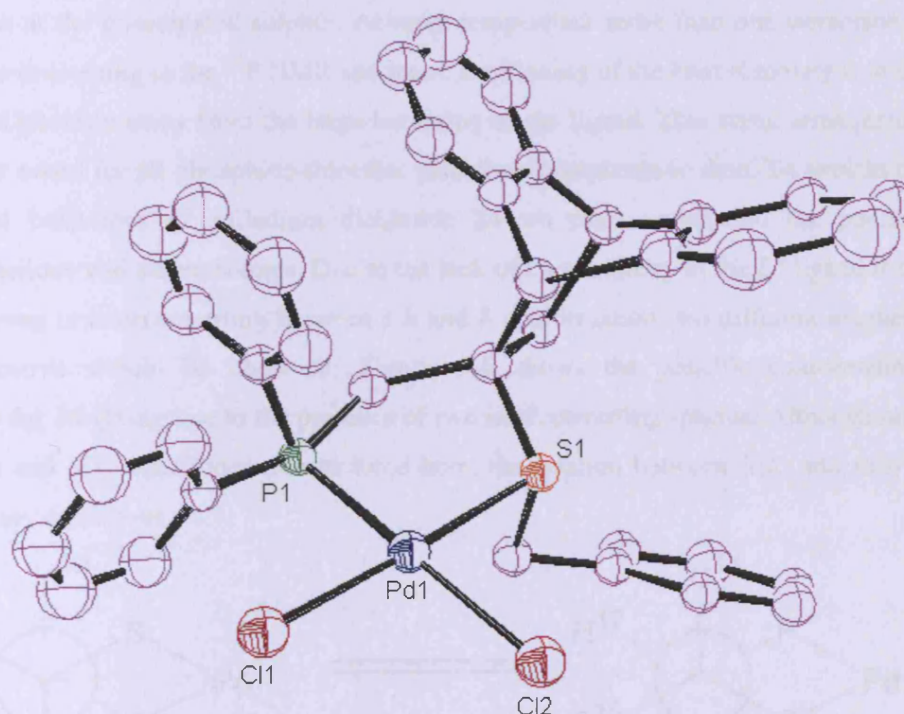
Figure 5-5: Crystal structure of Pd(L^2Bn)Cl$_2$ **24**. Hydrogen atoms are omitted for clarity. Thermal ellipsoids are drawn at 50% probability.

Crystallographic data in **Table 5-6** shows selected bond lengths and angles. The formation of the desired palladium phosphino-thioether was not expected from the spectroscopic data gathered before recrystallisation due to the fragments observed in the electrospray mass spectrum. These crystals were then re-dissolved in deuterated

chloroform and proton and phosphorus NMR data was gathered on the purified material.

Pd(1)-Cl(2)	2.4236(14)	Pd(1)-P(1)	2.2788(14)
Pd(1)-S(1)	2.2819(14)	Pd(1)-Cl(1)	2.3235(15)
P(1)-Pd(1)-S(1)	92.20(5)	Cl(2)-Pd(1)-P(1)	176.41(2)
Cl(1)-Pd(1)-S(1)	177.42(6)	Cl(2)-Pd(1)-S(1)	85.89(5)
Cl(1)-Pd-P(1)	85.25(5)	Cl(2)-Pd(1)-Cl(2)	85.89(5)

Table 5-6: Selected bond lengths (Å) and angles (°) of palladium complex **24**

The same spectrum was observed when compared to NMR data from the bulk material. This confirms that the $Pd(L^2Bn)Cl_2$ complex must be fluxional, most likely involving inversion at the coordinated sulphur. At room temperature more than one stereoisomer of **24** are coalescing in the ^{31}P NMR spectrum. Positioning of the benzyl moiety is in the expected position away from the large backbone of the ligand. This steric arrangement has been noted for all phosphino-thioether palladium complexes to date. To explain the fluxional behaviour of palladium dichloride **24** we must understand the possible conformations and stereoisomers. Due to the lack of C_2 symmetry in the L^2 ligand if the chelate ring is interconverting between a λ and δ conformation two different magnetic environments should be observed. **Figure 5-6** shows the possible conformations possible for **24** giving rise to the presence of two interconverting species. Although only the $S(\delta)$ and $S(\lambda)$ conformers are pictured here, the relation between $R(\lambda)$ and $R(\delta)$ is completely analogous.
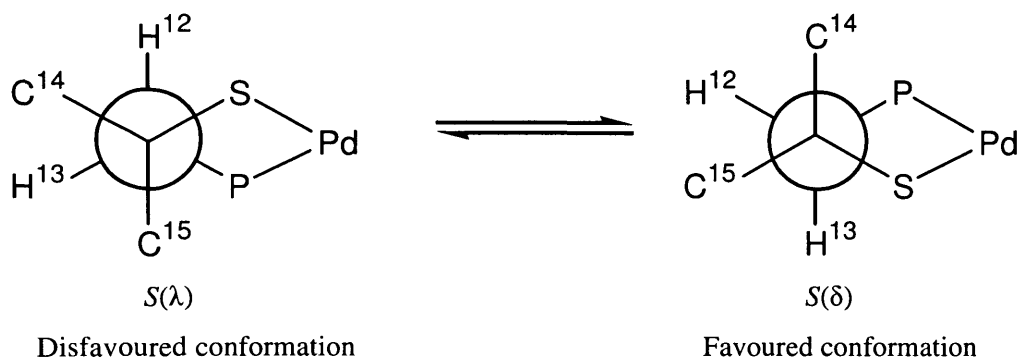

$S(\lambda)$

Disfavoured conformation

$S(\delta)$

Favoured conformation

Figure 5-6: Newman projection for the possible conformations of **24**.

5.5 Variable temperature NMR studies

To verify the presence and attempt to quantify which conformations of the complexes formed were preferred, variable temperature NMRs were recorded for the three palladium phosphino-thioether complexes formed in this chapter. Low-temperature ^{31}P and ^{1}H NMR spectra were recorded on a 500 MHz Bruker instrument, temperature ranges were selected between -50°C to 40°C at 10°C intervals. Chloroform was selected as the solvent for this study due to the solvent having a freezing point of -55°C.

Complex **24** was selected for the first VT experiments after being purified through recrystalisation. The major difficulty encountered with this procedure was the reduced solubility of complexes after recrystallisation. For all the complexes the same generic pattern was observed with the identification of four different signals at lower temperatures. With complex **24** having low solubility the lower temperatures precipitated the complex and proton NMRs at these temperatures were difficult to identify signals. Out of the three sets of complexes samples, phosphinothioether complex **26** gave most resolved spectra. This ligand had the highest solubility and produced spectra which gave the highest resolution. Shown below are the results of the phosphorus low temperature NMRs displayed in a stack plot (**Figure 5-7**).
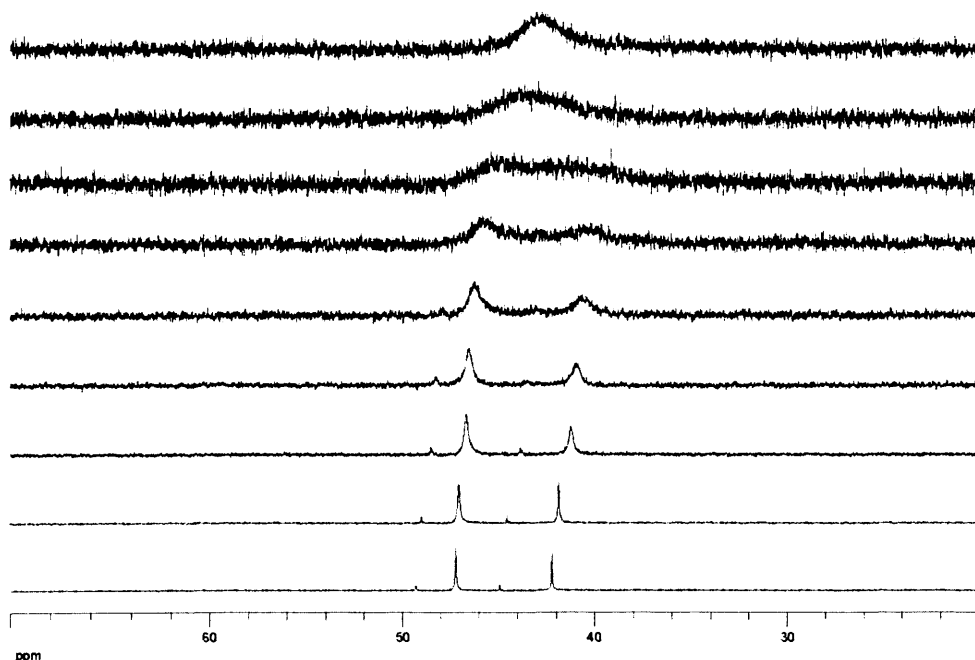

Figure 5-7: Stack plot of variable temperature ^{31}P NMRs of complex **26** dissolved in CDCl₃, temperatures between -50°C to 40°C.

At -50°C two sets of two complexes of different intensities were observed. The larger signals at δ_P 42.9 and δ_P 47.9 relate to the δ and λ conformers of the preferred sulphur arrangement as discussed previously which wouldn't give any energetic preference and therefore have almost equal intensity. The two peaks with the smaller integrated signals at chemical shifts of δ_P 45.3 and δ_P 49.8 are attributed to δ and λ conformers with sulphur inversion, placing the bulky thioether moieties on the same plane as the ligands backbone. Activiation energies range between 51-56 kJ Mol^{-1} which is required to inter-convert such large thioether moieties and therefore a preference is adopted for the lone pair of electrons of sulphur to stay *trans* to the axial hydrogen on the backbone of the ligand. Fluxional phosphinothioethers are reported in the work of Evans where an effective means of controlling the configuration at the sulphur is designed into the ligand [106]. This inter-conversion can further be demonstrated in the low temperature ^{1}H NMR spectra where signals in a room temperature NMR can be seen to convert into the four signals observed in the phosphorus NMR spectrum.
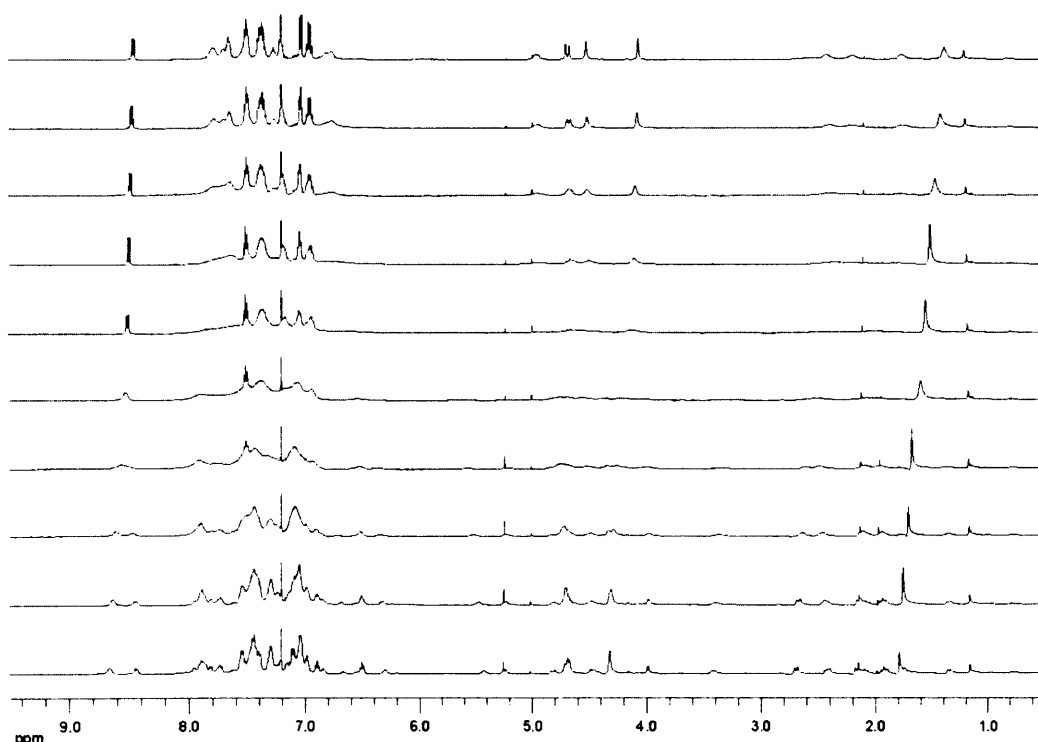

Figure 5-8: Stack plot of variable temperature ^{1}H NMRs of complex 26 dissolved in CDCl₃, temperatures between -50°C to 40°C.

Figure 5-8 shows the complete low temperature ^{1}H NMR spectra for complex 26 with signals converting in all areas of the spectrum. This shows that the stereogenic

131

centres of $\mathbf{L^11\text{-}MN}$ have an influence on all proton environments from saturated backbone ligand protons to aromatic phenyl protons. A good example of this can be seen in the aromatic section of the spectrum as illustrated in **Figure 5-9**. This shows the most resolved signal at 40°C and with the temperature gradually lowered shows the presence of two major products along with the shoulder signals which are the isomers with sulphur inversion.
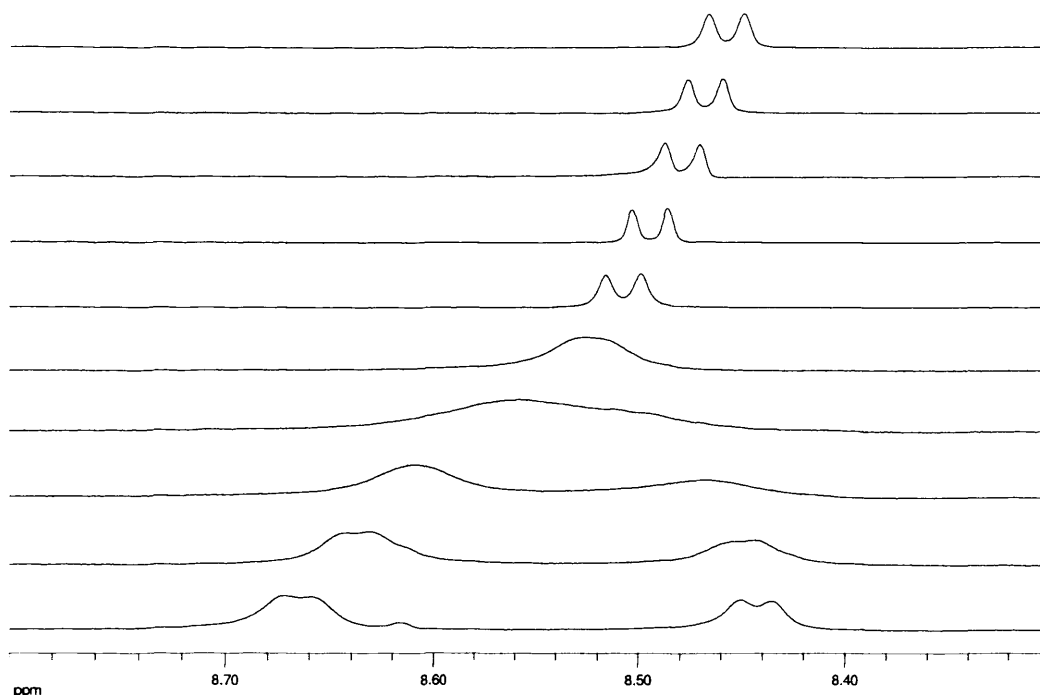
Figure 5-9: Stack plot of variable temperature ^{1}H NMRs of complex **26** dissolved in $CDCl_3$, temperatures between -50°C to 40°C in the aromatic region.

5.6 Iridium complexes

After the characterisation and complexation of the series of palladium phosphinothioethers we then turned our attention to coordination with iridium. The iridium cod chloride dimer which was synthesised using standard methods [129], was reacted with a half molar equivalent of $\mathbf{L^1Bn}$ dissolved in degassed CH_2Cl_2. This reaction afforded the iridium chloride species shown in **Scheme 5-10**. Through a counter ion exchange reaction using ammonium hexafluorophosphide dissolved in degassed water, complex **25** was isolated. The ^{31}P NMR spectrum shows the presence of a singlet at δ_P 36.5 and a septet at δ_P -143.2 (J_{PF} = 7.1 Hz).
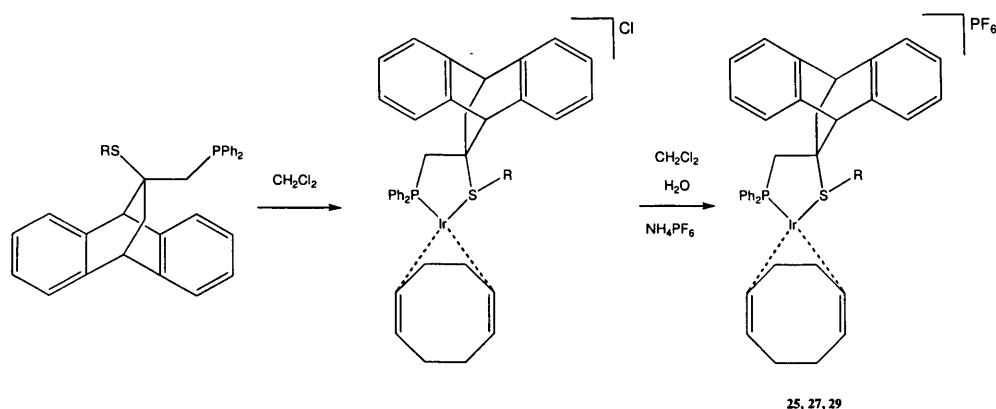
Scheme 5-10: Reaction scheme for the formation of $[Ir(L^2)(cod)]PF_6$ complexes **25, 27** and **29**

^1H NMR analysis gave a broad spectrum similar to that seen for the palladium counter part. Low temperature (-50°) NMR data shows that the interconversion was too rapid to isolate the spectrum of the interconverting species. ^{13}C NMR spectrum shows the formation of the desired complex with the correct number of saturated carbon signals observed. Electrospray mass spectrometry shows the major ion to be that of the iridium complex minus its hexafluorophosphide counter ion.

The series of iridium complexes are still air sensitive and must be treated using anhydrous degassed solvents when recording NMRs and attempts for recrystallisation. Formation of the analogous L^21-MN iridium complex was done using previously stated methods. Again the ^{31}P NMR spectrum shows the presence of a singlet at δ_P 35.8 for the ligand phosphorus and a septet at δ_P =143.2 for the counter ion with fluoride coupling J_{PF} = 6.4. ^1H NMR shows the broad spectrum at room and low temperatures. ^{13}C NMR data gives evidence of the formation of the desired complex. Phosphinothioether L^29-MAN shows all the same characteristic as the previous two complexes. Electrospray mass spectrometry shows the formation of complex **29** minus the phosphine counter ion.

We have demonstrated the differences between the small conformationally confined backboned phosphinothioether complexes (ML^1R) to that of the large phosphinothioether complexes (ML^2R) that contain a degree of rotational freedom around the chiral carbon. The fluxional properties of these metal complexes make characterising very difficult compared to the confined backboned complexes. The steric influence of the backbone does not lead to distortions of the metal-ligand bonding compared to ligand L^1 therefore we can conclude that simple phosphinothioethers would be used for catalytic reactions where steric interactions are required. However,

133

electronic diversity can be seen between the two types of complexes. Complex **24** shows a larger *trans* influence for the diphenylphosphino- groups therefore lowering the *trans influence* of the thioether moiety. Where electronic differences are required the bulky phosphinothiother complexes could demonstrate greater activity.

5.7 Experimental
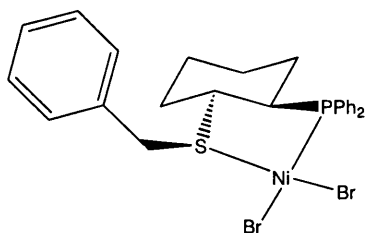
Preparation of Ni(C₇H₇SC₆H₁₀PPh₂)Br₂ 17. Diphenyl phosphine (1.63 g, 8.76 mmol) was charged with THF (30 ml) whilst stirring under argon. The solution was then cooled to 0°C using an ice bath and n-BuLi (2.5 M, 1.52 ml, 8.76 mmol) was added drop-wise turning the solution bright yellow. After one hour of stirring cyclohexene sulphide (1.00 g, 8.76 mmol) was dissolved in anhydrous THF (20 ml) and added to the reaction drop-wise at 0°C whilst stirring under argon turning the solution colourless. After one hour of stirring benzyl bromide (1.50 g, 8.76 mmol) was added drop-wise. NiCl₂.6H₂O (0.5 g, 2.1 mmol), **L¹Bn** (0.815 g, 2.1 mmol) and potassium bromide (0.72g, 6.3 mmol) were dissolved in anhydrous methanol (30 ml) whilst stirring under argon for two hours. The solvent was then removed and redissolved in dichloromethane (20 ml). Excess KBr was then filtered off leaving a purple solution. Evaporation of the solvent left a purple solid. Yield 0.129g (88%). δ$_P$ (CDCl₃, 121MHz) 60.0. Mass calculated for C₂₅H₂₇S₁P₁Ni₁Br₂(-Br) requires m/z 528.9, found m/z 529.0 (LRES).
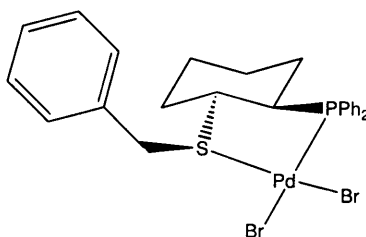
Preparation of Pd(C₇H₇SC₆H₁₀PPh₂)Br₂ 18. Diphenyl phosphine (1.63 g, 8.76 mmol) was charged with THF (30 ml) whilst stirring under argon. The solution was then cooled to 0°C using an ice bath and n-BuLi (2.5 M, 1.52 ml, 8.76 mmol) was added drop-wise turning the solution bright yellow. After one hour of stirring cyclohexene sulphide (1.00 g, 8.76 mmol) was dissolved in anhydrous THF (20 ml) and added to the reaction drop-wise at 0°C whilst stirring under argon turning the solution colourless. After one hour of stirring benzyl bromide (1.50 g, 8.76 mmol) was added drop-wise.

Pd(NCPh)$_2$Cl$_2$ (0.5 g, 1.3 mmol), **L^{1}Bn** (0.507 g, 1.3 mmol) and potassium bromide (0.56 g, 4.8 mmol) were dissolved in anhydrous methanol (30 ml) whilst stirring under argon for two hours. The solvent was then removed and redissolved in dichloromethane (20 ml). The KBr was then filtered off leaving an orange solution. Evaporation of the solvent left a yellow solid. Pd(**L^{1}Bn**)Br$_2$ **7** was isolated from slow evaporation of a CH$_2$Cl$_2$ solution. This method afforded orange block type crystals suitable for X-ray diffraction. Yield 1.033g (75%). δ_H (CDCl$_3$, 400MHz) 0.084 (2H, m, Cy), 1.12 (2H, m, Cy), 1.56 (2H, m, Cy), 1.70 (1H, d, Cy, $^2J_{HH}$ = 13.7), 1.86 (1H, d, Cy, $^2J_{HH}$ = 12.7), 2.07 (1H, m, Cy), 2.34 (1H, m, Cy), 4.25 (1H, d, C*H$_2$*, $^2J_{HH}$ = 13.6), 5.06 (1H, d, C*H$_2$*, $^2J_{HH}$ = 13.6) 7.16-7.72 (15H, m, Ar*H*). δ_P (CDCl$_3$, 121MHz) 65.9. Mass calculated for C$_{25}$H$_{27}$S$_1$P$_1$Pd$_1$Br$_2$(-Br) requires m/z 576.6, found m/z 576.9 (LRES).
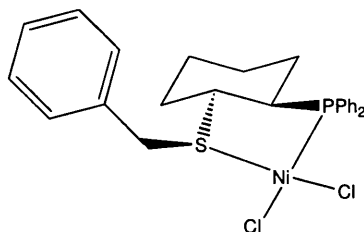
Preparation of Ni(C$_7$H$_7$SC$_6$H$_{10}$PPh$_2$)Cl$_2$ 19. NiCl$_2$.6H$_2$O (0.5 g, 2.1 mmol) and **L^{1}Bn** (0.815 g, 2.1 mmol) were dissolved in anhydrous CH$_2$Cl$_2$ (30 ml) whilst stirring under argon. The reaction mixture was then stirred at room temperature for 2 hours. Removal of the solvent left a purple solid. Ni(**L^{1}Bn**)Cl$_2$ **9** was isolated from slow diffusion of diethyl ether into a CH$_2$Cl$_2$ solution. This method afforded purple block type crystals suitable for X-ray diffraction. Yield 0.838 g (77%). δ_H (CDCl$_3$, 400MHz) 0.66 (1H, m, Cy), 0.82 (1H, m, Cy), 1.08 (1H, m, Cy), 1.46 (3H, m, Cy), 1.76 (2H, m, Cy), 2.07 (1H, m, Cy), 2.19 (1H, m, Cy), 3.81 (1H, d, C*H$_2$*, $^2J_{HH}$ = 13.5), 4.67 (1H, d, C*H$_2$*, $^2J_{HH}$ = 13.2) 7.26 (3H, t, Ar*H*, $^3J_{HH}$ = 7.6), 7.35-7.67 (10H, m, Ar*H*), 7.88 (2H, d, Ar*H*, $^2J_{HH}$ = 3.4) . δ_P (CDCl$_3$, 121MHz) 50.0. Mass calculated for C$_{25}$H$_{27}$S$_1$P$_1$Ni$_1$Cl$_2$ (-Cl) requires m/z 483.1, found m/z 483.0 (LRES).
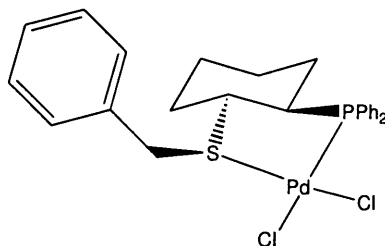
Preparation of Pd(C$_7$H$_7$SC$_6$H$_{10}$PPh$_2$)Cl$_2$ 20. PdCl$_2$(NCPh)$_2$ (0.122 g, 0.318 mmol) and **L^{1}Bn** (0.124 g, 0.318 mmol) were dissolved in anhydrous THF (30 ml) whilst stirring under argon. The reaction mixture was then stirred at room temperature for 2 hours. Removal of the solvent left a yellow solid powder. Yield 0.139 g (77%). δ_H (CDCl$_3$, 400MHz) 0.75 (1H, m, Cy), 0.87 (1H, m, Cy), 1.15 (1H, m, Cy), 1.58 (2H, m, Cy), 1.72 (1H, m, Cy), 1.88 (1H, m, Cy), 2.09 (1H, m, Cy), 2.36 (2H, m, Cy), 4.07 (1H, d, CH_2, $^2J_{HH}$ = 13.6), 4.94 (1H, d, CH_2, $^2J_{HH}$ = 13.6) 7.14-7.73 (15H, m, ArH). δ_P (CDCl$_3$, 121MHz) 63.2. Mass calculated for C$_{25}$H$_{27}$S$_1$P$_1$Pd$_1$Cl$_2$(-Cl) requires m/z 532.6, found m/z 537.1 (LRES).
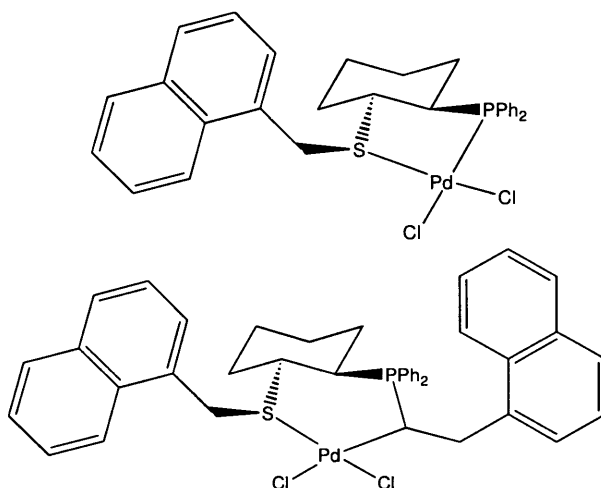
Preparation of Pd(C$_{11}$H$_9$SC$_6$H$_{10}$PPh$_2$)Cl$_2$ 21 and Pd(C$_{11}$H$_9$SC$_6$H$_{10}$PPh$_2$C$_{11}$H$_8$)Cl$_2$ 22. Pd(NCPh)$_2$Cl$_2$ (0.224 g, 0.321 mmol) and **L^{1}1-MN** (0.124 g, 0.321 mmol) were dissolved in anhydrous THF (30 ml) whilst stirring under argon. The reaction mixture was then stirred at room temperature for 2 hours. Removal of the solvent left a yellow solid.

Pd(L^{1}1-MN)Cl$_2$ 21 was isolated from slow diffusion of diethyl ether into a CH$_2$Cl$_2$ solution. Yield 0.109 g (55%). δ_H (CDCl$_3$, 400MHz) 0.75 (1H, m, Cy), 1.04 (1H, m, Cy), 1.26 (1H, m, Cy), 1.40 (2H, m, Cy), 1.63 (1H, m, Cy), 1.75 (1H, m, Cy), 1.81 (1H, m, Cy), 3.60 (1H, t, Cy, $^2J_{HH}$ = 6.3), 5.04 (1H, d, CH_2, $^2J_{HH}$ = 13.4), 5.56 (1H, d, CH_2, $^2J_{HH}$ = 13.7) 7.48-8.04 (16H, m, ArH), 8.58 (1H, d, ArH, $^2J_{HH}$ = 7.5). δ_P (CDCl$_3$, 121MHz) 68.5; exact mass calculated for C$_{29}$H$_{29}$S$_1$P$_1$Pd$_1$Cl$_2$(-Cl) requires m/z 581.0451, found m/z 581.0435 (ES).

137

Pd(1-MNL^{1}1-MN)Cl$_2$ 22 was isolated from slow diffusion of diethyl ether into a CH$_2$Cl$_2$ solution. This method afforded yellow block type crystals suitable for X-ray diffraction. Yield 0.025 g (11%). δ$_P$ (CDCl$_3$, 121MHz) 67.7.
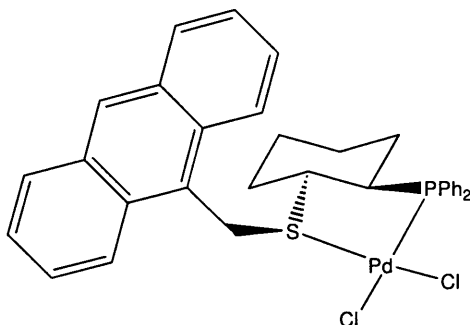
Preparation of Pd(C$_{15}$H$_{11}$SC$_6$H$_{10}$PPh$_2$)Cl$_2$ 23. Pd(NCPh)$_2$Cl$_2$ (0.224 g, 0.321 mmol) and **L^{1}9-MAN** (0.124 g, 0.321 mmol) were dissolved in anhydrous THF (30 ml) whilst stirring under argon. The reaction mixture was then stirred at room temperature for 2 hours. Removal of the solvent left a yellow solid. Pd(**L^{1}9-MAN**)Cl$_2$ was isolated from slow diffusion of diethyl ether into a CH$_2$Cl$_2$ solution. This method afforded orange block type crystals suitable for X-ray diffraction. Yield 0.174g (81%). δ$_H$ (CDCl$_3$, 400MHz) -0.17 (1H, m, Cy), -0.03 (1H, m, Cy), 0.62-1.00 (4H, m, Cy), 1.23 (H, m, Cy), 1.81 (1H, d, Cy, J$_{HH}$ = 12.9), 2.28 (2H, m, Cy) , 5.74 (1H, d, CH_2, $^2J_{HH}$ = 13.6), 5.97 (1H, d, CH_2, $^2J_{HH}$ = 13.6) 7.23-8.42 (19H, m, ArH). δ$_C$ (125MHz, CDCl$_3$) 34.15 (1C, s, Cy), 40.74 (1C, s, Cy), 44.90 (1C, s, Cy), 50.10 (1C, s, Cy), 56.87 (1C, s, Cy), 123.57 (1C, s, ArC), 123.71 (1C, s, ArC), 124.21 (1C, s, ArC), 124.43 (1C, s, ArC), 126.12 (1C, s, ArC), 126.13(1C, s, ArC), 126.36 (1C, s, ArC), 126.58 (1C, s, ArC), 142.06 (1C, s, ArC), 142.49 (1C, s, ArC), 142.89 (1C, s, ArC), 143.27 (1C, s, ArC). δ$_P$ (CDCl$_3$, 121MHz) 65.0; exact mass calculated for C$_{33}$H$_{31}$S$_1$P$_1$Pd$_1$Cl$_2$ (-Cl) requires m/z 631.0607, found m/z 631.0589 (ES).

138
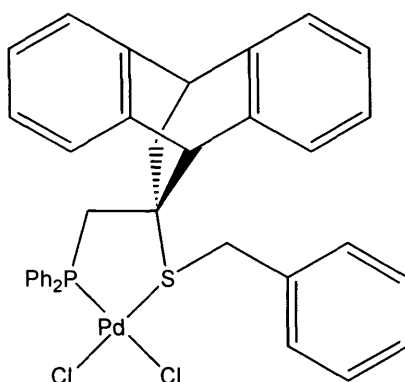
Preparation of Pd(C₇H₇SC₁₇H₁₄PPh₂)Cl₂ 24. Pd(NCPh)₂Cl₂ (0.52 g, 1.35 mmol) and **L²Bn** (0.71 g, 1.35 mmol) were dissolved in anhydrous dcm (30 ml) whilst stirring under argon. The reaction mixture was then stirred at room temperature for 2 hours. Removal of the solvent left a yellow solid. Yield 0.560 g (59%). Exact mass calculated for $C_{36}H_{31}S_1P_1Cl_1Pd_1$ (-Cl) requires m/z 667.0607, found m/z 667.0931 (ES).
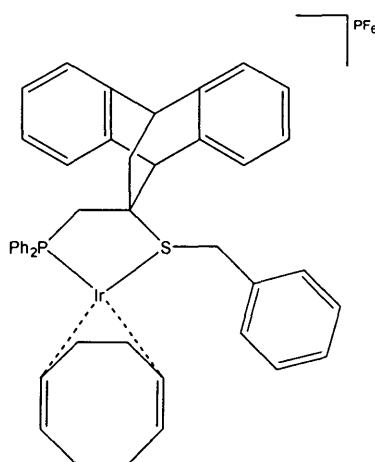
Preparation of [Ir(C₇H₇SC₁₇H₁₄PPh₂)(cod)]PF₆ 25. Ir(cod)Cl₂ (0.38 g, 0.566 mmol) and **L²Bn** (0.29 g, 0.551 mmol) were dissolved in anhydrous dichloromethane (30 ml) whilst stirring under argon. The reaction mixture was then stirred at room temperature for 12 hours. In a counter ion exchange ammonium hexafluorophosphide (0.1g, 0.614 mmol) dissolved in degassed water (20 ml) was added and stirred for 2 hours. The water was then extracted and removal of the solvent left a red solid. Yield 0.33 g (62%). δ_C (125MHz, ppm, CDCl₃) 14.31 (2C, s, CH_2(cod)), 29.93 (2C, s, CH_2(cod)), 30.73 (1C, s, CH), 41.56 (1C, s, CH), 50.97 (1C, d, C, $^2J_{CP}$ = 7.6), 54.00 (1C, s, CH_2) 64.95 (1C, s, CH_2), 65.69 (1C, d, CH_2, $^2J_{CP}$ = 7.6) 83.72 (2C, s, CH(cod)), 84.59 (2C, s, CH(cod)), 124.35 (1C, s, ArC), 124.51 (1C, s, ArC), 124.74 (1C, s, ArC), 124.83 (1C, s, ArC), 125.32 (1C, s, ArC), 125.56 (1C, s, ArC), 125.93 (1C, s, ArC), 126.62 (1C, s, ArC),

126.97 (1C, s, Ar*C*), 127.14 (1C, s, Ar*C*), 127.14 (1C, s, Ar*C*), 127.24 (1C, s, Ar*C*), 127.29 (1C, s, Ar*C*) 127.37 (1C, s, Ar*C*), 127.43 (1C, s, Ar*C*), 127.51 (1C, s, Ar*C*), 127.69 (1C, s, Ar*C*), 128.12 (1C, s, Ar*C*), 131.41 (1C, s, Ar*C*) 131.56 (1C, s, Ar*C*), 132.74 (1C, s, Ar*C*), 132.90 (1C, s, Ar*C*), 135.74 (1C, s, Ar*C*), 138.84 (1C, s, Ar*C*), 140.17 (1C, s, Ar*C*), 141.04 (1C, s, Ar*C*), 142.15 (1C, s, Ar*C*). δ_P (CDCl$_3$, 121MHz) 36.5 (s, *P*Ph$_2$), -143.2 (p, *P*F$_6$, $^7J_{PF}$ = 7.1). Exact mass calculated for C$_{44}$H$_{43}$S$_1$P$_1$Ir$_1$ (-P$_1$F$_6$) requires m/z 827.2374, found m/z 827.2369 (ES).
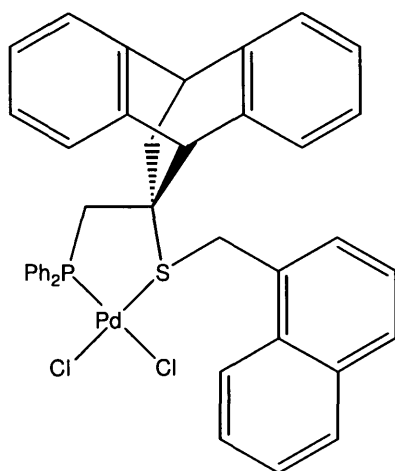
Preparation of Pd(C$_{11}$H$_9$SC$_{17}$H$_{14}$PPh$_2$)Cl$_2$ 26. PdCl$_2$(NCPh)$_2$ (0.160 g, 0.418 mmol) and **L^{2}1-MN** (0.226 g, 0.517 mmol) were dissolved in anhydrous dichloromethane (15 ml) whilst stirring under argon. The reaction mixture was then stirred for 2 hours at room temperature the solvent was evaporated leaving a pale orange solid. Yield 0.21 g (55%). Exact mass calculated for C$_{40}$H$_{33}$S$_1$P$_1$Cl$_1$Pd$_1$ (-Cl$_1$) requires m/z 717.0764, found m/z 717.0791 (ES).
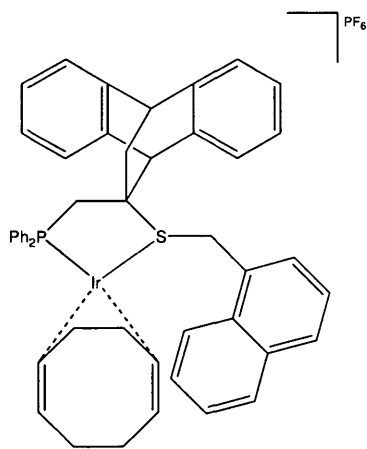
Preparation of [Ir(C₁₁H₉SC₁₇H₁₄PPh₂)(cod)]PF₆ 27. Ir(cod)Cl₂ (0.37 g, 0.551 mmol) and **L²1-MN** (0.32 g, 0.556 mmol) were dissolved in anhydrous dcm (30 ml) whilst stirring under argon. The reaction mixture was then stirred at room temperature for 12 hours. In a counter ion exchange ammonium hexafluorophosphide (0.1g, 0.614 mmol) dissolved in degassed water (20 ml) was added and stirred for 2 hours. The water was then extracted and removal of the solvent left a red solid. Yield 0.39g (69%). δ_C (125MHz, CDCl₃) 14.31 (1C, s, CH₂(cod)), 29.93 (1C, s, CH₂(cod)), 30.73 (1C, s, CH), 41.56 (1C, s, CH), 50.53 (1C, d, CH₂, $^2J_{CP}$ = 8.8), 54.00 (1C, s, C) 64.95 (1C, s, CH₂), 83.72 (1C, s, CH(cod)), 84.59 (1C, s, CH(cod)), 124.35 (1C, s, ArC), 124.51 (1C, s, ArC), 124.74 (1C, s, ArC), 124.83 (1C, s, ArC), 125.32 (1C, s, ArC), 125.56 (1C, s, Ar$C$), 125.93 (1C, s, Ar$C$), 126.62 (1C, s, Ar$C$), 126.97 (1C, s, Ar$C$), 127.14 (1C, s, Ar$C$), 127.14 (1C, s, Ar$C$), 127.24 (1C, s, Ar$C$), 127.29 (1C, s, Ar$C$) 127.37 (1C, s, Ar$C$), 127.43 (1C, s, Ar$C$), 127.51 (1C, s, Ar$C$), 127.69 (1C, s, Ar$C$), 128.12 (1C, s, Ar$C$), 131.41 (1C, s, Ar$C$) 131.56 (1C, s, Ar$C$), 132.74 (1C, s, Ar$C$), 132.90 (1C, s, Ar$C$), 135.74 (1C, s, Ar$C$), 138.84 (1C, s, Ar$C$), 140.17 (1C, s, Ar$C$), 141.04 (1C, s, Ar$C$), 142.15 (1C, s, Ar$C$). δ_P (CDCl₃, 121MHz) 35.8 (s, PPh₂), -143.2 (p, PF₆, $^7J_{PF}$ = 6.4); exact mass calculated for C₄₈H₃₅S₁P₁Ir₁(-P₁F₆) requires m/z 877.2609, found m/z 877.2607 (ES).
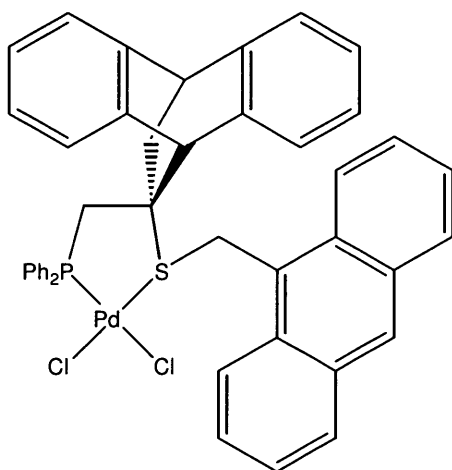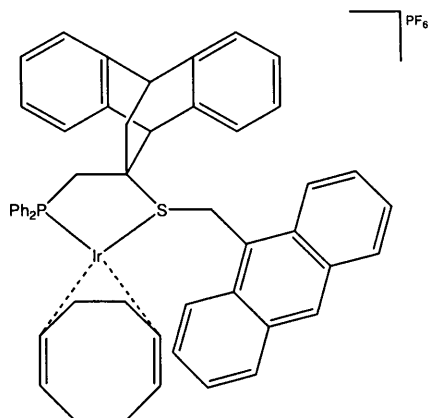

Preparation of Pd(C₁₅H₁₁SC₁₇H₁₄PPh₂)Cl₂ 28. Pd(NCPh)₂Cl₂ (0.24 g, 0.627 mmol) and **L²9-MAN** (0.39 g, 0.623 mmol) were dissolved in anhydrous dcm (30 ml) whilst stirring under argon. The reaction mixture was then stirred at room temperature for 2 hours. Removal of the solvent left a yellow solid. Yield 0.42 g (83%). Exact mass calculated for C₄₄H₃₅S₁P₁Cl₂Pd₁(-Cl) requires m/z 767.0920, found m/z 767.0931 (ES)

Preparation of [Ir(C$_{15}$H$_{11}$SC$_{17}$H$_{14}$PPh$_2$)(cod)]PF$_6$ **29.** Ir(cod)Cl$_2$ (0.431 g, 0.641 mmol) and **L^{2}9-MAN** (0.40 g, 0.638 mmol) were dissolved in anhydrous CH$_2$Cl$_2$ (30 ml) whilst stirring under argon. The reaction mixture was then stirred at room temperature for 12 hours. In a counter ion exchange ammonium hexafluorophosphide (0.11g, 0.675 mmol) dissolved in degassed water (20 ml) was added and stirred for 2 hours. The water was then extracted and removal of the solvent left a red solid. Yield 0.42g (62%). δ$_P$ (CDCl$_3$, 121MHz) 35.2 (s, P*Ph$_2$*), -143.1 (p, *P*F$_6$, $^7J_{PF}$ = 6.4); exact mass calculated for C$_{52}$H$_{47}$S$_1$P$_1$Ir$_1$(-PF$_6$) requires m/z 927.2765, found m/z 927.2726 (ES).

Chapter 6 Conclusion

To allow industry to commercially develop materials and methods, tuning of ligands, complex properties and synthetic stages are required. Ease of synthesis, availability of precursors and control of resulting materials is the key to commercialisation of such compounds. In order to scale-up resulting compounds, synthetic steps are required to be kept to a minimum. The use of commercially available substrates is therefore required to reduce the number of synthetic steps. In this study we reported two different approaches to ligand synthesis showing the pros and cons of synthesis using a simple one step process compared to a complex multi stage synthesis.

Most commercially available precursors are based on simple, low molecular weight substrates. They can increase the probability of a process being adopted by industry with a reduced number of synthetic steps using precursors which are already available on a large scale. However, the use of commercially available substrates can lead to ligands becoming restrictive of coordination geometries. As we have demonstrated the use of conformationally confined ligand L^1 can limit the versatility of bound species ability to for bridging species.

Using a complex synthetic route does have its problems with multi-step synthesis leading to the enhanced probability of cross contamination from substrates and by-products at each step of the reaction. Formation of L^2 demonstrates how cross contamination can influence the formation of undesired complexes, in this case being oxidised sulfinato complexes. Increasing the number of synthetic steps does have its advantages, the ability to design ligands to achieve a specific response in a catalytic reaction. The synthesis of ligand L^2 has demonstrated the advantages of forming a specifically designed backbone with greater steric influences and chiral freedom allow a set of diverse sulphur bridging complexes to be synthesised.

Through the use of group 10 metal precursors it was anticipated that square planar complexes would be synthesised coordinating our phosphinothiolate and phosphinothioether ligands. CFT and MO theory explained the basic principles behind forming square planar complexes. We have shown in this study that the backbone of the ligand can distort a metal complex geometry by their electronic and steric influences. **Figure 6-1** shows the numbering scheme of *cis* and *trans-* phosphinothiolate complexes to study the bond angles of the metal-ligand interactions.
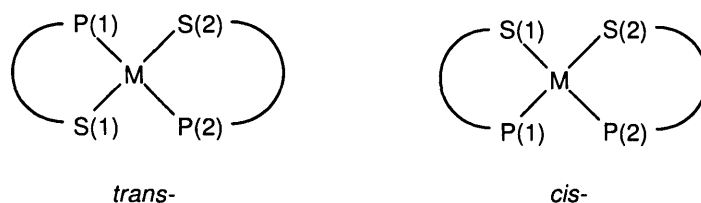
Figure 6-1: Ligand numbering scheme for *cis* and *trans* metal-ligand bond angle comparison

Ligand-metal bond angles are shown in **Table 6-1** for all monomeric phosphinothiolate complexes. We can see from the data that the geometry of *trans-* bis-chelates complexes is exactly square planar regardless of the type of ligand backbone. Distortions of the square planar geometry can be seen in *cis-* complexes where electronic factors including the *trans* effect determine the geometry of the complex placing bulky diphenylphosphino- groups in close proximity. Therefore steric interactions of the backbone do not play a part in the distortion of monomeric complexes, ligands L^1 and L^2 give almost identical ligand-metal bond angle for *cis* and *trans* geometries.

Complex	P(1)-M-S(1)	P(1)-M-P(2)	S(1)-M-S(2)	S(1)-M-P(2)
trans-Ni(L^1)$_2$ **7**	88.99(3)	180.00(4)	180.00(4)	91.01(3)
trans-Pd(L^1)$_2$ **8**	85.739(19)	180.00(3)	180.00(3)	94.261(19)
trans-Pd(L^2)$_2$ **12**	86.30(7)	180.00(10)	180.00(2)	93.41(3)
trans-Pd(L^2O_2)$_2$ **13**	83.59(3)	180.00(2)	180.00(2)	96.41(3)
cis-Pd(L^1)$_2$ **8**	86.74(19)	85.85(17)	100.57(17)	170.48(19)
cis-Pd(L^1)$_2$PdCl$_2$ **11**	88.30(4)	86.87(4)	102.66(4)	168.12(4)
PdCl$_2$[*cis*-Pd(L^2)$_2$Pd(H$_2$O)Cl$_2$]$_2$ **15**	86.22(7)	85.92(7)	102.04(7)	170.18(8)

Table 6-1: Monomeric phosphinothiolate ligand-metal bond angle (°) comparison

Regarding phosphinothioether complexes there are no interactions between ligands coordinated to the same metal therefore comparisons of metal-ligand bond angles can be made between the series of sterically diverse ligands. **Figure 6-2** shows the numbering scheme of phosphinothioether complexes to study the bond angles of the metal-ligand interactions.
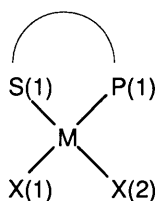

Figure 6-2: Phosphinothioether complex numbering scheme for metal-ligand bond angle comparison

144

All phosphinothioether complexes shown in **Table 6-2** have distorted square planar geometries similar to those seen in *cis*-bis-chelates complexes previously. In this case we see a correlation between the disortions and the steric interactions of the thioether moieties. With the increase in steric hinderence there is a pattern of increasing the diagonal planes to a closer fit to a standard square planar geometry. We also could predict that the steric interaction of ligand L^2 have an influence on the dihalide bond angle X(1)-M-X(2). For complexes **18**, **20** and **23** have X(1)-M-X(2) bond angles over 90°, the introduction of a larger backbone (L^2Bn) closes the metal-halide bond angle to 85.89(5)°. This is the first evidence that the backbone of the ligand has an impact on the geometry of the metal complex.

Complex	X(1)-M-P(1)	X(2)-M-S(1)	S(1)-M-P(1)	X(1)-M-X(2)	X(1)-M-S(1)
Pd(L^1Bn)Br$_2$ **18**	176.00(5)	174.67(5)	86.99(6)	91.91(5)	90.09(5)
Ni(L^1Bn)Cl$_2$ **20**	176.26(4)	174.94(4)	88.49(4)	93.21(4)	91.07(3)
Pd($L^1$9-MAN)Cl$_2$ **23**	173.15(4)	175.63(4)	87.55(4)	93.41(4)	89.58(3)
Pd(L^2Bn)Cl$_2$ **24**	176.41(2)	177.42(6)	92.20(5)	85.89(5)	85.89(5)

Table 6-2: Phosphinothioether ligand-metal bond angle (°) comparison

Through the successful synthesis of a number of square planar complexes this has led to a number of examples of the *trans influence* for phosphinothiolate and phosphinothioether complexes. For the first time in this study we compare metal-ligand bond lengths between phosphinothiolate and phosphinothioether complexes. **Figure 6-3** shows the numbering scheme of phosphinothiolate complexes to study the bond lengths of the metal-ligand interactions.

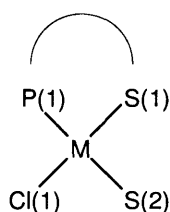**Figure 6-3:** Ligand numbering scheme for dimer and trimer metal-ligand bond length comparison

Table 6-3 shows metal-ligand bond lengths for all complexes formed which contain examples of *trans influence*. This data can confirm that changes in the backbone affect the electronic properties of the coordinating ligand moieties. We see that with increasing size of the ligand backbone and thioether moiety an increase in the *trans*

influence of the diphenylphosphino-group is also observed. With the diphenylphosphino- groups remaining relatively constant we can conclude that changes in the steric properties of the ligand backbone have a greater influence of the electronic properties of sulphur compared to phosphorus.

Phosphinothiolate	M-P	M-X	M-S(1)	M-S(2)	Difference
[Ni(L^1)Cl]$_2$ 9	2.1680(6)	2.1779(7)	2.1694(6)	2.2353(6)	0.0659
[Pd(dppet)Cl]$_2$ 10	2.2353(13)	2.3287(13)	2.2901(13)	2.3749(13)	0.0848
[Pd(L^2)Cl]$_3$ 16	2.2336(10)	2.3576(10)	2.2803(10)	2.3843(10)	0.1040
Phosphinothioether	M-P	M-S	M-X(1)	M-X(2)	Difference
Pd(L^{1}Bn)Br$_2$ 18	2.2461(16)	2.2757(16)	2.4177(9)	2.4730(10)	0.0553
Ni(L^{1}Bn)Cl$_2$ 20	2.1607(14)	2.1771(10)	2.1851(10)	2.2212(8)	0.0361
Pd(1-MNL^{1}1-MN)Cl$_2$ 22	2.068(3) (M-C)	2.2916(9)	2.3355(10)	2.3958(9)	0.0603
Pd(L^{1}9-MAN)Cl$_2$ 23	2.2207(10)	2.2792(10)	2.3101(10)	2.3842(10)	0.0741
Pd(L^{2}Bn)Cl$_2$ 24	2.2799(14)	2.2819(14)	2.3235(15)	2.4236(14)	0.1001

Table 6-3: Phosphinothiolate and phosphinothioether complex bond lengths (Å) showing relative *trans* influences

The main conclusions arisen from the study are as follows:

1. Conformationally confined ligand backbones can inhibit the ability for sulphur containing compounds to form bridging complexes.

2. Bis-chelate P, S complexes of the *cis* geometry require specific ligand backbone steric properties to orientate and accommodate complexation, with L^1 showing such properties.

3. Oxidation of sulphur upon coordination can be initiated through the inclusion of specific reagents and conditions.

4. Thioether moieties of varying steric hindrance can change the electronic and steric influence of sulphur upon coordination.

5. Conformationally confined phosphinothioethers can influence the preference of stereoisomers within a multi-chiral ligand backbone. Ligands with chiral rotational freedom can loose all stereospecificity leading to sulphur inverted fluxional compounds.

6. Overall bonding of sulphur with respect to coordination diversity from bis-chelate, dimer, trimer, pentimer, oxidation, is highly dependant upon steric bulk and or flexibility of the ligand backbone and number of synthetic steps.

This study has therefore increased our understanding of how the backbone of a ligand can influence the bonding and coordination of group 10 metal phosphinothiolate and phosphinothioether complexes. It has highlighted the need for ligand synthesis to be concise and limited to a minimal number of synthetic steps to reduce the likelihood of contamination. The following research strategies could be designed to follow up and elaborate on the results presented in this thesis.

1. Catalytic activity of structurally diverse sulphur bridging phosphinothiolate complexes.

2. Study the relationship between electronic differences and catalytic activity in phosphinothiother complexes.

3. Study the spontaneous mechanistic oxidation for the complexation of phosphinothiolate L^2H.

References

[1]. B. J. Dunne, R. B. Morris, A. G. Orpen, *J. Chem. Soc. Dalton Trans.*, **1991**, 653.

[2]. S. X. Xiao, W. C. Trogler, W. C. Ellis, Z. Yellin, *J. Amer. Chem. Soc.*, **1983**, 105, 7033.

[3]. D. S. Marynick, *J. Amer. Chem. Soc.*, **1984**, 106, 4064

[4]. N. G. Connelly, A. G. Orpen, *J. Chem. Soc. Chem. Commun.*, **1985**, 1310.

[5]. M. Braga, *Inorg. Chem.*, **1985**, 24, 2702

[6]. A. C. Tolman, *Chem. Rev.* **1977**, 77, 313

[7]. A. C. Tolman, *J. Amer. Chem. Soc.*, **1970**, 92, 2953

[8]. C. Carcedo, A. Dervisi, L. Ooi, *Advanced Synthesis & Catalysis*, **2006**, 348, 175

[9]. M. Bressan, C. Bonuzzi, F. Morandini, A. Morvillo, *Inorg, Chim. Acta* **1991**, 182, 153-156

[10]. I. del Rio, C. Claver and P. W. N. M. van Leeuwen, *Eur. J. Inorg. Chem.* **2001**, 11, 2719-2738

[11]. M. Beller, W. Magerlein, A. F. Indoese, C. Fisher, *Synthesis*, **2001**, 7, 1098-1109

[12]. M. Beller, W. Magerlein, A. F. Inolese, *Angew. Chem. Int. Ed.* **2001**, 40, 15, 2856

[13]. C. G. Arena, F. Nicolo, D. Drommi, G. Bruno, F. Faraone, *J. Chem. Soc., Chem. Commun.*, **1994**, 2251

[14]. K. Hiroi, Y. Suzuki, R. Kawagishi, *Tetrahedron Letters*, **1999**, 40, 715-718

[15]. A. Suzuki, *Journal of Organometallic Chemistry* **1999**, 576, 147-168

[16]. I. Ojima, *Catalytic Asymmetric Synthesis* Ed, VCH, **1993**

[17]. H. B. Kangan, T.-P. Dang, *J. Amer. Chem. Soc.* **1972**, 94, 6429-6433

[18]. A. Mishita, A. Yasuda, H. Tanaka, K. Toriumi, T. Ito, T. Sauchi, R. Noyori, *J. Amer. Chem. Soc.* **1980**, 102, 7932-7934

[19]. W. S. Knowles, M. J. Sabacky, B. D. Vineyard, *Adv. Chem. Ser.* **1974**, 132, 274

[20]. N. Sakai, S. Mano, K. Nozaki, H. Takaya, *J. Amer. Chem. Soc.* **1993**, 115, 7033

[21]. E. M. Padilla, C. M. Jensen, *Polyhedron* **1991**, 10, 89

[22]. Y. K. Jim, K. Osakada, K. Sugita, T. Yamamoto, A. Yamamoto, *Organometallics*, **1988**, 7, 2182

[23]. V. K. Jain, G. S. Rao, *Inorg. Chim. Acta*, **1987**, 127, 161

[24]. A. Singhai, V. K. Jain, *J. Organomet. Chem.* **1995**, 494, 75

[25]. M. T. Ashby, J. H. Enemark and D. L. Lichtenberger, *Inorg. Chem.* **1988**, 27, 191-197

[26]. H. Barrera and J. M. Vinas, *Polyhedron* **1985**, 12, 2027-2030

[27]. V. K. Jain *et al. Polyhedron* **1989**, 17, 2151-2155

[28]. J. Ruiz *et al. Polyhedron* **1998**, 17, 9, 1503-1509

[29]. A. Schnyder, L. Hintermann, A. Togni, *Angew. Chem.* **1995**, 107, 996-998

[30]. F. G. Mann, J. Watson, *J. Org. Chem.* **1948**, 13, 502-531

[31]. N. W. Alcock, A. W. G. Platt and P. Pringle, *J. Chem. Soc. Dalton Trans.* **1987**, 2273-2280

[32]. J. Heinicke, U. Jux, R. Kadyrov, M. He, Heteroatom Chem. **1997**, 8, 383

[33]. A. Schnyder, A. Togni, U. Wiesli, *Organometallics* **1997**, 16, 255-260

[34]. P. Blochl, A. Togni, *Organometallics* **1996**, 15, 4125-4132

[35]. J. M. Brown, D. J. Hulmes and F. J. Guiry, *Tetrahedron* **1994**, 50, 4493

[36]. K. Yonehiro, T. Hashizume, K. Mori, K. Ohe and S. Uemura, *Chem. Commun.* **1999**, 415-416

[37]. J. Sprinz, M. Kiefer, G. Helmchen, M. Reggelein, G. Huttner and L. Zsolnai, *Tetrahedron Lett.* **1994**, 35, 1523

[38]. J. Sprinz and G. Helmchen, *Tetrahedron Lett.* **1993**, 34, 1769

[39]. S. Kudis and G. Helmchen, *Angew. Chem. Int. Ed.* **1998**, 37, 21, 3047-3050

[40]. J. W. Faller, N. Sarantopoulos, *Organometallics* **2004**, 23, 2008-2014

[41]. F. Teixidor, C. Vinas, R. Benakki, *Inorg. Chem.* **1997**, 36, 1719-1723

[42]. J. R. Geigy, Fr. Pat. 1401930, 1965; *Chem Abstr.* **1965**, 63, 11615g

[43]. K. Issleib, K. D. Franze, *J. Prakt. Chem.* **1973**, 315, 471

[44]. P. H. Leung, J. W. L. Martin, S. B. Wild, *Inorg. Chem.* **1986**, 25, 3396-3400

[45]. G. S. White, D. W. Stephan, *Organometallics* **1987**, 6, 2169-2175

[46]. E. Block, G. Ofori-Okia, J. Zubieta, *J. Amer. Chem. Soc.* **1989**, 111, 2327-2329

[47]. S. Gladiali, A. Dore, D. Fabbri, *Tetrahedron: Asymmetry* **1994**, 5, 7, 1143-1146

[48]. O. Korpiun, R. A. Lewis, J. Chickos, K. Mislow, *J. Amer. Chem. Soc.,* **1968**, 90, 4842-4846

[49]. A. Albinati, J. Herrmann and P. S. Pregosin, *Inorganica Chimica Acta* **1997**, 264, 33-42

[50]. N. Brugat *et al. Tetrahedron: Asymmetry* **2002**, 13, 569-577

[51]. V. C. Gibson, N. J. Long, A. J. P. White, C. K. Williams and D. J. Williams, *Organometallics* **2002**, 21, 770-772

[52]. J. Duran, N. Brugat, A. Polo, C. Segura, J. Real, X. Fontrodona and J. Benet-Buchholz, *Organometallics* **2003**, 22, 3432-3438

[53]. A. Dervisi, R. L. Jenkins, K. M. Malik, M. B. Hursthouse and S. Coles, *Dalton Trans.* **2003**, 1133- 1142

[54]. T. H. Chan, J. R. Finkenbine, *J. Amer. Chem. Soc.*, **1972**, 94, 8, 2880-2882

[55]. W. E. Childers *et al. J. Org. Chem.* **1988**, 53, 5947-5951

[56]. V. Calo, L. Lopez, L. Marchese, G. Pesce, *J. Chem. Soc., Chem. Comm.*, **1975**, 621-622

[57]. J. S. Yadav, B. V. S. Reddy, C. S. Reddy and K. Rajasekhar, *J. Org. Chem.* **2003**, 68, 2525-2527

[58]. R. L. Pederson, K. C. Liu, J. F. Rutan, L. Chen and C-H. Wong, *J. Org. Chem.* **1990**, 55, 4897-4901

[59]. O. Varela and P. A. Zunazain, *J. Org. Chem.* **1993**, 58, 27, 7860-7863

[60]. M. Wieber, T. Z. Clarius, *Anorg. Allg. Chem.* **1995**, 621, 1288

[61]. P. H. Leung, A. C. Willis, S. B. Wild, *Inorg. Chem.* **1992**, 31, 1406-1410

[62]. J. R. Dilworth and N. Wheatley, *Coordination Chemistry Review* **2000**, 199, 89-158

[63]. G. Doyle, *J. Organomet. Chem.* **1975**, 101, 85

[64]. J. Chatt, J. Dilworth, J. A. Schmutz, *J. Chem. Soc., Dalton Trans.*, **1979**, 1595-1599

[65]. M. Savignac, P. Cadiot, *Inorg. Chimi. Acta,* **1980**, 45, L43-L44

[66]. D. W. Stephan, *Inorg. Chem.* **1984**, 23, 2207-2210

[67]. G. White, D. W. Stephan, *Inorg. Chem.* **1985**, 24, 1499-1503

[68]. D. Morales, R. Poli, P. Richard, J. Andrieu, E. Collange, *J. Chem. Soc., Dalton Trans.*, **1999**, 867-873

[69]. J. Real *et al. Inorganic Chemical Communications* **2000**, 3, 221-223

[70]. A. Benefiel, D. M. Roundhill, W. Fultz and A. L. Rheingold, *Inorg. Chem.* **1984**, 23, 3316-3324

[71]. N. Brugat, A. Polo, A. Alvarez-Larena, J. F. Piniella and J. Real, *Inog. Chem.* **1999**, 38, 4829-4837

[72]. J. R. Dilworth, A. J. Hutson, *Transition Metal Chemistry* **1994**, 19, 61-64

[73]. J. R. Dilworth, C. Lu, J. R. Miller, Y. Zheng, *J. Chem. Soc. Dalton Trans.*, **1995**, 1957-1964

[74]. J. R. Dilworth, D. Vaughan Griffiths, S. J. Parrott, Y. Zheng, *J. Chem. Soc., Dalton Trans.*, **1997**, 2931-2936

[75]. P. Perez-Lourido, J. Romero, J. Garcia-Vazquez, A. Sousa, *Inorg. Chem.* **1998**, 37, 3331-3336

[76]. P. Perez-Lourido, J. Romero, J. Garcia-Vazquez, A. Sousa, *Inorg. Chem.* **1998**, 37, 3331-3336

[77]. P. Perez-Lourido, J. Romero, J. A. Garcia-Vazquez, A. Sousa, Inorg. Chem. **1999**, 38, 1293-1298

[78]. Y. Qin, A. J. P. White, D. J. Williams, P. Leung, *Organometallics*, **2002**, 21, 171-174

[79]. D. Canseco-Gonzalez *et al. Journal of Organometallic Chemistry* **2003**, 679, 101-109

[80]. E. Cerrada, L. R. Falvello, M. B. Hursthouse, M. Laguna and C. Pozo-Gonzalo, Eur. *J. Inorg. Chem.* **2002**, 826-833

[81]. J. R. Dilworth, A. J. Hutson, J. S. Lewis, J. R. Miller, Y. Zheng, Q. Chen, J. Zubieta, *J. Chem. Soc., Dalton Trans.*, **1996**, 1093-1104

[82]. K. Ortner, L. Hilditch, Y. Zheng, J. R. Dilworth and U. Abram, *Inorg. Chem.* **2000**, 39, 2801-2806

[83]. K. A. Clark, T. A. George, *Inorg. Chem.* **2005**, 44, 416-422

[84]. G. Dyer, D. Meek, *Inorg. Chem.*, **1965**, 4, 10, 1398-1402

[85]. G. Dyer, M. O. Workman, D. Meek, *Inorg. Chem.*, **1967**, 6, 7, 1404-1407

[86]. J. F. Sieckhaus, T. Layloff, *Inorg. Chem.*, **1967**, 6, 12, 2185-2190

[87]. E. P. Ross, G. R. Dobson, *J. Inorg. Nucl. Chem.*, **1968**, 30, 2363-2366

[88]. F. G. Mann, I. T. Millar, *J. Chem. Soc.* **1952**, 3039-3046

[89]. E. Hauptman, P. J. Fagan and W. Marshall, *Organometallics* **1999**, 18, 2061-2073

[90]. O. Pamies, M. Dieguez, G. Net, A. Ruiz and C. Claver, *Organometallics* **2000**, 19, 1488-1496

[91]. J. Herrmann, P. S. Pregosin and R. Salzmann, *Organometallics* **1995**, 14, 3311-3318

[92]. D. A. Evans, K. R. Campos, J. S. Tedrow, F. E. Michael and M. R. Gagne, *J. Am. Chem. Soc.* **2000**, 122, 7905-7920

[93]. D. Morales-Morales *et al. Inorg. Chimi. Acta* **2002**, 328, 39-44

[94]. P. Barbaro, A. Currao, J. Herrmann, R. Nesper, P. S. Pregosin, *Organometallics* **1996**, 15, 1879-1888

[95]. M. O. Workman, G. Dyer and D. W. Meek, *Inorg. Chem.* **1967**, 6, 8, 1543-1548

[96]. G. Dyer, D. W. Meek, *J. Amer. Chem. Soc.,* **1967**, 89, 16, 3983-3987

[97]. D. M. Roundhill, W. B. Beaulieu and U. Bagchi, *J. Am. Chem. Soc.* **1979**, 101, 18, 5428-5431

[98]. D. M. Roundhill *et al. Inorg. Chem.* **1980**, 19, 3356-3373

[99]. A. Benefiel and D. M. Roundhill, *Inorg. Chem.* **1986**, 25, 4027-4031

[100]. J. R. Dilworth, J. R. Miller, N. Wheatley, M. J. Baker, J. G. Sunley, *J. Chem. Soc., Chem. Commun.*, **1995**, 1579-1581

[101]. P-H. Leung, S-K. Loh, K. F. Mok, A. J. P. White, D. J. Williams, *J. Chem. Soc., Dalton Trans.*, **1996**, 4443-4448

[102]. A. Albinati, P. S. Pregosin and K. Wick, *Organometallics* **1996**, 15, 2419

[103]. A. Albinati, J. Eckert, P. Pregosin, H. Ruegger, R. Salzmann and C. Stossel, *Organometallics* **1997**, 16, 579-590

[104]. M. Tschoerner, G. Trabesinger, A. Albinati, P. S. Pregosin, *Organometallics* **1997**, 16, 3447-3453

[105]. A. S. Abu-Surrah et al. *Polyhedron* **2000**, 19, 1601-1605

[106]. D. Evans, F. E. Michael, J. S. Tedrow and K. R. Campos, *J. Am. Chem. Soc.* **2003**, 125, 3534-3543

[107]. H. Lee, J. Bae, D. Kim, H. Kim, S. Kim, S. Cho, J. Ko and S. O. Kang, *Organometallics* **2002**, 21, 210-219

[108]. A. H. Eisenberg, M. V. Ovchinnikov and C. A. Mirkin, *J. Am. Chem. Soc.* **2003**, 125, 2836-2837

[109]. M. Bressan, C. Bonuzzi, F. Morandini, A. Morvillo, *Inorg, Chim. Acta* **1991**, 182, 153-156

[110]. R. L. Dutta, D. W. Meek, D. H. Busch, Inorg. Chem., 1970, **9**, 1215

[111]. P. G. Eller, J. M. Riker, D. W. Meek, J. Amer. Chem. Soc., 1973, **95**, 3540

[112]. S. S. Choinacki, Y-M. Hsiao, M. Y. Darensbourg and J. H. Reinspeies, *Inorg. Chem.*, 1993, **32**, 3573

[113]. D. C. Goodall, *J. Chem. Soc. (A)* **1968**, 887

[114]. M. S. Kharasch, R. C. Seyler, F. R. Mayo, *J. Amer. Chem. Soc.* **1938**, 60, 882

[115]. G. S. White and D. W. Stephan, *Organometallics*, 1988, 7, 903

[116]. T. Gerdau, W. Klein and R. Kramolowsky, *Cryst. Struct. Commun.*, 1982, **11**, 1163

[117]. S. E. Livingstone, T. N. Lockyer, *Inorg. Nucl. Chem. Lett.* **1967**, 3, 35

[118]. N. De Vries, A. Davison, A. G. Jones, *Inorg. Chimi. Acta* **1989**, 165, 9-10

[119]. J. Real, M. Pages, A. Polo, J. F. Piniella, A. Alvarez-Larena, *Chem. Comm.*, **1999**, 277-278

[120]. K. Michal-Pietrusiewicz, M. Zablocka, *Chem. Rev.* **1994**, 94, 1375-1411

[121]. T. M. Cocker and R. E. Bachman, *Inorg. Chem.* **2001**, 40, 1550-1556

[122]. E. Galardon, M. Giorgi and I. Artaud, *Chem Commun.* **2004**, 286-287

[123]. T. Tuntulani, G. Musie, J. H. Reibenspies and M. Y. Darensbourg, *Inorg. Chem.* **1995**, 34, 6279-6286

[124]. S. A. Mirza, M. A. Pressler, M. J. Kumar, R. O. Day and M. J. Maroney, *Inorg. Chem.* **1993**, 32, 977-987

[125]. S. W. Griffiths, J. King and C. L. Cooney, *The Journal of Biological Chemistry* **2002**, 277, 28, 25486-25492

[126]. I. K. Adzamli and E. Deutsch, *Inorg. Chem.* **1980**, 19, 1366-1373

[127]. S. Y. M. Chooi, P. H. Leung and K. F. Mok, *Inorg. Chimi. Acta* **1993**, 205, 245

[128]. L. A. Tyler, J. C. Noveron, M. M. Olmstead and P. K. Mascharak, *Inog. Chem.* **2000**, 39, 357-362

[129]. J. L. Herde, J. C. Lambert, C. V. Senoff, *Inorganic Synthesis*, vol. 15, 18-20

[130]. A. Spannenberg, W. Banmann, O. Rosenthal, *Organometallics* **2000**, 19, 3991-3993

[131]. L. R. Falvello, J. C. Ginés, J. J. Carbó, A. Lledós, R. Navarro, T. Soler, E. P. Urriolabeitia, *Inorg. Chem.* **2006**, 45, 6803-6815

[132]. G. Commenges, R. Chanvin, *Organometallics*, **2001**, 20, 808-810

[133]. A. M. Mazany, J. P. Fackler, *Organometallics*, **1982**, 1, 752-753

[134]. Y. Qin, A. J. P. White, D. J. Williams, P. Leung, *Organometallics*, **2002**, 21, 171-174

[135]. P. Mastrorilli, C. F. Nobile, G. P. Suranna, F. P. Fanizzi, G. Ciccarella, U. Englert and Q. Li, *Eur. J. Inorg. Chem.* **2004**, 1234-1242

[136]. R. Zuruwinski, B. Donnadieu, M. Mikolajczyk, R. Chauvin, *Journal of Organometallic Chemistry* **2004**, 689, 380-386

[137]. N. C. Yang and J. Libman, *J. Amer. Chem. Soc.* **1972**, 94, 1405

[138]. G. Kaupp, R. Dyllick-Brezinger and I. Zimmermann. *Angew. Chem. Internat. Edit.* **1975**, 14, 491

[139]. G.Kaupp. *Liebigs Ann. Chem.* **1977**, 254-275

[140]. E. Vedejs, J. P. Hagen, *J. Amer. Chem. Soc.* **1975**, 97, 6878

[141]. D. D. Perrin and W. F. A. Amarego, *Purification of Laboratory Chemicals*, Pergamon, Oxford, **1988**.